THE PHYSICAL REVIEW

VOLUME 47 Second Series NUMBER 5

MARCH 1, 1935

Published for the

AMERICAN PHYSICAL SOCIETY

by the

AMERICAN INSTITUTE OF PHYSICS

Lancaster, Pa., and New York, N. Y.

THE AMERICAN PHYSICAL SOCIETY

OFFICERS OF THE SOCIETY

[illegible] WOOD, *President*
[illegible] Johns Hopkins University
[illegible]more, Maryland

[illegible] L. SEVERINGHAUS, *Secretary*
Columbia University
New York, New York

[illegible] T. TATE, *Editor*
University of Minnesota
[illegible]neapolis, Minnesota

F. K. RICHTMYER, *Vice President*
Cornell University
Ithaca, New York

G. B. PEGRAM, *Treasurer*
Columbia University
New York, New York

L. B. LOEB, *Local Secretary for the Pacific Coast*
University of California
Berkeley, California

THE PHYSICAL REVIEW

BOARD OF EDITORS

JOHN T. TATE, *Editor*

J. W. BUCHTA, *Assistant Editor*

Associate Editors

K. K. DARROW
[illegible]C. HUBBARD
[illegible] R. RUARK

A. ELLETT
L. A. TURNER
G. E. UHLENBECK

W. V. HOUSTON
R. S. MULLIKEN
I. I. RABI

THE PHYSICAL REVIEW, which was established [illegible], is a journal of experimental and [illegible] physics. It is published for the American Physical Society by the American Institute of Physics Incorporated. There are two volumes annually with twelve issues in each volume.

[illegible] for publication should be submitted to [illegible], University of Minnesota, Minneapolis, [illegible]

[illegible] all correspondence concerning papers in the [illegible] publication, should be addressed to the Editorial [illegible] American Institute of Physics, 11 East 38th [illegible] York, New York.

[illegible] price: United States and Possessions and [illegible].00; Foreign, $16.50. Subscriptions and orders [illegible] members should be addressed to Prince and [illegible], Lancaster, Pennsylvania, or to the American [illegible] of Physics, 11 East 38th Street, New York, [illegible]

[illegible] is not accepted for the *Physical Review* but [illegible] is called to the *Review of Scientific Instruments with Notes and Views*, a companion publication of [illegible], and a medium through which the field of physics can be reached most effectively. Rates and other information will be furnished on request to the Editorial Secretary.

Changes of address and complaints of failure to receive the *Physical Review*, in the case of members of the American Physical Society, should be addressed to the Treasurer; in the case of other subscribers, to the Editorial Secretary. New copies can be sent free in response to complaints of non-delivery only if notice of non-delivery is received within three months of date of issue.

The Physical Review is published semi-monthly at Prince and Lemon Streets, Lancaster, Pennsylvania.

Entered at the Post Office at Lancaster, Pennsylvania, as second class matter.

Acceptance for mailing at special rate of postage provided for in section 1103, Act of October 3, 1917, authorized September 6, 1926.

THE
PHYSICAL REVIEW
A Journal of Experimental and Theoretical Physics
VOL. 47, NO. 5 MARCH 1, 1935 SECOND SERIES

Transmutations of Aluminum by Deutons

EDWIN MCMILLAN AND ERNEST O. LAWRENCE, *Radiation Laboratory, Department of Physics, University of California*
(Received January 12, 1935)

Aluminum bombarded by 2.2 mv deutons is found to emit protons, neutrons and alpha-particles, presumably accompanying reactions in which Al^{28} (radio-aluminum), Si^{28} and Mg^{25} are formed. The protons are the most abundant (about 8 per 10^7 deutons) and have a complex spectrum of ranges, in which groups with ranges 10, 21, 30 and 53 cm have been resolved. The maximum range of 62 cm corresponds to a reaction energy of 5.3 mv. The radioactive product, shown chemically to be an aluminum isotope, decays with a half-life of 156±5 sec., emitting negative electrons and intense gamma-rays. The maximum range of the electrons is 0.95 g/cm² of Al, corresponding to an energy limit of 2 mv. The excitation curve for the radioactivity agrees with Gamow's theory of nuclear penetration. The alpha-particles have a range of 6.5 cm, giving a reaction energy of 6.6 mv for the formation of Mg^{25}. They are only 1/100 as abundant as the protons.

INTRODUCTION

IN earlier experiments in this laboratory it has been found that aluminum under deuton bombardment gives off alpha-particles,[1] protons and neutrons,[2] and becomes radioactive.[3] This paper describes a more detailed investigation of these reactions.

The apparatus used for producing a beam of high speed deutons is described elsewhere.[4] For studying the emission of particles from the target during bombardment, the target was placed in the vacuum in the path of the deuton beam and the disintegration particles were allowed to emerge through a mica window, as shown in Fig. 1. For studying the radioactivity, the beam was sent through a thin aluminum window (about 1 cm air equivalent stopping power) so that the target, placed opposite the window, could be bombarded outside the vacuum, and therefore could be removed from the apparatus immediately after exposure.

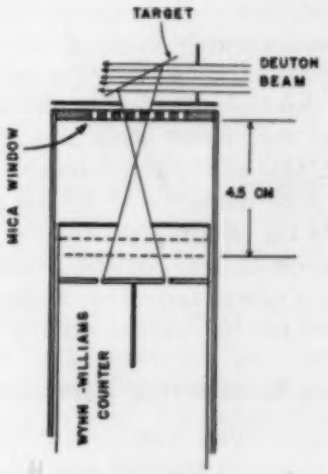

FIG. 1. Arrangement of target, screens and counter for bombarding in vacuum.

[1] G. N. Lewis, M. S. Livingston and E. O. Lawrence, Phys. Rev. **44**, 55 (1933).
[2] E. O. Lawrence and M. S. Livingston, Phys. Rev. **45**, 220 (1934).
[3] M. C. Henderson, M. S. Livingston and E. O. Lawrence, Phys. Rev. **45**, 428 (1934).
[4] E. O. Lawrence and M. S. Livingston, Phys. Rev. **45**, 608 (1934).

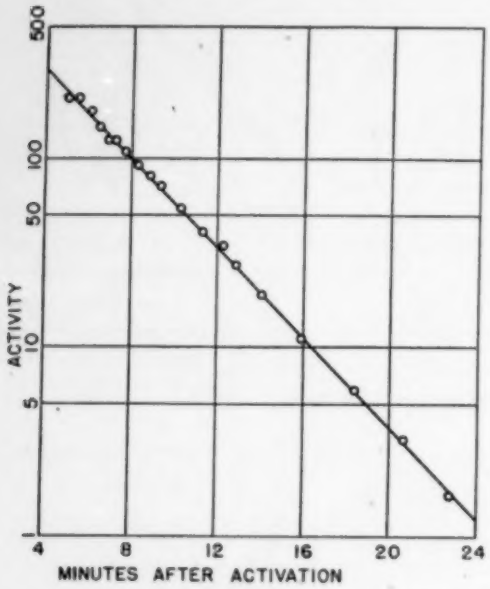

FIG. 2. Decay curve of Al radioactivity, with ordinates on a logarithmic scale.

RADIOACTIVITY

An aluminum target, exposed to ½ microampere of 1.9 mv deutons emerging from the window for a sufficient time to give saturation activity, was placed next to an ionization chamber containing a sensitive quartz fiber electroscope and provided with a thin aluminum window to admit beta-particles. The rate of discharge of the electroscope was followed over a sufficient time to allow the activity to decay by a factor of 120. A logarithmic plot of discharge rate against time (Fig. 2) was accurately linear, giving a half-life for the activity of 156±5 sec. The initial rate of discharge, extrapolated back to the time of removal from the deuton beam, was 50 divisions per second. One can compute roughly from the sensitivity (one division $=2\times10^6$ ion pairs), the geometry of the electroscope, and the ionization per centimeter of beta-particles, that this corresponds to a rate of activation of about 3 radioactive atoms per 10^7 deutons striking the target.

THE RADIOACTIVE RADIATIONS

The beta-particles were found by magnetic deflection to have a negative sign. Their absorption in aluminum was studied by placing foils between the target and the ionization chamber,

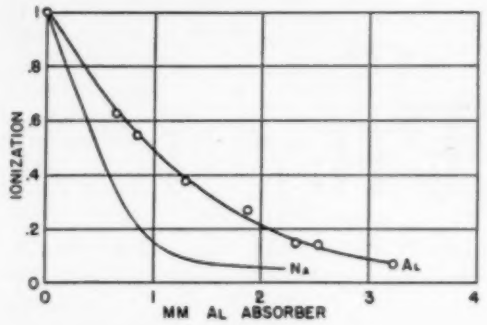

FIG. 3. Absorption of beta-particles from radio-aluminum in Al. Absorption of radio-sodium beta-particles shown for comparison.

with the results shown in Fig. 3. The curve obtained by Lawrence[5] for radio-sodium is given for comparison. As in the case of sodium, the aluminum beta-particles are accompanied by an intense gamma-radiation,[6] so that the ionization does not go to zero as more absorber is put in. Allowing for this background, the maximum range of the beta-particles is found to be 0.95 g/cm² of Al, corresponding, according to Feather's[7] formula, to a maximum energy of 2 mv. This value, in conjunction with the decay period, places the active body on Sargent's[8] upper curve.

The gamma-rays produce about 1/30 as much ionization as the beta-particles, which is the same ratio as was observed in the case of radio-sodium. This suggests, following Lawrence's[5] discussion of that case, that there is about one gamma quantum per beta-particle.

CHEMICAL IDENTIFICATION OF THE ACTIVE PRODUCT

The active product is presumably an element near Al, and most probably Mg, Al or Si. The possibility of Si was eliminated by dissolving an activated sample of thin Al foil in HF, evaporat-

[5] E. O. Lawrence, Phys. Rev. **47**, 17 (1935).

[6] Curie, Joliot and Preiswerk (reference 10) have reported evidence for the occasional disintegration of Al^{28} with the emission of a neutron. We looked for this interesting effect with negative results. An activated Al target placed against a sheet of paraffin in front of a Wynn-Williams ionization chamber did not produce a detectable number of recoil proton counts, indicating that in this case less than 1 in 1000 of the disintegrating atoms emits neutrons. It should be pointed out that in the experiments of Curie, Joliot and Preiswerk the Al^{28} was produced by a different nuclear reaction and may have different properties.

[7] N. Feather, Phys. Rev. **35**, 1559 (1930).

[8] B. W. Sargent, Proc. Roy. Soc. **A139**, 659 (1933).

ing to dryness, and observing that the activity remained behind. Then a similar sample was dissolved in HCl, some $MgCl_2$ was added, and then an excess of KOH was added until the magnesium came down as a precipitate of $Mg(OH)_2$ while the aluminum remained in solution. The precipitate was found not to carry the activity. In a third experiment the sample was again dissolved in HCl, and precipitated with an excess of NH_4OH, which brings the aluminum down as $Al(OH)_3$. The activity was all found in the precipitate, showing definitely that the active product is an aluminum isotope. It is interesting to note that the same active substance has been produced by Curie and Joliot[9] on bombarding Mg with alpha-particles, by Curie, Joliot and Preiswerk[10] on bombarding P with neutrons, by Fermi and his co-workers[11] on bombarding Si with neutrons, and by Amaldi, D'Agostino and Segré[12] on bombarding Al with neutrons.

Excitation Function of the Radioactivity

The number of radioactive atoms produced increases rapidly with the energy of the impacting deutons. The form of this variation was studied by using as a target a stack of thin Al foils (about 4 mm air equivalent stopping power each). Each foil receives precisely the same exposure to the deutons, with a difference in energy determined by the slowing down in the preceding foils. The measured activities of the foils are plotted against the corresponding deuton energies in Fig. 4. The circles are the experimental results, two different runs being shown on the plot.

This sort of experiment gives directly the differential excitation function. This can be compared to the theoretical curve of Gamow for the penetration of deutons through a nuclear potential barrier. In cases where the energy of the deutons is small compared to the height of the barrier, Gamow's formula states that the probability of penetration is proportional to

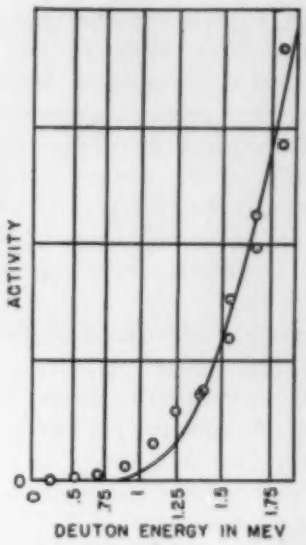

Fig. 4. Differential excitation curve of aluminum radioactivity.

$$(1/v^2)e^{-4\pi Ze^2/hv} \qquad (1)[13]$$

where v is the velocity of the deutons and Z the atomic number of the bombarded nucleus. This curve, for $Z=13$, and with the scale of ordinates adjusted to fit the higher experimental points, is shown in Fig. 4. It is seen that the fit with the experimental points is very good, except at the lower energies. This "tail" on the excitation curve may be due to a few faster deutons accompanying the main beam, or perhaps to a resonance penetration at low energies.

Nuclear Cross Section for Activation

The nuclear cross section for activation can be calculated when the form of the excitation function as well as the absolute intensity of activation of a thick target is known. The value obtained from the preceding data is 8×10^{-27} cm² at the maximum deuton energy of 1.9 mv.

Recoil of Activated Nuclei

When a high speed deuton reacts with a nucleus, its momentum is imparted to the products of the reaction. The radioactive nucleus

[9] I. Curie and F. Joliot, J. de phys. et rad. **5**, 153 (1934).
[10] I. Curie, F. Joliot and I. Preiswerk, Comptes rendus **198**, 2089 (1934).
[11] E. Fermi, E. Amaldi, O. D'Agostino, F. Rasetti and E. Segré, Proc. Roy. Soc. **A146**, 483 (1934).
[12] E. Amaldi, O. D'Agostino and E. Segré, La Ricerca Scientifica, November, 1934.

[13] Professor Oppenheimer informs us that there is an uncertainty as to the precise power of v in the factor multiplying the exponential. In Lawrence's paper on sodium $1/v$ is used.

receives most of this momentum plus a randomly directed momentum imparted by the other particle emitted in the reaction. Because of this randomness, the average momentum in the direction of motion of the deuton beam is just that imparted by the deuton. Dr. Kurie has kindly calculated that this gives the radioactive nuclei an average recoil range in the forward direction of about 0.6 mm of air for a deuton energy of 1.9 mv.

The existence of this recoil phenomenon has been noted previously,[14] and it has now been investigated more carefully in the case of aluminum. The experimental procedure was simply to replace the aluminum target by one of platinum, and to evacuate the space between the window and the target during the bombardment, so that the activated nuclei driven from the aluminum window by recoil would all be deposited on the platinum. It was found that the activity on the platinum was 1/20 as great as that on an aluminum target. From the form of the excitation curve it is calculated that this amount of activity is produced in a layer on the surface of the window of a thickness of 0.5 mm air equivalent. The depth of this layer is a fair measure of the average range of the recoil nuclei, and is in good agreement with the calculated value.

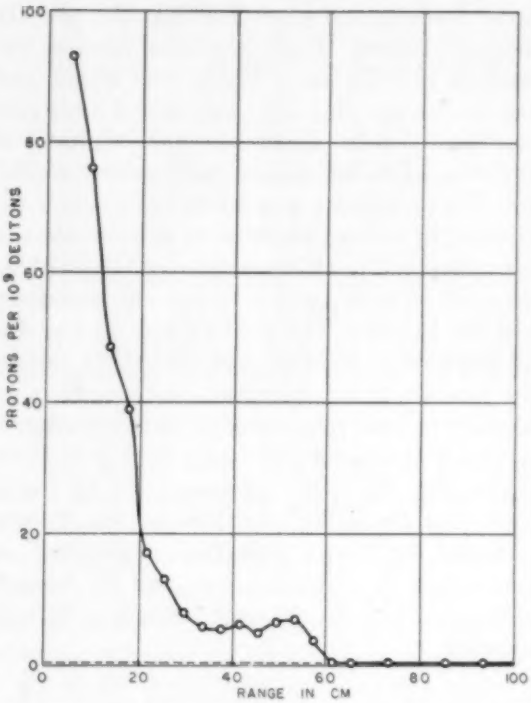

FIG. 5. Protons from a thick Al target bombarded with deutons. The counting rate (corrected to include the whole solid angle) is plotted against the air-equivalent thickness of absorber. The dotted line indicates the neutron background.

THE DISINTEGRATION PROTONS

The fact that the radioactive product is an aluminum isotope, which decays with the emission of a negative electron, suggests that the nuclear reactions concerned are:

$$Al^{27}+D^{2}\rightarrow Al^{28}+H^{1} \qquad (2)$$

$$Al^{28}\rightarrow Si^{28}+\epsilon^{-}. \qquad (3)$$

The protons emitted in reaction (2) were investigated by the arrangement shown in Fig. 1, in which the target was in the vacuum. The protons emerged through a mica window and were counted by a Wynn-Williams counter—a shallow (4 mm) ionization chamber and linear amplifier in conjunction with a cathode-ray oscillograph and thyratron counter. Diaphragms in the path of the deuton beam and between the target and the counter insured that only particles from the target could reach the counter. Aluminum absorbers were placed in front of the counter, to obtain range curves. The deuton voltage in these experiments was 2.2 mv, and the current was usually kept small (about 0.1 μA).

The first observations were made with a solid aluminum target, whose surface was carefully scraped to avoid contamination. The results are shown in Fig. 5 in which are plotted the numbers of protons emitted in all directions, calculated from the geometry of the apparatus. Each point represents about 500 proton counts. A diaphragm was put in front of the counter for the points below 20 cm, to obtain a reasonable counting rate. A small background of neutron counts is indicated by the dotted line.

It is known from other experiments (as pointed out by Lawrence[5] in his work on sodium) that a

[14] M. S. Livingston and E. McMillan, Phys. Rev. **46**, 437 (1934). The nitrogen activity reported in this letter, which occurs as a contamination on any target bombarded with deutons in air, is not sufficiently large to interfere with the measurements on aluminum. In some of the experiments reported above, the space between the window and the target was evacuated during the bombardment in order to be sure that this contamination is of no importance.

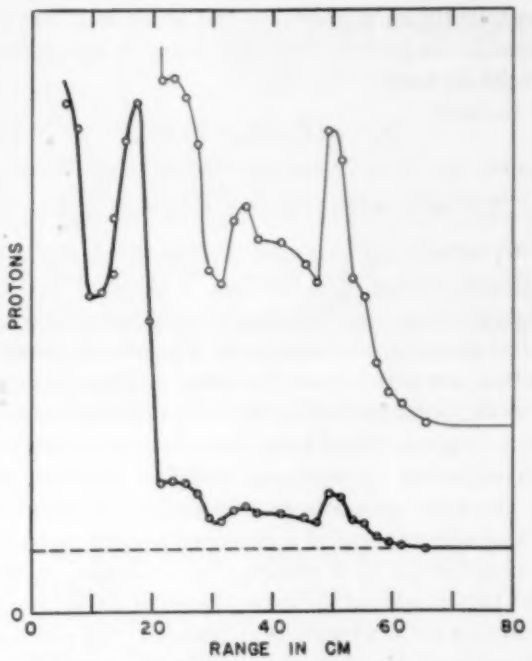

FIG. 6. Range distribution curve of protons from a thin Al target bombarded by deutons. The curve drawn with a finer line is the part beyond 20 cm with a larger scale of ordinates.

homogeneous group of protons, if present, is indicated by this counting arrangement as a sharp peak of half-width 2 cm. The question therefore arose as to whether these results were to be interpreted as showing a continuous distribution of proton energies, or a number of discrete groups that are too close together for resolution when using a thick target.

THIN-TARGET EXPERIMENTS

To settle the question of the nature of the proton distribution in energy, a target of thin Al foil was used (about 2 mm air equivalent thickness in the direction of the deuton beam). The results obtained in this way are shown in Fig. 6; the finer curve is simply the part beyond 20 cm plotted on a larger ordinate scale. As before, the readings below 20 cm were taken with a diaphragm in front of the counter, and each point represents about 500 proton counts. The number of proton counts is reduced by the use of the thin target, whereas that part of the neutron background not arising from the target is undiminished. Hence the neutron background appears relatively larger.

These results show that there are two very strong proton groups of 10 and 21 cm range, two weak but clearly resolved groups of 30 and 53 cm range, and still weaker groups between 30 and 48 cm as well as at least one more group with a maximum range of 62 cm. The ranges and relative intensities of the resolved groups, together with the reaction energies corresponding to the different ranges (obtained by allowing for the deuton energy and the recoil of the product nucleus), are summarized in Table I. The reaction energy of 5.3 mv presumably corresponds to the case in which the product nucleus is left in its lowest state, while in the others it is left in various excited states, with energies given by the differences in reaction energies. These excited nuclei should give rise to gamma-rays, evidence for which has been found by McMillan.[18]

TABLE I. *Proton ranges from radioactive aluminum.*

Range (cm)	Relative intensity	Reaction energy (mv)
10	7	0.6
21	6	1.8
30	1	2.9
53	0.8	4.6
62	—	5.3

YIELD OF PROTONS

The total number of disintegration protons can be found by integrating the curve of Fig. 5, using as unit abscissa interval the estimated half-width of a sharp proton peak, namely 2 cm. Such an integration, making a reasonable extrapolation to zero range, showed that there are 8 protons emitted in all directions per 10^7 deutons (of 2.2 mv energy) striking the target. The yield of radioactive atoms was found to be 3 per 10^7 deutons at 1.9 mv, a number which is in good agreement with the proton yield when the change in the reaction probability between 1.9 and 2.2 mv is allowed for. This gives further support to the view that the protons and the radioactivity arise from the same nuclear reaction.

NEUTRONS

The neutron background previously mentioned arises partly from the target and partly from other parts of the apparatus. It was investigated

[18] E. McMillan, Phys. Rev. **46**, 868 (1934).

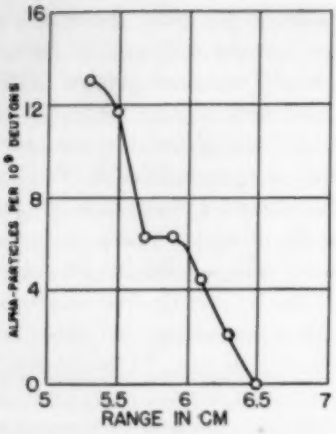

FIG. 7. Absorption curve of the alpha-particles from a thick Al target bombarded with deutons.

more carefully by placing a sheet of paraffin in front of the counter, and observing the number of counts with a thick Al target, and then with an inactive target in place. It was found that the counting rate was doubled by putting in the Al target. The total yield of neutrons from the Al calculated on the assumption that one per thousand traversing the counter was recorded, was 2 per 10^7 deutons. The reaction concerned is probably:

$$Al^{27}+D^2\rightarrow Si^{28}+n. \qquad (4)$$

ALPHA-PARTICLES

The counting circuit can be adjusted so as to record alpha-particles but not protons, and when this was done it was found that a few counts were still observed at short ranges. In this experiment the deuton current was made very small (0.007 μA) in order to avoid operation of the counter by the "piling up" of proton impulses, and the variation in range was obtained by moving the counter. The results, shown in Fig. 7, have been corrected for the variation in solid angle and are expressed in terms of the total number of alpha-particles emitted in all directions. The "step" in the curve was found in two separate runs, and is probably real.

Thus there appear to be two weak groups of alpha-particles, of ranges 5.7 and 6.5 cm, corresponding to reaction energies of 5.9 and 6.6 mv, respectively. The yield is about 6 per 10^9 deutons for each group, of the order of 1/100 as great as the proton yield. The reaction giving rise to the alpha-particles is:

$$Al^{27}+D^2\rightarrow Mg^{25}+He^4. \qquad (5)$$

EFFECTS WITH PROTON BOMBARDMENT

By admitting ordinary hydrogen to the apparatus instead of deuterium, a beam of hydrogen molecular ions (of course contaminated with a few deutons) was obtained. The proton energy in this case was 1.1 mv. By using a large current, a weak alpha-particle group was observed of the same range as found under deuton bombardment, accompanied by neutrons and fast protons, all in the same proportions as found with deutons. These effects were of a magnitude such as to be accounted for by a deuton contamination of one per two thousand protons. There is little doubt that this is the explanation, and that the protons themselves produce no appreciable number of disintegrations.[16]

ATOMIC MASSES

None of the masses concerned in any of the above reactions is known accurately from mass-spectrographic data, so that only differences can be computed. Assuming that the largest reaction energy in each case corresponds to the process which leaves the product nucleus in its normal state, and taking $H^1=1.0078$, $D^2=2.0136$, $He^4=4.0022$, we get:

From Eq. (2), $Al^{28}=Al^{27}+1.0001$;

From Eq. (5), $Al^{27}=Mg^{25}+1.9957$.

ACKNOWLEDGMENTS

The authors wish to thank Dr. M. Stanley Livingston for his collaboration in some of the radioactive work done while he was still in Berkeley. They also express their appreciation for the financial support given by the Research Corporation and the Chemical Foundation.

[16] In the early experiments of M. S. Livingston and E. O. Lawrence (Phys. Rev. **43**, 369, 1933) the Geiger-counter observations of the radiations from Al bombarded by protons which were thought to be alpha-particles, were doubtless due to soft x-rays.

Band Systems of MgCl, CaCl and SrCl

ALLAN E. PARKER, *Columbia University*

(Received December 7, 1934)

A vibrational analysis has been made of band systems due to MgCl, CaCl and SrCl. There are two systems due to MgCl with $\nu_E^* = 26{,}441.5$, $\omega' = 474.8$ and $\omega'' = 447.4$ for the more intense system and $\nu_E = 25{,}887.2$, $\omega' = 466.9$ and $\omega'' = 447.4$ for the less intense system. CaCl has three extensive systems with $\nu_E = 16{,}093.5$, $\omega' = 367.1$, $\omega'' = 364.5$; $\nu_E = 16{,}850.6$, $\omega' = 361.0$, $\omega'' = 364.0$; $\nu_E = 26{,}498.9$, $\omega' = 336.0$, $\omega'' = 368.3$, respectively. There are also three weakly developed systems. Two strong systems of SrCl are observed with the respective constants $\nu_E = 15{,}716.9$, $\omega' = 306.3$, $\omega'' = 301.6$ and $\nu_E = 25{,}245.5$, $\omega' = 280.4$, $\omega'' = 300.6$. SrCl has three poorly defined systems as well. The isotope effect due to Cl^{35} and Cl^{37} is observed in all transitions.

The rotational structure is partially resolved for most systems, and in the ultraviolet CaCl bands sufficiently to estimate that $B' = 0.24$ and $B'' = 0.26$. The electronic states and dissociation products are discussed. All values are expressed in cm^{-1}.

INTRODUCTION

THE existence of many of the bands whose analysis is recorded here, has been known for a considerable time. Olmsted[1] photographed a number of them and Mecke[2] using his data made an analysis of certain of these. Walters and Barratt[3] photographed the bands of MgCl, CaCl and SrCl in absorption using a prism instrument, but made no attempt at analysis. Hedfeld[4] has analyzed the visible CaCl and SrCl bands using spectrograms taken in the first order of a twelve-foot grating.

No analysis has been reported previously of the MgCl bands. While analyzing these it seemed worth while to investigate the bands of CaCl and SrCl as well, improving the measurements and thereby the accuracy of the analyses.

EXPERIMENTAL PROCEDURE

The SrCl, CaCl and MgCl bands were excited by means of an arc between a water-cooled nickel anode and a copper cathode in the form of a cup, the cup containing the anhydrous chloride whose diatomic spectrum it was desired to investigate. The arc current varied from 5–8 amperes with a 220 volt d.c. main. The arc was operated in a bulb containing helium, nitrogen or hydrogen at a pressure of 5–10 cm of mercury. Hydrogen was found to be the most suitable gas. The majority of the spectrograms were taken in the first and second orders of the twenty-one foot grating of Yale University, which is in a stigmatic mounting, giving a dispersion in the second order ranging from 2.2A/mm to a 2.5A/mm depending on the spectral region. Certain plates of CaCl were taken in the second order of the twenty-one foot grating of Columbia University which is in an astigmatic mounting and whose dispersion for the region and order investigated is 1.3A/mm.

The visible bands were photographed on Eastman hypersensitive panchromatic plates with the addition that the red SrCl band was also photographed on Eastman I-C plates. The ultraviolet bands were photographed on either Eastman 33 or Eastman 40 plates. The exposure times were of the order of fifteen minutes for the visible bands and several hours for the ultraviolet bands. An iron comparison spectrum was placed on each spectrogram.

The spectrograms were measured on the comparator of New York University, and I wish to thank Professor E. O. Salant for the opportunity of using it.

MgCl BANDS

The existence of bands in the ultraviolet due to MgCl was reported by Olmsted.[1] The bands have two heads and degrade to the violet. We can therefore assign them as the P_1 and P_2 heads of a $^2\Sigma - {}^2\Sigma$ or a $^2\Pi - {}^2\Pi$ transition. The $\Delta v = 0, \pm 1, \pm 2$ sequences are observed. The positions of the heads of the $MgCl^{35}$ band are

* $\nu_E = \nu_{\text{head}}^{(-1/2,\,-1/2)}$

[1] C. M. Olmsted, Zeits. f. wiss. Phot. **4**, 255, 293 (1906).
[2] R. Mecke, Zeits. f. Physik **42**, 390 (1927).
[3] O. H. Walters and S. Barratt, Proc. Roy. Soc. **A118**, 120 (1928).
[4] K. Hedfeld, Zeits. f. Physik **68**, 610 (1931).

TABLE I. *Vibrational assignments of the P_1 and P_2 heads of MgCl.*

$v'-v''$	+1		0		−1		−2	
v''	P_2	P_1	P_2	P_1	P_2	P_1	P_2	P_1
0	26963.4	26958.0	26477.6	26455.0				
1	84.0		516.3	503.2	26033.6	26019.4		
2	27003.9	98.3	40.7	33.1	75.1	57.3		
3	23.0	27016.9	65.5	57.8	103.3		25643.3	25625.7
4	40.5	35.1	87.5	81.3	28.2	118.4	66.6	58.0
5	56.8	50.7	609.2	604.7	49.4		87.3	
6	75.3	68.8	27.3					
7	91.5		45.6					
8	104.8	99.0						

given in Table I, the $\Delta v=+2$ sequence being omitted as these bands were too weak for accurate measurements. From the $\Delta G(v)$ values given in Table II the following equation is set up:

$$\nu=26441.5+[474.8(v'+\tfrac{1}{2})-2.5(v'+\tfrac{1}{2})^2]-[447.4(v''+\tfrac{1}{2})-1.6(v''+\tfrac{1}{2})^2].$$

A noticeable feature of these bands is the fact that bands involving the $v'=0$ level are markedly shifted from their normal position. This is doubtless due to a perturbation which has a maximum value at the head of the band. Further perturbations though not of the same magnitude exist in the $v'=7$ level and possibly $v'=8$ as well. Bands due to $MgCl^{37}$ are observed in the appropriate positions.

Besides the bands comprising this system, three others of quite appreciable intensity were observed whose frequencies are: 25,896.1 cm^{-1}, 25,915.1 cm^{-1} and 25,932.8 cm^{-1}. The assumption can be made that they are the (0,0), (1,1) and (2,2) bands, respectively, of a weaker MgCl system. Assuming that the final state is common to both systems we can fit them to the equation

$$\nu=25,887.2+[466.9(v'+\tfrac{1}{2})-2.3(v'+\tfrac{1}{2})^2]-[447.4(v''+\tfrac{1}{2})-1.6(v''+\tfrac{1}{2})^2].$$

The bands observed by Querbach[5] in the region of 7800–8100A, which he thought might be attributed to MgCl, were sought by using Eastman I-N plates but the bands were not observed.

TABLE II. *Average $\Delta G(v)$ values for the X and B states of MgCl.*

v	0	1	2	3	4	5	6	7
X	445.6	442.3	438.0	435.9	431.3	429.5	429.7	
B	484.3	467.2	462.7	458.4	453.0	447.6	448.1	445.9

[5] J. Querbach, Zeits. f. Physik **60**, 109 (1931).

CaCl Bands

CaCl has a number of band systems and of these three are well developed. Two systems in the red are observed with the $\Delta v=0, \pm1$ sequences and one system in the ultraviolet with the $\Delta v=0, \pm1, \pm2, \pm3$ sequences. The band system furthest to the red degrades to the violet and has four heads. Hence it is a $^2\Sigma$, $^2\Pi$ transition and the head-forming branches are the P_1, Q_1, P_2 and Q_2 branches. Table III lists the heads of this system due to $CaCl^{35}$. Several bands not recorded by Hedfeld[4] are observed in the $\Delta v=\pm1$ sequences and therefore his (v', v'') assignments must be increased. Table IV contains the average $\Delta G(v)$ values for both Q branches. The equations obtained for the Q heads are:

$$\nu=16,093.5+[367.1(v'+\tfrac{1}{2})-0.91(v'+\tfrac{1}{2})^2]-[364.5(v''+\tfrac{1}{2})-0.80(v''+\tfrac{1}{2})^2],$$

$$\nu=16,164.0+[355.3(v'+\tfrac{1}{2})-0.45(v'+\tfrac{1}{2})^2]-[352.6(v''+\tfrac{1}{2})-0.33(v''+\tfrac{1}{2})^2].$$

Besides this system there is another system in the red as reported by Hedfeld, and our measurements agree with his for the most part. Each band has but a single head and hence we are led to assume that the system is a $^2\Sigma-{}^2\Sigma$ or a $^2\Pi-{}^2\Pi$ system with the same doublet splitting in both states. As the bands degrade to the violet, the heads are due to the P_1 and P_2 branches. The positions of the heads are recorded

TABLE III. *Vibrational assignments of the P and Q heads of the $A-X$ $CaCl^{35}$ bands.* The subscripts should be interchanged for this and subsequent band systems if the lower state is a $^2\Pi$ state instead of a $^2\Sigma$ state.

$v'-v''$	+1			0				−1			
v''	Q_1	P_2	Q_2	P_1	Q_1	P_2	Q_2	P_1	Q_1	P_2	Q_2
0	16452.0	16493.8	16509.9	16062.5	16094.8	16141.8	16164.3				
1	54.2	98.7	13.7	64.1	97.3	44.1	66.9	15704.7	15722.1	15782.0	15803.2
2	56.4	502.4	16.7	65.9	99.6	46.4	69.3	10.5	27.8	87.2	08.2
3	58.2	05.9	19.6	67.5	101.8	47.3	71.3	15.3	33.1	91.7	12.8
4	59.7		21.9	68.6	03.8		73.2	19.9	38.4	96.2	17.5
5	60.7		24.3	69.5	05.6		74.8	24.3	43.3	800.6	21.7
6	61.6		26.3	70.1	07.0		76.1	27.8	48.3	04.5	25.4
7	62.1		28.1		08.2		76.8	32.1	52.2	08.2	
8			29.5				78.1	35.6	56.3		
9			30.8				78.8	42.0	60.1		
10			31.7						63.7		
11			32.4						66.9		
12									69.9		
13									72.6		
14									75.0		
15									77.3		

TABLE IV. *Average $\Delta G(v)$ values for the Q heads of the $A-X$ $CaCl^{35}$ transition.*

	X		A	
v	Q_1	Q_2	Q_1	Q_2
0	363.7	352.1	366.2	354.7
1	362.1	351.6	364.1	354.0
2	360.6	350.9	362.8	353.0
3	358.9	350.1	360.9	352.2
4	357.3	349.3	359.1	350.9
5	355.5	348.8	357.0	350.1
6	354.1		355.3	

TABLE V. *Vibrational assignments of the P heads of the $B-X$ $CaCl^{35}$ bands.*

$v'-v''$	+1	0	−1
v''	P	P	P
0	17207.0	16847.5	
1	00.0	43.3	
2	192.6	39.7	
3	84.6	35.7	16478.9
4	77.3	31.3	75.2
5	68.0	26.6	71.6
6	58.6	21.5	67.4
7		16.2	
8		10.5	
9		04.5	
10		798.0	
11		91.4	
12		84.2	
13		76.6	
14		68.5	
15		59.3	
16		51.5	

in Table V for $CaCl^{35}$. In Table VI are given the values of $\Delta G(v)$ from which the following equation is derived for the heads:

$$\nu = 16{,}850.6 + [361.0(v'+\tfrac{1}{2}) - 1.2(v'+\tfrac{1}{2})^2] - [364.0(v''+\tfrac{1}{2}) - 1.0(v''+\tfrac{1}{2})^2].$$

In the ultraviolet there is a system of CaCl bands observed by Olmsted.[1] These bands exhibit four heads degrading to the red. These must be the R_1, Q_1, R_2 and Q_2 heads of a transition between a $^2\Sigma$ and a $^2\Pi$ state. The vibrational assignments for these bands are given in Table VII for the $CaCl^{35}$ molecule. The $\Delta G(v)$ values are recorded in Table VIII. By means of these we arrive at the following equation to represent the stronger Q heads

$$\nu = 26{,}498.9 + [336.0(v'+\tfrac{1}{2}) - 1.4(v'+\tfrac{1}{2})^2] - [368.3(v''+\tfrac{1}{2}) - 1.5(v''+\tfrac{1}{2})^2].$$

TABLE VI. *Average $\Delta G(v)$ values for the $B-X$ $CaCl^{35}$ bands.*

v	0	1	2	3	4	5
X			358.9	356.9	355.3	352.9
B			354.9	352.5	350.5	347.8

The most interesting feature of these bands is that the rotational structure is particularly open. In fact as will be discussed later estimates can be made of B' and B''.

TABLE VII. *Vibrational assignments of the R and Q heads of the C−X $CaCl^{35}$ bands.*

v'	v''	0	1	2	3	4	5	6
0	R_2	26563.5						
	Q_2	26558.8	26191.8					
	R_1	26486.5						
	Q_1	26482.8	26115.4	25750.5				
1	R_2							
	Q_2	26893.4		26161.1	25793.6			
	R_1	26820.9				25368.8		
	Q_1	26816.4	26451.0	26084.5	25715.6	25364.2		
2	R_2		26856.7					
	Q_2	27216.6	26852.3					
	R_1		26785.2					
	Q_1	27141.1	26780.7	26419.7	26059.3	25694.1	25330.6	
3	R_2		27185.9	26820.9				
	Q_2		27183.8	26816.4				
	R_1	27460.1	27111.4					
	Q_1	27457.4	27108.7			26024.5	25667.0	
4	R_2							
	Q_2							
	R_1							
	Q_1			27073.1	26718.4		26003.7	25636.1
5	R_2							
	Q_2							
	R_1							
	Q_1				27040.8			
6	R_2							
	Q_2							
	R_1				27358.3			
	Q_1				27354.7			

Besides these well-developed systems there are several fragmentary systems. Walters and Barratt[3] observed CaCl bands in the ultraviolet beyond the system last mentioned. These bands were very weak in absorption and such was found to be the case in emission. Table IX gives the position of what is apparently the $\Delta v=0$ sequence of a group of single-headed bands arising from a $^2\Sigma-{}^2\Sigma$ or a $^2\Pi-{}^2\Pi$ transition with the same or negligible separations of the substates. For $v=2$, 8, 9 and 10, two heads are observed. This is probably due to perturbations in the upper state. There are a few additional weak bands in the region from 31,000 cm^{-1} to 33,000 cm^{-1} but not sufficient to form any definite sequence.

In the neighborhood of the red bands, there are two groups of weak bands comprising portions of two additional systems. One group apparently consists of two branches of a single sequence. The positions of these bands are given

TABLE VIII. *Average $\Delta G(v)$ values for the C−X $CaCl^{35}$ transition.*

v	0	1	2	3
X	360.6	364.1	361.3	358.4
C	334.4	332.2	326.7	

TABLE IX. *Vibrational assignments of the far ultraviolet $CaCl^{35}$ bands.* An atomic line partially obscures the (6,6) head.

v		
0	33685.6	
1	78.3	
2	68.2	64.9
3	52.7	
4	43.1	
5	31.7	
6	20.3	
7	07.7	
8	595.2	90.3
9	85.5	81.6
10	65.2	58.2
11	52.3	

TABLE X. *Additional weak bands of CaCl.*

16392.3	16408.9	15646.9
93.2	09.8	47.4
94.2	11.1	48.0
96.0	13.0	48.7
97.5	15.0	49.7
	16.7	50.6
	18.9	
	20.8	

in Table X. The small separation between the heads of the sequence shows that the ω values of the states involved are quite comparable. Another group of bands of similar spacing is also observed and likewise recorded in Table X. However these two groups cannot be related to one another except as the components of a $^2\Sigma$, $^2\Pi$ transition, for the separation between the two lowest bands bars the possibility of their being different sequences of the same system.

SrCl Bands

SrCl gives rise to two intense band systems one in the red and one in the ultraviolet. The red bands for which the $\Delta v = 0, \pm 1 + 2$ sequences are observed, exhibit four heads, P_1, Q_1, P_2 and Q_2. Table XI lists the bands of this system due to $SrCl^{35}$. From the $\Delta G(v)$ values in Table XII, we obtain the following equations for the heads of the Q branches:

$$\nu = 15{,}109.5 + [302.6(v'+\tfrac{1}{2}) - 0.82(v'+\tfrac{1}{2})^2] - [296.7(v''+\tfrac{1}{2}) - 0.93(v''+\tfrac{1}{2})^2],$$

$$\nu = 15{,}716.9 + [306.3(v'+\tfrac{1}{2}) - 0.76(v'+\tfrac{1}{2})^2] - [301.6(v''+\tfrac{1}{2}) - 0.63(v''+\tfrac{1}{2})^2].$$

The ultraviolet bands contain some members of the $\Delta v = 2$ sequence as well as the $\Delta v = 0, \pm 1$ sequences. These bands degrade to the red and the four R_1, Q_1, R_2 and Q_2 branches form heads. These are listed in Table XIII for $SrCl^{35}$ and the $\Delta G(v)$ values in Table XIV. The following equations may be deduced for the Q heads:

$$\nu = 25{,}245.5 + [280.4(v'+\tfrac{1}{2}) - 0.56(v'+\tfrac{1}{2})^2] - [300.6(v''+\tfrac{1}{2}) - 0.78(v''+\tfrac{1}{2})^2],$$

$$\nu = 25{,}401.7 + [279.3(v'+\tfrac{1}{2}) - 0.80(v'+\tfrac{1}{2})^2] - [298.9(v''+\tfrac{1}{2}) - 1.3(v''+\tfrac{1}{2})^2].$$

In addition to these bands several fragmentary systems are observed in the region of the red transition. These scattered sequences are apparently portions of three additional band systems. The positions of the various heads are given in Table XV for the best developed group.

TABLE XI. *Vibrational assignments of the $A - X$ $SrCl^{35}$ bands.* As remarked above, the subscripts must be interchanged if the ground state is the $^2\Pi$ state.

$v'-v''$	+1		0		−1		−2
v''	Q_1	Q_2	Q_1	Q_2	Q_1	Q_2	Q_1
0	15420.6	16028.6	15115.3	15721.6			
1	25.1	30.4	22.5	26.5	14821.8	15422.1	
2	29.6	32.9	29.3	30.8	28.7	27.1	14529.2
3	33.8	34.6	36.0	35.1	35.6	31.8	38.9
4	39.8	36.5	42.6	39.0	42.7	36.5	48.1
5	42.4	38.4	48.9	43.1	49.4	41.0	56.4
6		39.9	55.6	46.9	55.9	45.2	
7		41.5		50.3	62.5	50.1	70.0
8		43.0				55.2	
9						59.2	
	P_1	P_2	P_1	P_2	P_1	P_2	
0	15401.5	16007.6	15101.2	15712.8			
1	06.4	09.9	07.2	17.3	14797.7	15401.5	
2	11.2	12.7		21.6	804.6	06.4	
3	16.0	15.0		25.6	11.8	11.2	
4		17.0		29.6	18.6	16.0	
5		18.8		33.4			
6		20.4		37.2			
7		22.0					

TABLE XII. *Average $\Delta G(v)$ values for the Q heads of the $A-X$ $SrCl^{35}$ transition.*

	X		A	
v	Q_1	Q_2	Q_1	Q_2
0	300.8	295.8	305.8	301.8
1	299.5	294.1	303.8	300.0
2	298.4	292.4	302.7	298.4
3	297.1	290.3	301.0	296.9
4	295.7		299.8	
5	294.7		298.5	
6	293.2		296.6	

Here we appear to have two sequences of a system, presumably the $\Delta v=0$, -1 sequences, which forms but one head. Besides these there are two groups, listed in Table XV, which cannot be correlated with each other or with the stronger group. One of these groups is single-headed and the other double-headed. The positions of the bands, the magnitudes of the separations between the bands of a sequence or the increase or decrease in the values of these separations prohibit the correlation of these groups either with one another or with the strong band system in this region. The fact that Walters and Barratt failed to observe them in absorption may be due to their low intensity or to the fact that the lower state of these bands is not the ground state of the SrCl molecule.

CaCl Rotational Structure

With few exceptions all the bands whose analysis is given above exhibit partially resolved rotational structure. In the near ultraviolet CaCl system, the rotational structure was more completely resolved than in any of the other band systems. The rotational structure of the (0,0) band was especially noticeable as the two P branches are completely resolved to the origin which is quite remarkable for a molecule both of whose atoms have atomic weights of this magnitude. A number of weak lines associated with the P_1 and P_2 lines of high J value are of the appropriate intensity for lines due to $CaCl^{37}$

TABLE XIII. *Vibrational assignments of the $B-X$ $SrCl^{35}$ bands with subscripts provisionally indicated.*

$v'-v''$	+1		0		−1		−2
v''	Q_2	Q_1	Q_2	Q_1	Q_2	Q_1	Q_2
0	25673.5	25514.8	25392.0	25235.5			
1	52.7	494.1	72.8	15.3	25097.3	24934.8	
2	30.9	72.4			80.7	16.4	
3	12.0	52.1			57.2	898.9	
4		32.2			40.5	80.7	
5					22.6	63.1	24747.6
6						45.7	32.8
7							17.9
8							03.1
9							689.0
10							74.5
11							60.5
12							46.6
	R_2	R_1	R_2	R_1	R_2	R_1	R_2
0	25678.5	25520.6	25396.9	25240.2			
1	58.5	498.7	78.1	20.3	25102.5	24940.5	
2	37.8	77.2			085.8	22.2	
3	16.8	55.6			63.3	04.1	
4					46.2	886.0	
5					30.1	68.5	24754.4
6					13.1	50.7	
7							
8							
9							
10							681.6

TABLE XIV. *Average $\Delta G(v)$ values for the Q heads of the $B-X$ $SrCl^{35}$ transition.*

	X		B	
v	Q_1	Q_2	Q_1	Q_2
0	297.7	300.1	278.5	279.9
1	292.1	299.0	279.9	278.8

and they are in the appropriate position for these lines. The P_1 and P_2 lines for both $CaCl^{35}$ and $CaCl^{37}$ are given in Table XVI. The fact that the bands have four heads indicates that they are due to a transition between a $^2\Sigma$ and a $^2\Pi$ state. We may estimate the values of B' and B'' in the following manner. For such a transition, the separation of the P lines near the origin is approximately $B'+B''$. The separations of the heads of the R branches from their respective origins is given by the expression

$$\nu(R_{\text{head}}) = -(B'+B'')^2/4(B'-B'').$$

By means of these two relationships we can deduce that:

$B''=0.26$ cm^{-1} $\quad$ $B'=0.24$ cm^{-1}
$I''=106(10)^{-40}$ g cm $\quad$ $I'=115(10)^{-40}$ g cm
$r''=1.86(10)^{-8}$ cm $\quad$ $r'=1.93(10)^{-8}$ cm
$\omega r^3=2340$ cm^2 $\quad$ $\omega r^3=2430$ cm^2.

The values of B'' and B' are the average of the values obtained from the sub-ones and the sub-twos. An approximate value of A can be secured from the separation of the lowest P lines, assuming negligible splitting in the $^2\Sigma$ state. On this basis A is 77.4 cm^{-1}. Hence $Y=|A|/B$ is 310 and we see that the $^2\Pi$ state is close to case a.

ELECTRONIC STATES

In Table XVII the following constants: ν_E, A^*, ω_h, $x_h\omega_h$, r, D and $\nu_E+D'-D''$ are collected for the various alkaline-earth chlorides. A^* represents the separation of the two substates as determined from the separation of the two (0,0) bands and is not the true A value unless one of the electronic states involved has negligible doubling. The values of r are estimated from the empirical relationship that ωr_e^3 is approximately 3000. The values of Fredrickson and Hogan[6] for BeCl are included in this table as are the values of the writer[7] for BaCl. The bands of BeCl previously reported in an abstract[8] have since been found to be spurious. From the work of Walters and Barratt we know that the bands,

[6] W. R. Fredrickson and M. E. Hogan, Jr., Phys. Rev. **46**, 454 (1934).
[7] A. E. Parker, Phys. Rev. **46**, 31 (1934).
[8] A. E. Parker, Phys. Rev. **45**, 752 (1934).

TABLE XV. *Additional weak bands of SrCl.* The two missing heads in the first sequence are due to superposed atomic lines. The first two sequences may be correlated with the v numbering shown.

$v'-v''$	+1	0	P	P	P
v''	P	P			
0	16164.5	15470.8	16469.4	16475.1	16846.9
1	67.0	75.3	50.5	55.2	43.4
2	69.4	79.4	31.8	34.7	39.7
3	71.8	83.3	14.5	17.0	35.3
4	73.2	86.9	398.3	02.6	31.1
5	74.9	90.5	85.3	389.7	26.0
6	76.1	94.1			21.2
7		97.7			15.5
8		501.0			10.0
9		04.1			804.0
10					797.7
11		10.4			90.9
12		14.1			
13		16.8			
14		19.7			
15		22.6			
16					
17		27.7			
18		30.5			

TABLE XVI. *Rotational assignments of the P lines of the (0,0) band of the near ultraviolet C−X CaCl system. M* is used as the quantum number since the proper *J* values cannot be determined.

	P_1		P_2			P_1		P_2	
M	$CaCl^{35}$	$CaCl^{37}$	$CaCl^{35}$	$CaCl^{37}$	*M*	$CaCl^{35}$	$CaCl^{37}$	$CaCl^{35}$	$CaCl^{37}$
0	26473.43		26550.76		35	26440.30	26442.08	26521.58	
1	72.91		50.26		36	39.08		20.46	
2	72.38		49.72		37	37.84		19.29	
3	71.80		49.12		38	36.60		18.08	
4	71.09		48.55		39	35.19		16.86	
5	70.36		47.93		40	33.83		15.55	
6	69.68		47.35		41	32.46		14.36	
7	68.92		46.72		42	31.04		13.07	
8	68.27		46.09		43	29.66	31.79	11.78	
9	67.58		45.40		44	28.18	30.31	10.52	
10	66.80		44.69		45	26.74	28.84	09.13	
11	65.97		43.97		46	25.32	27.37	07.91	
12	65.30		43.23		47	23.77	25.87	06.59	
13	64.37		42.47		48	22.27	24.43	05.12	
14	63.50		41.71		49	20.75		03.78	26505.82
15	62.72		40.99		50	19.22	21.52	02.32	04.38
16	61.74		40.17		51			00.92	
17	60.95		39.35		52			499.55	00.55
18	58.86		38.51		53			97.97	
19	57.91		37.65		54			96.43	498.56
20	57.19		36.78		55			95.00	97.09
21	56.17		35.88		56			93.48	95.58
22	55.23		34.98		57			92.11	
23	54.08		34.01		58			90.42	
24	53.02		33.10		59			88.87	91.18
25	52.01		32.15		60			87.08	89.57
26	50.95		31.21		61			85.81	88.13
27	49.65		30.20		62			84.08	
28	48.28	26450.17	29.16		63			82.40	
29	47.19	48.74	28.18		64			80.75	
30	46.34		27.11		65			79.22	
31	45.27		26.08		66			77.60	
32	44.12		24.94		67			76.15	78.09
33	42.87		23.87		68			74.69	76.71
34	41.56		22.72		69			72.91	75.62

other than BeCl, involve the ground state of the molecule as they appear in absorption. Now Hedfeld has advanced the hypothesis that the ground state is a $^2\Pi$ state, on the basis of a comparable doublet separation of certain of the bands of particular molecules. This agreement is found in the case of only one chloride, CaCl, as is readily seen from Table XVII. BeCl and SrCl are represented by transitions between $^2\Sigma$ states and $^2\Pi$ states and it is impossible to decide which of these is the ground state. The bands of MgCl are either $^2\Sigma-^2\Sigma$ or $^2\Pi-^2\Pi$ transitions and here too no decision may be reached. In the case of BaCl which was discussed previously[7] the assignment of the lower state as a $^2\Sigma$ state may be made on the basis of the fact that the ultraviolet bands are a single-headed transition and hence are either a $^2\Sigma-^2\Sigma$ or a $^2\Pi-^2\Pi$ transition. If the latter is the case it would be extremely fortuitous if the *A* constants of the two states were identical as would be necessary for the production of a single-headed band system. However negligible spin-doubling of the $^2\Sigma$ states is to be expected and on this basis the assignments in reference 7 were made. The approximate agreement of the doublet separation of the ultraviolet CaCl bands and the $A-X$ red CaCl bands makes Hedfeld's hypothesis feasible for this molecule. But the single-headed $B-X$ CaCl bands must then be explained as a $^2\Pi-^2\Pi$ transition with identical *A* values for the two states which seems dubious.

TABLE XVII. *Constants of the alkaline-earth chlorides.* All values are expressed in cm^{-1} with the exceptions that r is expressed in Angstroms and that the atomic excitation, $\nu_E+D'-D''$ is also given in volts. A* represents the doublet separation of the bands.

	State	ν_E	A^*	ω_e	$x_e\omega_e$	r	D	$\nu_E+D'-D''$	
	A	27970.5		824.2	6.0	1.5	28,100	21,000	2.59
BeCl	X			846.6	5.1	1.5	35,100		
	B	26441.5	22.6	474.8	2.5	1.9	23,000	18,200	2.25
	A	25887.2		466.9	2.3	1.9	21,700	16,300	2.02
MgCl	X			447.4	1.6	1.9	31,300		
	D	33689		357					
	C	26498.9	76.0	336.0	1.4	2.1	20,200	23,600	2.91
	B	16850.6		361.0	1.2	2.0	27,400	11,600	1.45
	A	16093.5	70.5	367.1	0.91	2.0	37,000	11,800	1.46
				368.3	1.5	2.0	23,100		
				364.0	1.0	2.0	32,600		
CaCl	X			364.5	0.80	2.0	41,300		
	B	25245.5	156.3	280.4	0.56	2.2	22,500	18,800	2.32
	A	15716.9	607.4	306.3	0.76	2.1	30,800	7,400	0.91
				300.6	0.78	2.1	28,900		
SrCl	X			301.6	0.63	2.1	39,100		
	C	27097.3		311.5	0.93	2.1	25,500	34,600	4.27
	B	25496.9		304.6	1.04	2.1	22,300	29,800	3.68
	A	19450.1	387.2	285.0	0.79	2.2	15,800	16,800	2.08
				278.8	0.75	2.2			
				279.1	0.78	2.2			
BaCl	X			280.5	0.80	2.2	18,000		

DISSOCIATION PRODUCTS

The question of dissociation products is one of particular interest. The molecules whose constants are listed in Table XVII are all alkaline-earth chlorides. The lowest states of the Cl atom are the $(3p)^5\ ^2P_{1/2,\,3/2}$ levels whose separation is 0.11 volt. The next lowest state of Cl is 9 volts higher. So we see that the atomic excitation differences, given by $\nu_E+D'-D''$ in Table XVII represent the excitation of the alkaline-earth atom. Now the accurate determination of this quantity depends on several facts. First there is the question of the effect of higher power terms in the expression for $G(v)$ which will certainly cause a decrease in D. This effect is to some extent minimized as the decrease in both states may make the relative change smaller. This might be expected to be the case for states such as those under consideration here. Then there is the question of the accuracy of the determination of $x_e\omega_e$. The dissociation energy is quite sensitive to small changes in $x_e\omega_e$ and so our values of the atomic excitation will be in error from this cause as well. Hence definite assignments of dissociation products cannot be made but estimates may be given.

Fredrickson and Hogan have correlated the excitation of the Be atom resulting from the dissociation of the two states of BeCl with the $(2s)(2p)\ ^1P$ and $(2s)(3d)\ ^1D$ levels of Be. These levels are separated by 2.70 volts. But this assignment is open to considerable question as they have since informed me by private communication. For equally good agreement between atomic and molecular values may be obtained by using the separation of the $(2s)^2\ ^1S$ and $(2s)(2p)\ ^3P$ states which is 2.70 volts or the separation of the $(2s)(2p)\ ^3P$ and $(2s)(2p)\ ^1P$ states which is 2.54 volts.

For the MgCl molecule it seems probable that the two excited states give rise to the same dissociation products. The best agreement with atomic spectra is the separation of the $(3s)(3p)\ ^3P$ and the $(3s)(3p)\ ^1P$ which lies 1.63 volts above it. The ground state of Mg is a $(3s)^2\ ^1S$ state and it lies 2.69 volts below the $(3s)(3p)\ ^3P$ state. It seems more probable that the molecular value is too high as a greater effect is to be expected for the higher order terms in the $G(v)$ equation for the excited state than for the ground state. Hence it seems probable that the first of the two possibilities is the correct one.

In the case of CaCl and of SrCl, no definite assignments may be made, while for BaCl this has been discussed previously[7] with the conclusion that the ground state of BaCl does not dissociate into a Ba atom in its ground state and that the probable products of the X and A states of BaCl are, respectively, $(6s)(5d)\,{}^1D$ and $(6s)(6d)\,{}^1D$ states of Ba.

For both MgCl and BaCl it seems likely that the ground state gives rise upon dissociation to an excited Mg and Ba atom, respectively. From the spectra of CaH, SrH and BaH, we know that the dissociation of these molecules gives rise to an excited atom. And by analogy we may assume that the same is true for CaCl and SrCl. Finally we may arrive at the conclusion that an atom in a ground $(ns)^2\,{}^1S$ state will not in general form a stable molecule. This fact has been previously discussed by Lessheim and Samuels[9] and others.

The author wishes to thank Professor L. W. McKeehan for the opportunity of using the facilities of the Physics Laboratory of Yale University, where most of the spectrograms were obtained. The advice and interest of Professor W. W. Watson are also gratefully acknowledged.

[9] H. Lessheim and R. Samuels, Zeits. f. Physik **84**, 637 (1933).

MARCH 1, 1935 PHYSICAL REVIEW VOLUME 47

The Band Spectra of the Hydrides of Lithium

Part I: $Li^{(7)}D$

F. H. CRAWFORD AND T. JORGENSEN, JR., *Physics Research Laboratory, Harvard University*

(Received December 28, 1934)

The $^1\Sigma \rightarrow {}^1\Sigma$ spectrum of LiD has been photographed in absorption in the second order of a 21-foot grating giving a dispersion of 1A/mm. The spectrum is a headless concourse of lines stretching from λ3200 to λ4300A. About 80 percent of the lines (over 1400 in all) have been measured and assigned to 35 two-branch bands. The initial and final double differences, Δ_2F_v' and Δ_2F_v'', for $Li^{(7)}D$ have been represented as functions of J by a semigraphical method; these represent the observed data on the average to within ± 0.023 cm^{-1} for the upper state and ± 0.019 cm^{-1} for the ground state. This gives $B_e' = 1.6060$,* $D_e' = 4.8 \times 10^{-4}$, $B_e'' = 4.2338$ and $D_e'' = 2.756 \times 10^{-4}$. By using the rotational constants so determined the origins of the bands involved were computed and the values of $\Delta G'(v+\frac{1}{2})$ and $\Delta G''(v+\frac{1}{2})$ represented by least-square expressions in $(v+\frac{1}{2})$. The $\Delta G'$-values require a fifth degree polynomial while the $\Delta G''$ values are represented closely by a cubic. The corresponding expression for the origins of the whole system represents the data with an average deviation of ± 0.04 cm^{-1}. Here $\omega_e' = 183.12$, $\omega_e' x_e' = -12.741$, $\omega_e'' = 1055.12$, and $x_e'' \omega_e'' = 13.228$, with the electronic origin at $\nu_e = 26{,}512.05$. The corresponding vibrational constants for $Li^{(7)}H$ are computed from the simple isotope theory and although they differ considerably from the results of Nakamura, represent the isotope shifts within the rather large uncertainty involved. The question of possible l-uncoupling is examined and no *conclusive evidence is found for an appreciable l-uncoupling in either state of* $Li^{(7)}D$. This is contrary to the accepted interpretation of the anomalies of the spectrum.

INTRODUCTION

THE spectra of the hydrides of the alkali metals are of unique interest among diatomic spectra because of the presence of certain anomalies. If we represent the total energy, E/hc (in inverse cm), of a rotating vibrator in the usual notation[1]

$$E/hc = \nu_e + G(v) + F_v(J), \tag{1}$$

where

$$G(v) = \omega_v(v+\tfrac{1}{2}) = \{\omega_e - x_e\omega_e(v+\tfrac{1}{2}) + y_e\omega_e(v+\tfrac{1}{2})^2 + z_e\omega_e(v+\tfrac{1}{2})^3 + \cdots\}(v+\tfrac{1}{2}) \tag{2}$$

and

$$F_v(J) = B_vJ(J+1) + D_vJ^2(J+1)^2 + H_vJ^3(J+1)^3 + \cdots. \tag{3}$$

Then in a normal band spectrum certain general-

[1] Jevons, *Report on Band Spectra*, Cambridge, 1932. Here, to avoid confusion the coefficient of $J^3(J+1)^3$ in Eq. (3) has been written H_v instead of F_v.

izations can be made regarding certain of the coefficients involved. Thus the coefficients x_e, y_e, $z_e \cdots$ in Eq. (2) decrease in magnitude in this order and x_e is normally positive and of such value that as more and more vibrational energy is added the vibrational rate decreases steadily from its value for small vibrations to the necessary limit of zero at dissociation. If likewise we represent B_v, D_v and H_v as functions of $(v+\frac{1}{2})$ we have

$$B_v = B_e + \alpha_1(v+\tfrac{1}{2}) + \alpha_2(v+\tfrac{1}{2})^2 + \cdots, \quad (4)$$

$$D_v = D_e + \beta_1(v+\tfrac{1}{2}) + \beta_2(v+\tfrac{1}{2})^2 + \cdots, \quad (5)$$

$$H_v = H_e + \gamma_1(v+\tfrac{1}{2}) + \gamma_2(v+\tfrac{1}{2})^2 + \cdots, \quad (6)$$

where $|\alpha_1| \gg |\alpha_2|$, etc., and in general α_1 is negative causing B_v to *decrease* monotonically with v. Since $B_e = h/8\pi^2 cI_e$ this implies that the asymmetry of the vibrations together with the centrifugal effect of rotation causes the average of $h/8\pi^2 c\mu r^2$, where μ is the reduced mass of the molecule and r the distance between nuclei, to decrease steadily with v.

Now in the case of the $^1\Sigma \rightarrow {}^1\Sigma$ bands of the alkali hydrides, x_e' is *negative* and α_1' is *positive* so that both ω_v' and B_v' at *first* increase with v', attain maximum values (at different values of v') and thereafter decrease in regular fashion. This anomalous behavior is observed only in excited states and decreases rapidly in importance from LiH to KH. Furthermore in molecules in which the rotation does not affect the quantization of the l-vector the coefficient D_v in Eq. (3) is determined by the centrifugal stretching of the molecule. Hence as Kratzer[2] has shown for the vibrationless state it depends only on the curvature of the potential curve at the minimum, i.e.,

$$D_e = -4(B_e)^3/\omega_e^2, \quad (7)$$

a relation fairly closely verified by observation.

In the case of LiH Nakamura[3] has photographed the spectrum both in emission and absorption and carried out the analysis of the $Li^{(6)}H$ and $Li^{(7)}H$ bands. As Weizel[4] has pointed out Nakamura's results seemed to indicate that the empirically determined coefficients of $J^2(J+1)^2$ in Eq. (3) were numerically much too small compared with the coefficients of $J(J+1)$ and hence that Kratzer's relation, Eq. (7), was not even approximately true [i.e., observed values of D_e' were only half of those computed from Eq. (7)]. If this is true it would suggest that the coefficients in Eq. (2) had lost their normal mechanical significance. But as Hill and Van Vleck[5] and Dieke[6] have shown in the presence of the rotational uncoupling of the l-vector of a single p-electron in a $p-{}^1\Sigma$ state—when the uncoupling effect of rotation is *small*—we may write the rotational energy of Eq. (3) (to a constant) as

$$F(J) = XJ(J+1) + ZJ^2(J+1)^2 + \cdots, \quad (8)$$

where now X and Z have lost their purely mechanical significance. In fact

$$X = B(1-1/(Y-2)) \quad \text{and} \quad Z = D + 16B/(Y-2)^3,$$

etc., where YB gives the separation in cm^{-1} between the Π and Σ states formed from the same p-electron. Here Y is positive or negative according as the Π state is *above* the Σ state or below it. If Y is positive (and large) this causes X to be smaller than B and $|Z|$ to be smaller than $|D|$. Although of course Eq. (8) holds rigorously only for the vibrationless molecule, presumably a somewhat similar relation exists in the presence of vibration. If then as in the case of helium[6] increasing vibration increases the binding energy between the nuclear axis and l, Y should increase. Hence a Y_v might be defined which would be proportional to the separation in energy between Π and Σ levels of the same v-value. In effect therefore we should expect the empirical coefficients X_v to be of the form $(B_e+\alpha_1'(v+\frac{1}{2})+\cdots)\,[1-1/(Y_v-2)]$ where α_1' has the negative value determined by the slowly expanding molecule. If then Y_v increases sufficiently rapidly with v the second factor predominates at first causing an initial rise in X_v. Ultimately the first factor predominates and causes the ultimate fall of X_v. Using the data of Nakamura for LiH and estimating the values of

[2] Kratzer, Ann. d. Physik **67**, 127 (1922).
[3] G. Nakamura, Zeits. f. physik. Chemie **B80** (1929); Zeits. f. Physik **59**, 218 (1930). G. Nakamura and T. Shidei, Proc. Imp. Acad. Japan **7**, 303 (1930); Jap. J. Phys. **7**, 33 (1931).
[4] Weizel, Zeits. f. Physik **60**, 599 (1930).
[5] Hill and Van Vleck, Phys. Rev. **32**, 269 (1928).
[6] Dieke, Zeits. f. Physik **57**, 71 (1929).

$\alpha_1 \cdots \beta_1 \cdots$ in Eqs. (4) and (5), the authors[7] calculated the succession of Y_v values which must obtain if uncoupling were the *sole* cause of the anomalous behavior. Although the original data were taken at rather low dispersion and rather uncertain below $v'=2$ there seemed to be evidence for such a set of $^1\Pi$ levels lying only a few hundred cm^{-1} above the corresponding upper $^1\Sigma$ levels. Hence transitions from those levels should give a $^1\Pi \rightarrow {}^1\Sigma$ system overlying the known $^1\Sigma \rightarrow {}^1\Sigma$ bands.

Furthermore since the bands of LiD should give the same[8] progression of Y_v values (to within a constant of proportionality) but quite different B_v' and D_v' values, measurements on its spectrum should be of the greatest value in conjunction with more precise data on LiH.

Accordingly the present work was undertaken, the results of which will be reported in this and subsequent parts. Part I contains a summary of the data for $Li^{(7)}D$.

Experimental Procedure

For the study of the hydrides in absorption an electric furnace was constructed through which passed a steel tube whose ends were attached to short Pyrex cylinders. Several grams of pure metallic lithium were placed at the center of the tube, quartz windows attached and the system exhausted, with the metal just molten, for several hours. Then pure tank H_2 or D_2 (produced by the action of metallic calcium on samples of heavy water of 99.5 percent purity) was introduced and allowed to combine with the lithium with a sufficient excess of gas to prevent too rapid diffusion of the hydride. The same tube was never used for both gases. A parallel beam of light from a 500-watt tungsten lamp* was then passed through the heated tube and focused on the slit of a 21-foot grating (dispersion 1A/mm in the second order). A series of exposures were then made at temperatures varying from a dull red heat to about 900°C.

Eastman plates of fine grained type (Type IV–0) were employed and iron arc exposures were made before and after the hydride exposure. The iron arc exposures were of quite different intensity so that once the absence of any shift during the exposure was established, the standard lines could be measured on that exposure which gave the optimum density for precise settings. In all cases the narrowest slit widths feasible (around 0.015 mm) and the lowest temperatures sufficient to bring out the lines desired were employed. This was quite necessary because of the large Doppler broadening for such light molecules.

Plate Measurements and Analysis of Data

Since these spectra present no obvious heads, but rather an irregular concourse of lines, often 3 or 4 in the space of an Angstrom, the recognition of individual bands presents some difficulty. It was finally found that the lines could more quickly and certainly be arranged into branches by first making densitometer records of the plates, beginning with those taken at the lowest temperatures. Then with a millimeter scale and the line shapes and relative blackenings as a guide practice soon enabled a single branch to be picked out in a few minutes. In this way some 5000 lines belonging to $Li^{(6)}H$, $Li^{(7)}H$, $Li^{(6)}D$ and $Li^{(7)}D$ were provisionally assigned to bands. The lines due to the $Li^{(6)}$ isotope were of course found on only the higher temperature plates, where the $Li^{(7)}$ spectra were very much richer and superposition was more bothersome. This assignment included probably 80 percent of the measurable lines and when an attempt was made to assign *all* of the visible lines on the LiD plates most of the faintest lines were found to be due to $Li^{(7)}H$ present as an impurity. In no *single* case was a band discovered having more than a single P or R branch. If such are present they must be very faint indeed. It is more likely that the feeble lines remaining unidentified were simply the few central members of branches of higher initial vibrational progressions.

The plates were measured on a tested comparator and to render the wavelength estimates more precise correction curves were drawn for each 50 or 75A section of a plate from the large

[7] F. H. Crawford and T. Jorgensen, Jr., Phys. Rev. **45**, 737 (1934).

[8] Except for the small difference between the potential energy curves of hydrides and deuterides observed by Holst and Hulthén (Nature **133**, 496 (1934) and discussed theoretically by Kronig (Physica, p. 617, May, 1934)). See also F. H. Crawford and T. Jorgensen, Jr., Phys. Rev. **46**, 746 (1934).

* A carbon arc was used for the lower wavelength region.

TABLE I. *Vacuum frequencies of* $^1\Sigma \rightarrow {}^1\Sigma$ *bands of* $Li^{(7)}D$.

	(4−2) Band 23,000 cm^{-1}		(5−1) Band 24,000 cm^{-1}		(6−1) Band 25,000 cm^{-1}		(10−0) Band 27,000 cm^{-1}		(11−0) Band 27,000 cm^{-1}		(13−0) Band 27,000 cm^{-1}		(15−0) Band 28,000 cm^{-1}	
J''	$R(J)$	$P(J)$	$R(J)$	$P(J)$	$R(J)$	$P(J)$	$R(J)$	$P(J)$	$R(J)$	$P(J)$	$R(J)$	$P(J)$	$R(J)$	$P(J)$
0	—		—		—		1674.58		1966.13?		2552.95		2140.22	
1	1974.23	—	—	—	1509.83	1499.98	672.64	1662.95	964.17	1954.25	550.85	2541.44	137.90	2128.55
2	968.02	1951.64	2233.16	2216.77	503.22*	486.87	665.49	649.46	956.97	941.03	543.42?	527.86	130.34	114.89
3	957.06	934.21	221.61	198.78	491.68	468.88	653.20	630.77	944.58	922.31	530.91	508.87	117.50	096.06
4	941.39	912.00	205.18*	175.83	475.26	445.93	635.79	606.67?	927.05	898.43	513.14	484.96	099.34	071.82
5	920.91	885.13	183.89	148.06	453.89	418.13	613.20	578.08	904.32	869.41	490.07	455.75	075.97	042.34
6	895.77	853.56	157.67	115.46	427.66	385.48	585.51	544.03	876.45	835.30	461.85	421.37	047.27*	007.60
7	—	817.24*	126.52	—	396.51	347.96	—	504.93	843.48	796.04	428.44	381.86*	2013.33	1967.66
8	831.24	776.37	090.53	2035.65	360.49	305.66	514.75	460.84	805.31	751.76	389.84	337.15	1974.21	922.55
9	791.90	730.86	049.66	1988.48*	319.57	258.53	471.74	411.65	762.11	702.41	346.08	287.35	929.80	872.28
10	747.86	680.73	2003.95	936.71*	273.90	206.60	423.69	357.47	713.84	648.04	297.25	232.55	880.24	816.89
11	—	625.98	1953.47	880.04	223.33	149.96	370.61	298.39	—	588.74	243.26	172.69	825.54	756.35
12	645.94	566.78	898.11	818.70	168.04	088.61	312.51	234.34	602.14	524.44	184.28	107.93*	765.64*	690.86
13	587.99	502.93	837.92	752.71	107.93	1022.58	249.51	165.44	538.85	455.31	120.26	2038.11	700.82	620.28
14	525.44	434.61	773.09	681.97	1043.08	0951.92	181.58	091.70	470.58	381.31	2051.27	1963.39	630.85	544.86?
15	458.30	361.81	703.51	606.64*	0973.54	876.64	108.77	1013.15	397.48	302.45	1977.29	883.82	555.92*	464.38
16	386.59	284.57	629.22	526.83	899.40*	796.87	1031.09	0929.85?	319.45	218.87	898.43*	799.46	476.01	379.10
17	310.35	202.92	550.27	442.47	820.51	712.47	0948.61	841.86	236.65	130.59	814.77	710.39*	391.25	289.05*
18	229.60	116.91	467.62	353.56	737.00	623.60	861.40	749.21	149.06	1037.63	726.26	616.58	301.63	194.19
19	144.39	1026.60	378.62	260.20	649.03	530.29	769.49	—	1056.79	0940.04	633.02	518.18	207.14	1094.69
20	1054.76	0931.97	285.88	162.39	556.51	432.72	—	550.20	0959.78	837.89	535.11	415.17	107.93*	0990.40
21	0960.72?	833.07	188.71	1060.20	459.50	330.71	571.68	443.98	858.25	731.31	432.53	307.56	1004.04	881.63
22	862.58	730.00	1087.02	0953.75	358.17	224.49	465.94	333.29	752.12	—	325.33	195.52	0895.51	768.31
23	759.64	622.75	0980.92	0843.05	252.39	113.92	355.79	218.26			213.70	1091.70?	782.41	650.63
24			0870.50	728.08			241.18	098.95			1097.42*	0959.30?	664.84	528.49
25													542.78	402.05

number of good iron standards available in the region (λ3200 to λ4300). The results are consequently probably dependable to ±0.004A, or about ±0.025 cm^{-1}, in the most favorable regions. This is in agreement with the fact that the data on the double differences could in all cases be represented by empirical expressions to about this uncertainty. The vacuum frequencies of the lines, of which about 1400 of $Li^{(7)}D$ have been measured, were then arranged in bands and the first double differences $\Delta_2F_v'(J)$ and $\Delta_2F_v''(J)$ determined. The measurement of so many lines was necessitated by the fact that with no head formation whatever as a guide and the early lines in a branch usually faint—the origins could only be computed subsequent to the complete rotational analysis. The 35 bands obtained included 17 bands of the $(v',0)$, 7 of the $(v',1)$, 6 of the $(v',2)$, 4 of the $(v',3)$ and a single faint band of the $(v',4)$ progression. For obvious reasons of space actual vacuum frequencies of only 7 bands are given here. These are recorded in Table I and include about one-fifth of the lines measured. To save space at the head of each pair of columns is given a number which is to be *added* to the number opposite any J-value to give the appropriate vacuum frequency for the branch of the band in question. Since in the more intense parts of the LiD plates there are over twenty branches of $Li^{(7)}D$, 6 or 8 of $Li^{(7)}H$ and probably 8 or 10 of $Li^{(6)}D$ overlapping, the number of accidental superpositions, unresolved blendings, etc., is necessarily rather large. When the densitometer records indicated that a measurement is of questionable value for any of these reasons the line is marked by an asterisk. Question marks indicate the fact that a number of lines occur (usually weak and of similar intensity) so close together as to render identification doubtful. Blanks occur where lines were too near the end of a plate for trustworthy measure-

TABLE II. *Values of* $\Delta_2F_v''(J)$.

J	(11−0) Band	(15−0) Band	Ave. of all $(v',0)$ bands	Ave. −Calc.
1	25.10	25.33	25.14_3	−0.022
2	41.86	41.84	41.86_8	− .022
3	58.54	58.52	58.51_4	+ .020
4	75.17	75.16	75.17_0	+ .003
5	91.75	91.74	91.78_5	− .016
6	108.28	108.31	108.29_1	− .004
7	124.69	124.72	124.70_9	+ .011
8	141.07	141.05	141.05_4	+ .004
9	157.27	157.32	157.25_8	+ .030
10	173.37	173.45	173.39_0	− .005
11	189.40	189.38	189.36_1	+ .010
12	—	205.26	205.19_9	+ .006
13	220.83	220.78	220.87_1	+ .013
14	236.40	236.44	236.39_4	+ .007
15	251.71	251.75	251.75_8	− .016
16	266.89	266.87	266.91_5	− .022
17	281.82	281.82	281.83_6	− .009
18	296.61	296.55	296.61_9	− .009
19	311.17	311.23	311.17_5	+ .014
20	325.48	325.51	325.49_2	− .016
21	—	339.62	339.58_5	− .023
22	—	353.41	353.36_9	+ .053
23	—	367.02	367.00_3	+ .036
24	—	380.36	380.38_6	+ .023
		Av. deviation		± .016 cm^{-1}

TABLE III. *Values of* $\Delta_2F_{11}'(J)$.

J	Obs. (11,0) Band	(Obs. −Calc.)	J	Obs. (11,0) Band	(Obs. −Calc.)
1	(9.57)	+0.002	13	83.54	+0.002
2	15.94	− .004	14	89.27	+ .039
3	22.27	+ .018	15	95.03	− .041
4	28.62	− .003	16	100.58	− .005
5	34.91	+ .008	17	106.06	+ .003
6	41.15	+ .034	18	111.43	− .019
7	47.44	− .033	19	116.75	− .022
8	53.55	+ .033	20	121.89	+ .006
9	59.70	+ .005	21	126.94	− .013
10	65.80	− .031	22	(131.87)	+ .038
11	(71.74)	+ .023	23	(136.68)	+ .008
12	77.70	− .007		Ave. dev.	±0.017 cm^{-1}

ment or were obscured by the occultor supports or where the wrong line was measured. (With such a wealth of data a few missing lines caused very little trouble.)

From the data so arranged the upper state and lower state double differences $\Delta_2F_v'(J)$ and $\Delta_2F_v''(J)$ were computed. Since so many bands involved common lower states very trustworthy averages could be obtained by using only those differences which were above suspicion. A typical pair of these sets for $v''=0$ is given in Table II together with the final averages of the values from the 15 strongest bands. The last column of this table gives the differences (average—calculated) obtained from equations of the form of Eq. (10) with the constants given in Table V.

In the case of $\Delta_2F_v'(J)$-values, those from two or three and often only one band were available. In order to obtain the most likely values for use in determining rotational constants all the $\Delta_2F_v'(J)$-values for a constant J were plotted to scale against v. Almost without exception when a point was noticeably (say more than ±0.06 cm^{-1}) off the smooth curve through the points it was found to involve a line (or lines) whose $\Delta_2F_v''(J)$-value departed from the average in the appropriate direction. Careful reexamination of the plates in several dozen test-cases showed without exception that one or both of the frequencies were in doubt because of incomplete resolution, misidentification or a blunder in measuring. It therefore seemed legitimate thereafter to smooth such values by interpolation. Extrapolation was not resorted to. Values interpolated in this way are in parentheses in Table III which gives $\Delta_2F_{11}'(J)$ as observed together with those computed from the constants of Table V (below).

DETERMINATION OF ROTATIONAL CONSTANTS

Since the Fortrat diagrams for the bands are parabola-like curves of extreme narrowness it is not possible to determine the origins at all closely by any direct graphical method, particularly when the early lines are either very faint or altogether missing. It was therefore necessary to determine the rotational constants for each vibrational level with considerable precision and compute the origins from the lines themselves.

If we represent the double difference $\Delta_2F_v(J)=F_v(J+1)-F_v(J-1)$ as a power series in J it is of course possible to evaluate the coefficients in the usual least-squares fashion. Besides being rather laborious this has the disadvantage of ignoring the theoretical relations which must exist between the coefficients (as for example those of J^3 and J^4). If again we write from Eq. (3),

$$\Delta_2F_v(J)=(4J+2)[B_v+2D_v(J^2+J+1)+\cdots] \quad (9)$$

and plot $\Delta_2F_v(J)/(4J+2)$ against J we have a parabola-like curve with vertex at $J=-\frac{1}{2}$ and intersecting this line at $B_v+3/2D_v$. This, however, involves the extrapolation of a curve which is rising rapidly when $|D_v|$ is large. It further does not permit a precise evaluation of D_v when the data are such as to require higher terms in the energy expression, Eq. (3). Our data very definitely do require at least one more term.

We have consequently employed a graphical method due to Knave[9] which is so satisfactory as to warrant much wider use than it has thus far received. A little algebraic reduction shows that from Eq. (3) we may most conveniently write Eq. (9) as a function not of $J(J+1)$ but of $(J+\frac{1}{2})$. The result is

$$\Delta_2F_v(J)=4(J+\tfrac{1}{2})[(B_v+3/2D_v+27/16H_v)$$
$$+2(D_v-17/4H_v)(J+\tfrac{1}{2})^2+3H_v(J+\tfrac{1}{2})^4+\cdots] \quad (10)$$

$$\text{or}\quad \Delta_2F_v(J)/4(J+\tfrac{1}{2})=a_0+a_1x+a_2x^2+\cdots, \quad (11)$$

where $x=(J+\frac{1}{2})^2$. Hence if $\Delta_2F_v(J)/4(J+\frac{1}{2})$ is plotted against x we have a curve whose departure from a straight line gives a measure of a_2, whose initial slope is a_1 and whose intercept at

[9] E. Bengtsson Knave, Nova Acta Reg. Soc. Sci. Uppsala, Series IV **8**, 1 (1932).

$x=0$ is a_0 (see Fig. 1). Further since a_0, a_1, a_2 are of the order of 1, 10^{-4} and 10^{-8}, respectively, in magnitude the procedure is rapid and certain. In practice the data were plotted to a generous scale (this was repeated using a different scale to avoid systematic errors) and the best straight line through the first 8 or 10 points determined by the criterion that the computed values of a_2 must not increase or decrease with x. The constants so determined were then used in Eq. (11) and the complete set of $\Delta_2F_v(J)$-values computed. In most cases the differences between calculated and observed values were satisfactorily small and irregular. In other cases it was possible to improve the fit somewhat by small trial and error variations of a_2 and a_3, particularly when the scale chosen was inadequate for the precision of the data. In the last columns of Tables II and III are given the values of Δ_2F(calculated) $-\Delta_2F$(observed) for typical cases. In Tables IV and V are recorded the values of B_v, D_v and H_v for the lower and upper $^1\Sigma$ states, respectively, together with the averages for each value of v of the departures of Δ_2F(calculated) from Δ_2F(observed). These average departures are seen in all but one case to be less than 0.03 cm^{-1}. It is believed accordingly that the data are rather more consistent than most published molecular data.

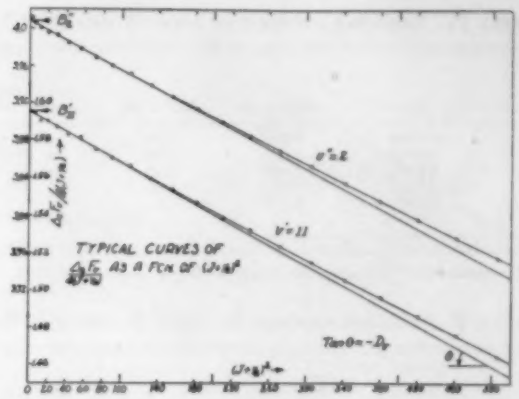

FIG. 1. Here are shown typical curves of $\Delta_2F_v(J)/4(J+\frac{1}{2})$ plotted against $(J+\frac{1}{2})^2$ for the upper and lower $^1\Sigma$ states of $Li^{(7)}D$. The curves are practically linear—the departure from linearity determining H_v in Eq. (3) and the slope, D_v. The regularity of the points enable these constants to be determined with rather greater than the usual precision. The departure from linearity in all cases was definite and marked though small.

The rotational constants of both states were then represented as power series in $(v+\frac{1}{2})$ by the least-square method of Birge and Shea.[10] The lower state constants are represented by the following expressions where the number in parenthesis is in each case the average departure of the observed constants from those calculated. The departures from linearity are small.

$$B_v''=4.23384-0.09198(v''+\tfrac{1}{2})+0.0006714(v''+\tfrac{1}{2})^2, \quad (\pm 0.0002), \tag{12}$$

$$-D_v''\times 10^4=2.756-0.0663(v''+\tfrac{1}{2})+0.00575(v''+\tfrac{1}{2})^2, \quad (\pm 0.001), \tag{13}$$

$$H_v''\times 10^8=2.1175-0.105(v''+\tfrac{1}{2}), \quad (\pm 0.05). \tag{14}$$

In the case of the upper state constants, however, fifth degree polynomials are required for adequate representation of the data. The results with the average departures from the observed values of Table V are:

$$B_v'=1.60602+0.0145042(v'+\tfrac{1}{2})-0.00184351(v'+\tfrac{1}{2})^2+0.0000546903(v'+\tfrac{1}{2})^3$$
$$-1.08582\times 10^{-6}(v'+\tfrac{1}{2})^4+8.43455\times 10^{-9}(v'+\tfrac{1}{2})^5, \quad (\pm 0.00035), \tag{15}$$

$$-D_v'\times 10^4=4.0188-1.12148(v'+\tfrac{1}{2})+0.20873(v'+\tfrac{1}{2})^2-0.019880(v'+\tfrac{1}{2})^3$$
$$+9.2475\times 10^{-4}(v'+\tfrac{1}{2})^4-1.6576\times 10^{-5}(v'+\tfrac{1}{2})^5, \quad (\pm 0.010), \tag{16}$$

$$H_v'\times 10^8=11.663-6.4585(v'+\tfrac{1}{2})+1.50170(v'+\tfrac{1}{2})^2-0.16791(v'+\tfrac{1}{2})^3+0.00900623(v'+\tfrac{1}{2})^4$$
$$-0.000185934(v'+\tfrac{1}{2})^5, \quad (\pm 0.08 \text{ to } v'=15). \tag{17}$$

Values of B_v' and H_v' are plotted in Fig. 2.

[10] Birge and Shea, Univ. of Cal. Publ. in Math. **2** (5), 67–118 (1927).

TABLE IV. *Rotational constants for lower* $^1\Sigma$ *state of* $Li^{(7)}D$.

v''	B_v''	$-D_v''\times10^4$	$H_v''\times10^4$	(Ave. Δ_2F_v'' calc. $-\Delta_2F_v''$ obs.)
0	4.1882	2.726	1.96	±0.016
1	4.0970	2.670	1.86	± .017
2	4.0082	2.625	1.75	± .017
3	3.9204	2.593	1.8$_4$	± .027
4	3.833$_4$	2.$_6$	—	
				Average = ±0.019

Constants for $v''=4$ are quite doubtful due to faintness of lines.

TABLE V. *Rotational constants for upper* $^1\Sigma$ *state of* $Li^{(7)}D$.

v'	B_v'	$-D_v'\times10^4$	$H_v'\times10^4$	(Ave. Δ_2F'calc. $-\Delta_2F'$obs.)
1	1.6238	2.775	4.9	±0.027
2	1.6316	2.206	2.25	.015
3	1.6365	1.939	1.7	.019
4	1.6383	1.746	1.2	.018
5	1.6382	1.626	0.92	.021
6	1.6358	1.557	0.93	.021
7	1.6310	1.495	0.91	.026
8	1.6243	1.432	0.83	.027
9	1.6162	1.399	0.89	.026
10	1.6057	1.357	0.88	.028
11	1.5955	1.345	0.81	.017
12	1.5824	1.317	0.74	.018
13	1.5678	1.293	0.78	.024
14	1.5534	1.289	0.75	.025
15	1.5361	1.290	0.59	.020
16	1.5197	1.304	1.1	.032
17	1.5002	1.302	0.9	.021
				Av. = ±0.023

VIBRATIONAL DATA

With reliable values of the rotational constants the origin of each band was then computed independently from the first 8 or 10 lines in each branch excluding questionable lines. These gave values whose consistency was a further check on the precision of the measurements and whose average was taken as the true origin. Thus for a typical set (from the (6−1) band) as M the ordinal number of a line runs from $M=+10$ (R branch) to $M=-10$ (P branch) the origins computed are 26,508.18 cm^{-1} −0.03, ±0.00, ±0.00, ±0.00, −0.02, ±0.00, −0.01, +0.01, +0.03, −0.01, ±0.00, +0.03, −0.01, −0.01, +0.00, −0.01, +0.02, +0.03 and −0.01 in order. (Here the line $M=+1$ is missing.) In Table VI are recorded the origins so determined where the *horizontal* and *vertical* differences, $\Delta G''(v+\frac{1}{2})$ and $\Delta G'(v+\frac{1}{2})$ are indicated in italics.

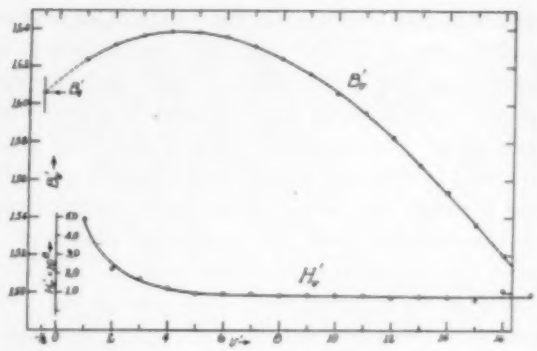

FIG. 2. The upper and lower curves show, respectively, the observed values of B_v' and H_v' [Eq. (10)]. The upper curve attains a maximum value between $v'=4$ and $v'=5$ and thereafter falls steadily. The observed B_v'' values fall steadily from the origin.

TABLE VI. *Origins of* $^1\Sigma\rightarrow{}^1\Sigma$ *bands of* $Li^{(7)}D$. Values involving uncertainty in the tenth's place were not used in the least-square computation of the origins. These are indicated with the last digit in smaller type.

v'	v'' 0		1		2		3		4
1					24255.71	*978.*$_5$	23277.2		
					224.62		*224.*$_6$		
2			25483.94	*1003.61*	24480.33	*978.55*	23501.78		
			239.92		*239.92*		*239.91*		
3	26752.8	*1028.*$_9$	25723.86	*1003.61*	24720.25	*978.56*	23741.69	*953.84*	22787.85
	252.$_1$		*252.16*		*252.19*		*252.19*		
4	27005.08	*1029.06*	25976.02	*1003.58*	24972.44	*978.56*	23993.88		
	262.03		*262.03*		*262.03*				
5	27267.11	*1029.06*	26238.05	*1003.58*	25234.47				
	270.15		*270.13*		*270.15*				
6	27537.26	*1029.08*	26508.18	*1003.56*	25504.62				
	276.69		*276.69*						
7	27813.95	*1029.08*	26784.87						
	282.01		*281.98*						
8	28095.96	*1029.11*	27066.85						
	286.13								
9	28382.08								
	289.28								
10	28671.36								
	291.60								
11	28962.96								
	293.08								
12	29256.04								
	293.78								
13	29549.82								

v'	$v''=0$
13	29549.82
	293.90
14	29843.72
	293.34
15	30137.06
	292.11
16	30429.17
	290.41
17	30719.58
	288.$_6$
18	31007.6
	285.$_2$
19	31292.8

The extremely close agreement whenever two independent values have been found is gratifying. Least-square solutions for $\Delta G''$ and $\Delta G'$ were then obtained and vibrational constants determined. Because of the regular decrease of the $\Delta G''(v+\frac{1}{2})$ values a cubic expression in $(v''+\frac{1}{2})$ is adequate while for the $\Delta G'(v+\frac{1}{2})$ values the approximation afforded by even a fifth power expression in $(v'+\frac{1}{2})$ could probably be improved. We find the origins of the 36 measured bands are represented with an average deviation of ± 0.04 cm^{-1} by an expression of the usual form,

$$\nu \text{ origin} = 26{,}512.05 + u'[\omega_e' - x_1'u' + x_2'(u')^2 + x_3'(u')^3 + x_4'(u')^4 + x_5'(u')^5 + \cdots], \quad (18)$$

where $u = v+\frac{1}{2}$, $x_1 = x_e\omega_e$, $x_2 = y_e\omega_e$, etc.,

where the values of the constants ω_e, $x_e\omega_e$, etc., are those given in Table VII. The extreme size

TABLE VII. *Vibrational constants for $Li^{(7)}D$.*

	Ground $^1\Sigma$ state	Upper $^1\Sigma$ state
ω_e	1055.12	183.1246
$x_e\omega_e = x_1$	+13.2282	−12.74161
$y_e\omega_e = x_2$	+0.1300	−0.8778501
x_3	−0.00667	+0.04261680
x_4		-1.332244×10^{-3}
x_5		$+1.808235\times10^{-5}$

of the higher powers of $(v+\frac{1}{2})$ necessitates the number of decimals given. Inasmuch as $\Delta G'(v+\frac{1}{2})$ attains a maximum at about $v'=13.5$ and it is not possible to follow the system much beyond $v'=18$ or 19 the attempt to extrapolate Eq. (2) to dissociation leads to very uncertain results.

COMPARISON WITH LiH

Assuming the simple isotope theory the vibrational and rotational constants of the ground $^1\Sigma$ state are in as good agreement with the published results of Nakamura as his lower dispersion would permit. See Table VIII.

The upper state constants, however, present certain discrepancies. If $\rho = (\mu/\mu^i)^{\frac{1}{2}}$ where μ and μ^i are the reduced masses of $Li^{(7)}D$ and $Li^{(7)}H$, respectively, and the atomic masses of Bainbridge[11] are used we have $\rho = 1.33245$, $\rho^2 = 1.77542$,

[11] K. T. Bainbridge, Phys. Rev. **42**, 1 (1932); **43**, 103 (1933); **44**, 56 (1933).

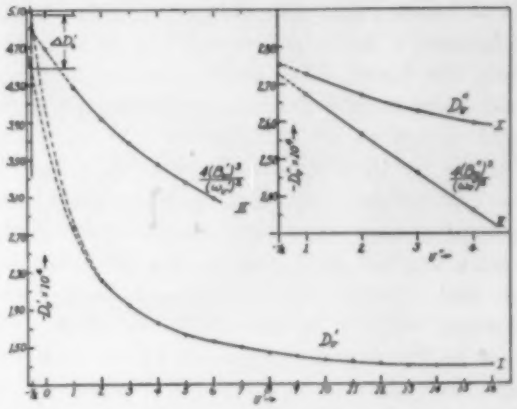

FIG. 3. The insert shows observed values of D_v'' (I) and $4(B_v'')^3/(\omega_v'')^3$ (II) plotted against v''. The difference between the intercepts at $v''=-\frac{1}{2}$ is small but probably real. In the other part of the figure are the corresponding curves for the upper state. Since the extrapolation of the lower curve to $v'=-\frac{1}{2}$ is rather uncertain the two dotted curves are drawn from the least-square representations of the data for $v'=1$ to 6 with D_1' taken, respectively, as 0.04×10^{-4} *above* and *below* the observed value. These are seen to extrapolate above and below the $v'=-\frac{1}{2}$ intercept of the upper curve (II) and hence indicate—if the present vibrational numbering is correct—no definite uncoupling in the upper state. The expression [Eq. (16)] which represents the actual observations from D_1 to D_{17}, due to the extreme flatness of the curve at the right end is not at all trustworthy for extrapolation outside of this range. Hence the initial constant in that equation is of little significance. The average of the dotted curves is taken as giving the most probable value, i.e., $D_e' = -4.8\times10^{-4}$ $(\pm0.3\times10^{-4})$.

$\rho^3 = 2.36566$, etc. Hence by the usual isotope theory $B_e^i = B_e\rho^2$, etc., and the calculated B_e' values agree to within about 5 percent with Nakamura's results and much closer with our most recent remeasurements for $Li^{(7)}H$. The vibrational data, however, cannot be made to agree with Nakamura's constants though the vibrational numbering used in this paper seems the most nearly consistent. Now with the values of ρ, ρ^2, ρ^3, etc., given above and the data of Table VII we obtain the corresponding vibrational constants for $Li^{(7)}H$ from the simple isotope theory. These are given in columns I and

TABLE VIII. *Vibrational constants for $Li^{(7)}H$.*

	Ground $^1\Sigma$ state		Upper $^1\Sigma$ state		
	Isotope theory	Nakamura	Isotope theory	Nakamura	Nakamura recalculated
ω_e	1405.895	1406.1	244.004	287.91	279.84
x_1	23.485	22.73	−22.622	−9.13	−9.5642
x_2	.307		−2.0766	+.318	+.06015
x_3			+0.13433		−.038719
x_4			−0.00556		+.0011546

III of Table VIII while columns II and IV give Nakamura's published values.[3] It is seen that while the lower state constants are in pretty good agreement, for the upper state the agreement is not at all satisfactory, the ω_e'-values differing by 16 percent and the $\omega_e'x_e'$-values by over 100 percent. We have made a recalculation by least squares of these constants from Nakamura's original data and obtain the results in the *last* column where ω_e' and $\omega_e'x_e'$ have changed slightly in the right direction. This gives as the system origin for $Li^{(7)}H$ 26,479.66 cm^{-1} as against 26,457.9 cm^{-1} obtained by Nakamura. Furthermore with the exception of one faint band the vibrational constants obtained from our $Li^{(7)}D$ data by the simple isotope theory reproduce the observed isotope shifts with no more systematic deviations than Nakamura's constants give (either as originally recorded or as recomputed). We therefore conclude that more precise observations are required before any inference can be drawn as to the actual electronic isotope shift or the failure of the simple isotope theory.

On the other hand, the following considerations lend independent support to the present vibrational numbering in the upper state. In Fig. 3 (insert) are drawn two curves, I being the observed values of $-D_v''$ and II, values of $+4(B_v'')^3/(\omega_v'')^2$. Each should extrapolate to the same value at $v''=-\frac{1}{2}$ if Kratzer's relation is true. The first actually gives $D_e''=-2.756\times10^{-4}$ while the other gives -2.728×10^{-4} a difference which is small but probably real and an indication perhaps of a *very* small amount of uncoupling in the ground state. In the other part of the same figure are drawn the corresponding curves for the upper state. Here unfortunately the most crucial point, the value of D_1' in curve I, is experimentally the least accurately known and therefore renders extrapolation to $v'=-\frac{1}{2}$ rather uncertain. We have, however, by trial and error found that D_1' cannot depart from the value -2.775×10^{-4} by more than ±0.04 and allow B_1' and H_1' in Eq. (10) to be changed in such a way as to represent the observed $\Delta_2F_1'(J)$-values. Consequently using the observed values of D_v' for the 6 lowest values of v', least-squares calculations were made with D_1' set equal to -2.810 and -2.730×10^{-4}, respectively.[12] The results are plotted as the dotted curves in the figure. It is seen that the intercept at $v'=-\frac{1}{2}$ of curve II is well within the range of uncertainty implied by the dotted curves. Since a shift of numbering of ±1 unit would cause a very large difference between D_e' and $-4(B_e')^3/(\omega_e')^2$ this would imply an uncoupling so marked as to influence markedly the linearity near the origins of the upper state curves of the type of that in Fig. 1. The present numbering seems therefore quite necessary. Thus within the range of experimental uncertainty there is *no evidence of appreciable uncoupling in either state of LiD*. This means therefore that the peculiar behavior of the observed B_v' and ω_v' values must be ascribed to peculiarities in the potential energy curve alone.

It becomes further apparent why attempts to calculate D_e' for LiH by extrapolation (of rather uncertain values) from say $v'=2$ to $v'=-\frac{1}{2}$ was bound to give results much below the true values and hence to suggest that both B_v' and D_v' had lost their mechanical significance. It is further apparent that although D_e' depends only on the curvature of the potential curve at the minimum, its rate of change with v is very sensitive to the precise way in which this curve alters as we leave the equilibrium position. A detailed examination of the empirical form of the potential curve will be possible when the remaining data on LiH have been adequately summarized.

We wish at this time to express our thanks for a generous grant from the Milton Fund of Harvard University which has defrayed part of the expenses of this investigation.

---

[12] It must be borne in mind that when a curve changing as rapidly at one end and as nearly constant at the other as that of D_v' is represented by a power series by the method of least squares—the expression so obtained is not dependable for extrapolation. It is much more certain if a few points near one end or the other are used. For this reason the constant term in Eq. (16) is of no significance. The midpoint of the dotted curves of Fig. 3 is accordingly taken for D_e'. This gives $D_e'=-4.8\ (\pm0.3)\times10^{-4}$.

Incoherent Scattering and the Concept of Discrete Electrons*

ARTHUR H. COMPTON, *University of Chicago and Oxford University*

(Received December 21, 1934)

Experiment has shown that scattered x-rays contain both a coherent and an incoherent portion. Classical electron theory provides a formula for scattering closely similar to that based on wave mechanics, but includes both coherent and incoherent components only if the atom consists of discrete electrons. From a comparison of the classical and wave-mechanics theories of scattering it is concluded that the most accurate classical analog of Schrödinger's $\psi\psi^*$ is the probability of occurrence of discrete electrons, and that a particular electron is associated with each particular function $\psi_n\psi_n^*$.

EXPERIMENT shows that two types of scattered x-rays occur, one of which is of the same wavelength as the primary rays and the other of greater wavelength. Definite phase relations occur between the unmodified rays scattered by neighboring portions of matter, whence these rays are described as *coherent*. The modified rays, differing from each other in wavelength, can have no fixed phase relations, and are described as *incoherent*. Theoretical descriptions of the origin of the two types of rays have been given on the basis of (1) photons, (2) wave mechanics and (3) classical electromagnetic theory. It is a point of no little interest that whereas according to wave mechanics both types of scattered rays are interpreted in terms of wave functions distributed continuously throughout space, according to classical electromagnetic theory discrete electrons are required if incoherent rays are to occur. A comparison of the various theories of scattering is thus helpful in understanding the realm within which the concept of the electron is applicable.

It was first recognized from a consideration of the interaction of atoms and photons[1] that in addition to coherent scattering, collisions should occur involving changes of the photon's energy, which would mean a change of frequency and hence incoherence. Whereas Compton and Debye concerned themselves primarily with electrons which were knocked free from the atom by the photon's impact, Smekal noted also that any possible energy change of the atom might give to the scattered photon a frequency described by

$$h\nu_s = h\nu + W_i - W_f, \qquad (1)$$

where W_i and W_f are the initial and final energies. In the hands of Jauncey and others[2] the concept of photons colliding with electrons moving within the atom has shown itself capable of describing in quantitative form the distribution of energy between the coherent and the incoherent rays.

According to the wave-mechanics theory,[3] under the influence of the field of the incident electromagnetic wave the characteristic functions for higher energy states of an atom assume finite values, and the radiation which it emits has the frequencies described by Eq. (1). If the final state of the atom is identical with the initial state i, the frequency is unchanged, and coherent radiation is emitted. In calculating this part of

* Based on an address presented at the Symposium on X-Ray Scattering at the St. Louis meeting of the Am. Phys. Soc., Dec. 1, 1934.

[1] A. H. Compton, Bull. Nat. Res. Council No. **20**, 19 (1922); Phys. Rev. **21**, 483 (1923); **24**, 168 (1924). P. Debye, Physik. Zeits. **24**, 161 (1923). A. Smekal, Naturwiss. **11**, 873 (1923).

[2] G. E. M. Jauncey, Phil. Mag. **49**, 427 (1925); Phys. Rev. **25**, 314 (1925). J. W. M. Dumond, Phys. Rev. **33**, 643 (1929). S. Chandrasekhar, Proc. Roy. Soc. **A125**, 231 (1929).

[3] This wave-mechanics theory includes the main features of the theory of dispersion by virtual oscillators introduced by H. A. Kramers, Nature **113**, 673 (1924); **114**, 310 (1924), and extended by H. A. Kramers and W. Heisenberg, Zeits. f. Physik **31**, 681 (1925), whose theory included the incoherent radiation of the frequency given by Eq. (1). E. Schrödinger's first wave-mechanical theory of scattering, Ann. d. Physik **81**, 109 (1926), was approximately equivalent to that of Kramers, giving only the coherent term. O. Klein, Zeits. f. Physik **41**, 407 (1927), in sections 5 and 6 of his paper, gives a detailed and lucid account of the origin of the coherent and incoherent radiation according to wave mechanics. This theory was extended by Wentzel, Zeits. f. Physik **43**, 1, 779 (1927), who first derived Eq. (6) from wave-mechanical principles. Eq. (3) is due to I. Waller, Phil. Mag. **4**, 1228 (1927); Zeits. f. Physik **41**, 213 (1928); and especially good for clarity of interpretation, I. Waller and D. R. Hartree, Proc. Roy. Soc. **A124**, 119 (1929), who corrected Wentzel's theory by taking into account the limitations of Pauli's exclusion principle.

the scattering, only the ψ functions of the normal state o of the atom are therefore concerned. That is, the coherent scattering is identical with that from an atom having a continuous distribution of electric charge of density

$$\rho = -e\psi_0\psi_0^*. \tag{2}$$

If the final state differs from the initial state, the scattered ray is by Eq. (1) incoherent with the primary. The possible final states which may occur are all of those permitted by Pauli's exclusion principle, which is equivalent to the statement that an electron may be transferred to any level allowed by the selection rules, and not already occupied in the normal atom. Since the most probable transitions would in any case be those corresponding to complete ionization, this limitation is not stringent. It has the effect, however, of making the inner electrons of a Bohr atom less effective in incoherent scattering than are the outer ones.[4]

The formula thus developed by Waller[3] from wave mechanics may be written as

$$R_w \equiv \frac{I_a}{I_e} = \underbrace{(\sum_1^z f_n)^2}_{\text{content}} + \underbrace{\sum_1^z (1-f_n^2) - \sum_{mn}''(f_{mn}^2)}_{\text{incoherent}}. \tag{3}$$

[$\sum_{mn}''$ = sum over all pairs of electrons with the same spin, and $m \neq n$.]

Here I_a is the scattering by an atom, I_e that by an electron according to classical electron theory, f_n and f_{mn} are defined by the expressions,

$$f_n = \int\int\int \psi_n\psi_n^* e^{i\mathbf{k}\cdot\mathbf{r}} d\tau, \tag{4}$$

$$f_{mn} = \int\int\int \psi_m\psi_n^* e^{i\mathbf{k}\cdot\mathbf{r}} d\tau, \tag{5}$$

where ψ_n is Schrödinger's wave function corresponding to the nth electronic state in the normal atom, $\mathbf{k} = 2\pi(\mathbf{s}' - \mathbf{s})/\lambda$, where $\mathbf{s}'$ and $\mathbf{s}$ are unit vectors in the directions of the scattered and the primary rays respectively, $\mathbf{r}$ is the vector distance of the volume element $d\tau$ from the center of the atom and Z is the atomic number. Thus f_{mn} is the amplitude of the scattered wave due to the m to n transition, in terms of that due to a point charge electron as unity. The first term thus represents the scattering for the unchanged atom, which is coherent. The second term, as Wentzel shows, represents the scattering for all transitions for which $m \neq n$, and the third term takes account of those transitions which are disallowed by the Pauli exclusion principle. These terms thus describe the incoherent scattering.

In this theory, both radiation and atom are treated as distributed continuously through space. Its relation to the photon-electron theory described above corresponds to de Broglie's theorem of the equivalence of waves and particles. They may be considered as alternative views of the same phenomenon.[5]

It is noteworthy that classical electrical theory leads to a formula (Eq. (6)) almost identical with that derived from wave mechanics (Eq. (3)), but only if the atom is assumed to consist of discrete electrons. Woo's extension of Raman's classical theory[6] gives the expression,

$$R_c = (\sum_1^z f_n)^2 + \sum_1^z (1-f_n^2), \tag{6}$$

where f_n has the same significance as in Eq. (4) except that $\psi_n\psi_n^*$ is replaced by p_n, where $p_n d\tau$ is the probability that the nth electron will lie in the volume element $d\tau$. If we should assume on the other hand that $\sum p_n d\tau$ is the portion of the continuously distributed electric charge in the volume element $d\tau$, and that this volume element has the same ratio of charge to mass as does an electron, we should obtain merely[7]

[4] In most cases the effect of the negative term representing the Pauli exclusion principle is practically negligible. G. G. Harvey, P. S. Williams and G. E. M. Jauncey, Phys. Rev. **46**, 365 (1934), have recently shown, however, that in the diffuse scattering from crystals this term may become of experimental importance.

[5] The photon theories of Jauncey and others are not in their present forms precisely equivalent to Eq. (3), though there is no apparent reason why they could not be so made. It seems possible from wave mechanics, however, to arrive more easily at a rigorously derived formula.

[6] The classical theory of coherent scattering by the electrons in an atom was first treated extensively by P. Debye, Ann. d. Physik **46**, 809 (1915). That incoherent scattering must occur was pointed out from classical principles by A. H. Compton, *X-Rays and Electrons*, p. 171 (1926), and the theory was developed independently by C. V. Raman, Ind. J. Phys. **3**, 357 (1928) and A. H. Compton, Phys. Rev. **35**, 925 (1930), leading to Eq. (9). Eq. (6) was derived by Y. H. Woo, Phys. Rev. **41**, 21 (1932), following an extension of Raman's theory by G. E. M. Jauncey, Phys. Rev. **37**, 1193 (1931).

[7] This result is implicit in Wentzel's wave-mechanics theory (reference 5), and is derived explicitly by A. H.

$$R_c' = (\sum_1^s f_n)^2. \qquad (7)$$

Since definite phase relations exist between the rays scattered by the various volume elements of charge, this expression represents coherent radiation. Raman has shown[6] that the second term of Eq. (6) arises from the fact that in an atom composed of discrete electrons the positions of these electrons are continually changing, giving variable phase relations. There is thus a portion of the radiation from each electron (represented by the nth term in the summation) which is incoherent with that from the rest of the atom.

To the last term in Eq. (3) there seems to be no exact classical analog. It represents constraints upon each electron's motion due to the presence of the other electrons. If an attempt were made to build an atom out of electrons according to classical principles, such constraints would necessarily arise, but they could not be expected to introduce a term in the scattering formula identical with that resulting from Pauli's exclusion principle. According to classical electron theory, electrons should partially shield each other from the action of the electric field of the primary wave due to (1) the electrostatic field of the displaced neighboring electrons, and (2) the radiation field resulting from this acceleration. The former effect is an aspect of refraction, the latter is an increase of the electrical inertia due to proximity of the electrons. Both effects are dimensionally different from the Pauli exclusion effect, and of a smaller order of magnitude.

Further differences arise if the wave-mechanical theory is developed in sufficient detail to take into account the recoil of the scattering electrons and the corresponding increase in wavelength of the incoherent rays. Here the classical analog of radiation pressure gives a term of entirely the wrong order of magnitude. Nevertheless even here a treatment of the change in wavelength as a Doppler effect has, in the hands of Jauncey and DuMond[2] shown that momenta can be properly ascribed to the electrons within the atom, thus emphasizing their discrete existence.

Compton and S. K. Allison in their *X-Rays in Theory and Experiment*, Van Nostrand, New York, 1935, p. 138.

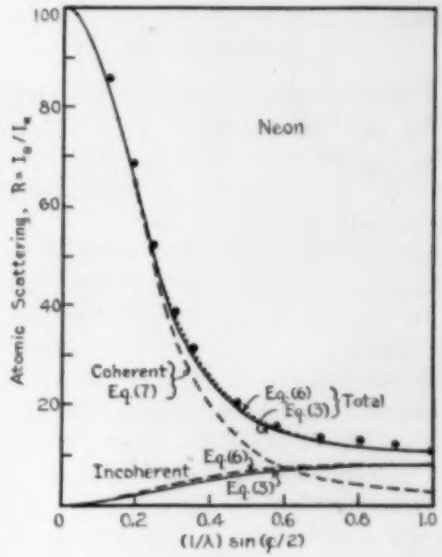

FIG. 1. Scattering of x-rays by neon. Experiments, Wollan. Theories based on Hartree electron distribution.

To a first approximation (Eq. (7)), a classical counterpart of the wave-mechanics atom is thus given by supposing the atom to consist of a continuously distributed charge of density given by Eq. (2). As will be seen from Fig. 1 this represents the most important part of the scattering at small angles. A second and much closer approximation (Eq. (6)) is obtained by replacing the continuous charge distribution with discrete electrons, the probability of occurrence of the nth electron being given by,

$$p_n d\tau = \psi_n \psi_n^* d\tau. \qquad (8)$$

Attempts to arrive at a still closer approximation by taking into account the constraints on the electron's motions cannot be expected to give the third term of Eq. (3).

It is noteworthy also that in order to get the closest classical analog to the wave-mechanical atom, we must assume that each electron has its own characteristic region within which it moves, i.e., $p_n \neq p_m$ (except where n and m differ only in the direction of the electron's spin). If each electron in the atom is assumed to have the same probability of occurrence at any point as every other electron, all the p_n's and hence all the f_n's will be alike (Eq. (4)), and Eq. (6) reduces to the form derived by Raman and

Compton,[8]

$$R_e = Z^2 f^2 + Z(1-f^2), \qquad (9)$$

where f is the common value of the structure factor for all of the electrons. This is no longer identical with the first two terms of Eq. (3), and is found[8] to be in somewhat less satisfactory agreement with the experiments.

Though we are accustomed to think of the Schrödinger ψ_n functions as distributed continuously throughout space, these functions are strictly speaking in $3n$-dimensional space. The apparent overlapping of the functions is merely a convenient 3-dimensional approximation. Thus the discreteness of the electrons in the classical theory corresponds on the wave-mechanics theory to equally discrete ψ_n functions, which are completely separated by being in different dimensions.

The closest classical analog to the wave-mechanical atom is thus one composed of discrete electrons, each of which has its own characteristic probability $\psi_n \psi_n^* d\tau$ of occurring within a given volume element.[9] It is accordingly proper not only to speak of electrons occurring within the atom, but also to distinguish each individual electron by the name of the corresponding quantum state. That is, K electrons are distinguishable from L electrons, etc. Thus for treatment of scattering problems, individual electrons grouped within the atom form the most nearly adequate classical picture corresponding to the continuous de Broglie waves of the wave-mechanics atom.

[8] G. Herzog, Zeits. f. Physik **69**, 207 (1931); E. O. Wollan, Rev. Mod. Phys. **4**, 241 (1932).

[9] Cf. A. H. Compton, Phys. Rev. **35**, 931 (1930), and Tech. Rev. Mass. Inst. **33**, 19 (1930). The conclusion there drawn was that the observed presence of incoherent scattering indicated that the discrete electron interpretation of $\psi\psi^*$ was necessary to bring agreement between theory and experiment. This argument was criticized by G. Herzog (reference 8), because of a supposed lack of agreement between the classical and quantum formulas, and because the concept of discrete electrons does not enter into the quantum theory of scattering. The statement that the best *classical* interpretation of $\psi\psi^*$ is the probability of occurrence of discrete electrons seems to be the legitimate conclusion from the considerations here advanced.

MARCH 1, 1935 PHYSICAL REVIEW VOLUME 47

The Arc Spectrum of Samarium and Gadolinium. Normal Electron Configurations of the Rare Earths

WALTER ALBERTSON, *George Eastman Research Laboratory of Physics, Massachusetts Institute of Technology*

(Received January 11, 1935)

A partial analysis which includes most of the low temperature lines is presented for Sa I and Gd I: 453 lines, 175 levels for Sa I; 71 lines, 35 levels for Gd I. The normal configuration and lowest state of Sa I is $4f^6 6s^2\ {}^7F$; for Gd I is $4f^7 5d 6s^2\ {}^9D$. It is also shown that the normal configuration for Tm I is probably $4f^{13} 6s^2$. There exists in the rare earth group the same type of variation of relative binding between the $4f$ and $5d$ electrons as exists between the s and d electrons in the long periods. In the rare earth group the $5d$ electron is most tightly bound at the beginning and middle of the group and has a minimum just before the middle and at the end of the group.

INTRODUCTION

THE region of the periodic table least investigated by spectroscopists is that occupied by the fourteen elements from cerium to lutecium, inclusive,—the so-called rare earths. With the exception of thulium, ytterbium and lutecium, the arc and spark spectra of the rare earths are of extreme complexity. Indeed, the number of lines obtained appears to depend only on the amount of exposure given. Even if one adheres to the strictest selection rules for L, S, J and parent terms, a fundamental electron transition in neutral gadolinium can yield more than 20,000 lines, and if only the J selection rule is retained, there is a possibility of more than 18,000,000 lines, whereas the identical electron jump in

caesium gives two lines. These figures indicate the apparent futility of an attempt by any worker to push the observation of a rare earth spectrum to its limit.

With the exception of the three elements mentioned above, by far the greater number of the intense lines of an arc exposure belong to the ionized rare earth atom. The work of King[1] on the furnace spectra of the rare earths has shown that the spectrum of the neutral atom is very poorly developed in an arc source. Many neutral lines that are comparatively well developed in the furnace appear so faint in the arc that they have not been measured, while a large number more are masked in the arc by the more intense ionized lines. It is practically impossible to analyze the spectrum of the neutral atom with only the use of arc and spark exposure data. Additional data from the furnace or from absorption measurements must be added.

The most characteristic rare earth spectra are shown by the end-group, thulium, ytterbium and lutecium, and by europium, which precedes the middle. Many of the lutecium and ytterbium lines have already been explained by Meggers and Scribner[2] and by Meggers and Russell[3] as resulting from transitions involving s, p and d electrons. The $4f$ shell is completely filled and contributes nothing to the term types. The europium spectrum is quite complex, but it does have a special character due to a small group of lines of outstanding intensity. These lines have been explained by the writer[4] and by Russell and King.[5] They result from transitions involving s, p and d electrons and configurations built on the parent term $4f^7\ {}^8S$, which does not contribute to the L value of the resulting terms. Thus, although the most intense rare earth lines have been classified, no terms have been found for which the $4f$ electrons contribute to the L value.

[1] Numerous articles in Astrophys. J., Spectroscopic bibliography, R. C. Gibbs, Rev. Mod. Phys. **4**, 278 (1932).
[2] W. F. Meggers and B. F. Scribner, Bur. Standards J. Research **5**, 73 (1930).
[3] W. F. Meggers and H. N. Russell, unpublished material. C. E. Moore, *Term Designations for Excitation Potentials*, Princeton Observatory and Carnegie Institute at Mt. Wilson.
[4] W. E. Albertson, Phys. Rev. **45**, 499 (1934).
[5] H. N. Russell and A. S. King, Phys. Rev. **46**, 1023 (1934).

Analysis of the Arc Spectrum of Samarium

Experimental Data

Following the above-mentioned elements, the next most characteristic spectra are those of samarium, gadolinium, dysprosium and holmium. An extensive temperature classification of samarium has recently been completed by King.[6] The author is greatly indebted to Dr. King, who was generous enough to send a duplicate list of the neutral lines prior to publication. The list contains 422 Class I and II lines, many of which are comparatively intense in the arc and reversed in the furnace, and more than 1200 Class III, IV and V lines. The latter classes appear in two distinct wavelength regions; one from the long waves to about 5100A, the other, from 3900A to short waves. King's data have been supplemented with absorption data recorded by Paul.[7] These data for 337 lines extend from 7755A to 3527A. Although absorption lines were found out to 8700A, none of them belonged to samarium. Nearly all the Class I and the strong Class II lines in this region and strong Class III lines of wavelength less than 3900A appear in absorption.

Results

The results of the analysis of the data are given in Tables I and II. Table I contains all the classified lines (453) that involve levels which are probably real. Over 200 lines are omitted from the list as they involve levels that do not show enough combinations to be accepted with confidence as being real. Most of these levels are no doubt real but they are all omitted as at present there is no way of telling which ones are spurious. Table I also contains all unclassified Class I lines of wavelength less than 7756A. Column 1 gives the wavelength from King's data; Column 2 the arc intensity; Column 3 the furnace intensity with temperature class; Column 4, absorption intensity; Column 5, the wave number in vacuum; Column 6, term combinations. The absorption intensities can be compared only over a small wavelength range. Table II contains the level number, energy of level in cm^{-1} and tentative J value.

[6] A. S. King, unpublished material.
[7] F. W. Paul, M.Sc. Thesis, M. I. T. (1934).

As is seen from Table II, the analysis has yielded a set of seven low levels, each having a different J value, increasing in order. A systematic search has shown that there are no other levels below 12,000 cm^{-1} that combine readily with the middle and high levels already found. This is quite in agreement with the fact that only a few absorption lines remain to be explained.

At the present time all books on the subject state that the normal electron configuration for a rare earth is $4f^n5d6s^2$ where n increases progressively from 1 for cerium to 14 for lutecium. If such were the fact, then the normal configuration for samarium should be $4f^5 5d6s^2$. $4f^5$ gives rise to the following terms:

$$^2PDFGHIKLMNO \quad ^4SPDFGHIKLM \quad ^6PDH.$$

Most of the quartet and doublet terms appear several times for each value of L. Let us consider just the ^6H multiplet, since it will be the lowest and most important. The addition of the $5d$ electron to ^6H gives rise to a pentad of septet and quintet multiplets, all expected to be fairly low in Sa I. Since only a single septet multiplet accounts for nearly all the low temperature lines and no other low levels could be found, the normal configuration of Sa I is obviously not $4f^5 5d6s^2$. Another configuration likely to be found low is $4f^6 6s^2$. This configuration yields only one septet multiplet, ^7F. Furthermore it is known that when a d shell lacks a single electron of being half filled, i.e., d^4, there is but a single multiplet of highest multiplicity, and it lies far below all other levels from the same configuration. These facts suggest quite strongly that the normal configuration of Sa I is $4f^6 6s^2$.

The chief electron configurations and transitions of Sa I are expected to be

(1) $4f^6 6s^2 - 4f^6 6s6p$,
(2) $4f^6 6s^2 - 4f^5 5d6s^2$,
(3) $4f^5 5d6s^2 - 4f^5 5d6s6p$,
(4) $4f^6 6s6p - 4f^5 5d6s6p$.

In (1) the chief multiplets will be built on the ^7F parent term. The upper configuration will yield the triads $^7F6s6p(^9, ^7DFG, ^7, ^5DFG)$. Although the identification is uncertain, it is believed that most of the nonet and septet levels have been found. They occur at energy values quite near those for the corresponding multiplets built on ^8S of Eu I[5]. Table III gives a typical multiplet ^7FG, the first complete septet multiplet yet found.

The configurations involving the $5d$ electron will yield an enormous number of multiplets. Most of the middle and high levels in Table II, probably belong to $4f^5 5d6s^2$.

Numerous recurring frequency differences among the intense long wavelength Class III and IV lines have been found with the aid of the mechanical interval sorter.[8] Thus far they have defied attempts to link them together. These intervals probably belong to the configurations involving a $5d$ electron.

The Normal Electron Configuration for the Rare Earths

The normal configuration of Eu I has already been shown by Russell and King[5] to be $4f^7 6s^2$ instead of the previously supposed $4f^6 5d6s^2$. This result, with that of Sa I, suggested that the normal configuration of Gd I is $4f^8 6s^2$ giving identical multiplets with Sa I but inverted. King's data for gadolinium[9] is not complete (4680–3840A) but it does cover the most important region of the spectrum. The results of an analysis of these data are presented in Tables IV and V. Table IV contains all the Class I and II lines and Table V the energy values of the levels with tentative J values. It is seen that nearly all of King's lines result from transitions between middle levels and a low regular multiplet of five levels. The low multiplet eliminates $4f^8 6s^2$ and answers quite well for ^9D, the expected normal state from $4f^7 5d6s^2$.

The unpublished data of King for Tm I[10] indicate an extremely simple structure for the low levels. Only a few lines appear, most of which are strong and reversed. The two most probable configurations are $4f^{12} 5d6s^2$ and $4f^{13} 6s^2$. The former configuration yields 107 levels and the latter only 2. The experimental data, although they have thus far defied analysis favor $4f^{13} 6s^2$.

---

[8] G. R. Harrison, R. S. I. **4**, 581 (1933).
[9] A. S. King, Astrophys. J. **72**, 221 (1930).
[10] A. S. King, unpublished material; Phys. Rev. **38**, 583 (1931).

TABLE I. *Classified lines of* Sa I.

I.A.	Int. and Temp. Class Arc	Fur.	Abs.	ν(vac)	Designation
8027.5	1	15 IIA		12,453.8	6 – 15
7907.48	5	40 IA		12,642.78	5 – 11
7787.02	8	60 IA		12,838.35	7 – 20
7755.32	?	80 IA	1	12,890.83	4 – 9
7686.70	8	60 IA	1	13,005.91	6 – 17
7580.91	5	60 IA	2	13,187.40	3 – 8
7554.14	8	60 IA	2	13,234.14	5 – 13
7513.3	2	8 IIA		13,306.1	5 – 15
7446.2	1	5 IIA		13,426.0	4 – 11
7403.30	8	60 IA	3	13,503.78	$^7F - {}^9G$
7378.04	5	60 IA	2	13,550.01	4 – 12
7367.9	1	4 IIA		13,568.6	3 – 9
7332.65	60	100 I	2	13,633.88	7 – 27
7279.25	80	100 I	4	13,733.90	6 – 20
7262.69	3	20 IIA		13,765.21	6 – 21
7213.82	80	100 I	10	13,858.47	5 – 17
7172.67	40	30 I	1	13,937.88	5 – 18
7141.13	30	100 I	10	13,999.53	1 – 8
7131.80	100	150 I	12	14,017.84	4 – 13
7114.50	10	80 I	3	14,051.93	3 – 10
7106.23	100	150 I	10	14,068.29	$^7F - {}^9G$
7104.54	150	200 I	10	14,071.63	$^7F - {}^9G$
7101.46	10	50 I	1	14,077.74	4 – 14
7096.33	100	150 I	12	14,087.91	2 – 9
7095.50	150	200 I	15	14,089.56	4 – 15
7091.16	100	150 I	4	14,098.19	$^7F - {}^9G$
7088.30	150	250 I	20	14,103.87	3 – 11
7056.55	40	40 I		14,167.33	
7026.62	100	200 IA	12	14,227.67	3 – 12
7002.03	2	60 IA		14,277.64	7 – 34
6912.79	3	100 IIA	1	14,461.96	6 – 26
6880.86	20	200 II	3	14,529.07	6 – 27
6860.93	300	300 I	15	14,571.27	2 – 10
6853.92	15	150 IIA	2	14,586.17	5 – 20
6839.23	10	100 IIA	1	14,617.50	5 – 21
6827.81	40	150 IA	2	14,641.95	4 – 17
6802.96	50	150 IA	2	14,695.43	3 – 13
6790.88	30	60 IA	1	14,721.57	4 – 18
6779.16	100	200 IA	5	14,747.03	2 – 12
6775.30	60	150 IA	3	14,755.43	3 – 14
6759.25	60	15 III		14,790.46	7 – 41
6725.88	300	200 I	10	14,863.85	1 – 10
6671.51	800	400 I	3	14,984.98	
6588.91	500	300 I	4	15,172.83	6 – 34
6580.53	50	200 IA	2	15,192.16	
6566.36	80	100 I	2	15,224.94	6 – 36
6563.52	150	200 I	2	15,231.53	5 – 24
6562.64	10	80 IA		15,233.57	7 – 48
6558.18	8	50 IA	1	15,243.95	7 – 49
6551.80	200	300 I	3	15,258.77	
6544.95	40	150 IA	3	15,274.75	2 – 14
6536.83	30	150 IA	3	15,293.72	5 – 25
6533.96	200	300 I	5	15,300.44	
6532.25	200	300 I	5	15,304.44	
6528.02	200	250 I	4	15,314.36	5 – 26
6509.44	50	300 IA	6	15,358.07	2 – 16
6501.00	25	100 IA		15,378.01	6 – 39
6492.05	5	25 IIA		15,399.11	3 – 18
6491.28	15	100 IA		15,401.03	4 – 21
6425.90	200	250 I	2	15,557.73	5 – 29
6387.79	4	100 IA		15,650.55	1 – 16
6373.50	10	100 IIA		15,685.64	6 – 41
6373.29	4	60 IIA		15,686.16	5 – 30
6371.01	150	150 I	2	15,691.77	7 – 52
6367.41	250	250 I	5	15,700.64	4 – 22
6295.97	15	80 IIA		15,878.80	2 – 19
6273.29	15	100 IA	2	15,936.20	5 – 32
6258.94	4	30 IIA		15,972.74	4 – 23
6242.39	60	200 IA	2	16,015.08	4 – 24
6229.07	3	20 IIA		16,049.33	6 – 45
6226.70	100	20 II		16,055.44	5 – 35
6222.55	15	30 IA		16,066.15	6 – 46
6218.23	50	150 IA	1	16,077.31	5 – 36 4 – 25
6198.37	30	125 IA	2	16,128.82	6 – 48
6196.83	2	25 IIA		16,132.83	7 – 56
6194.39	200	200 I	3	16,139.18	6 – 49
6174.45	150	150 I	2	16,191.30	
6159.56	150	200 I	2	16,230.45	5 – 39
6117.79	40	150 IA	2	16,341.26	4 – 29
6103.95	3	15 IIA		16,378.31	3 – 22
6099.90	40	200 IA	3	16,389.19	
6096.55	6	80 IA	1	16,398.19	2 – 19
6084.12	400	250 I	4	16,431.69	
6070.06	300	200 I	4	16,469.75	4 – 30
6045.00	300	150 I	3	16,538.03	5 – 41
6027.52	40	100 IA		16,585.99	4 – 31
6027.16	150	150 I	2	16,586.98	6 – 52
6004.18	200	200 I	5	16,650.46	3 – 23
5995.09	125	100 I	2	16,675.71	5 – 42
5989.68	50	150 IA	2	16,690.77	1 – 19
5979.38	200	200 I	4	16,719.52	4 – 32
5936.92	2	8 IIA		16,839.10	4 – 35
5927.89	20	60 IIA		16,864.75	6 – 54
5916.36	80	150 IA	3	16,897.61	2 – 22
5914.91	12	40 IA		16,901.76	5 – 45
5909.04	80	40 I	1	16,918.54	5 – 46
5906.05	50	40 I	1	16,927.11	4 – 37
5902.60	80	40 I	1	16,937.00	5 – 47
5895.35	4	20 IA		16,957.83	3 – 28
5883.68	10	50 IIA	1	16,991.47	5 – 49
5875.92	40	100 IA	1	17,013.91	4 – 39
5874.21	200	150 I	3	17,018.86	3 – 29
5871.06	150	125 I	2	17,027.99	6 – 56
5868.61	200	125 I	2	17,035.10	7 – 63
5867.79	250	80 II	2	17,037.48	6 – 57
5866.23	1	20 III		17,042.01	7 – 64
5860.78	4	40 IIA		17,057.86	6 – 58
5822.61	5	40 IA		17,169.68	2 – 23
5802.84	300	100 I	4	17,228.17	5 – 50
5790.91	8	50 IA		17,263.67	3 – 31
5798.38	200	80 I	3	17,271.21	6 – 59
5779.24	200	100 I	3	17,298.53	4 – 40
5746.50	5	50 IIA		17,397.08	3 – 32
5741.19	3	4 I		17,413.18	3 – 33
5732.95	300	150 II	2	17,438.20	7 – 68
5726.06	3	10 IIA		17,459.18	4 – 42
5720.19	125	60 II	2	17,477.10	2 – 28
5711.45	40	60 II	1	17,503.84	5 – 53
5707.22	3	25 IA		17,516.82	3 – 35
5706.75	80	80 I	1	17,518.26	
5706.20	300	100 rII	2	17,519.95	4 – 44
5686.98	20	20 I		17,579.16	7 – 69
5678.74	3	15 IIA		17,604.67	3 – 37
5659.86	400	200 rII	3	17,663.39	3 – 38
5652.84	30	40 I	2	17,685.33	4 – 45
5642.67	6	20 IIA		17,717.20	5 – 54
5641.59	8	10 II		17,720.59	4 – 47
5626.01	250	150 rII	3	17,769.67	1 – 28
5621.79	200	100 I	3	17,783.00	2 – 31
5591.17	20	40 IA	1	17,880.39	5 – 56
5588.20	100	30 II	1	17,889.90	5 – 57
5581.83	10	20 II		17,910.31	5 – 58
5575.59	15	20 I		17,930.36	6 – 63
5574.89	80	30 II	2	17,932.61	2 – 33
5573.42	100	60 II	2	17,937.34	6 – 64
5561.37	50	20 II		17,976.20	3 – 40
5550.40	300	200 rII	4	18,011.73	4 – 50
5548.95	150	125 I	3	18,016.44	
5517.87	1	4 III		18,117.91	6 – 66
5516.09	500d	300 rII	4	18,123.76	5 – 59 2 – 37
5512.10	200	100 I	4	18,136.88	3 – 42
5511.09	60	40 I	1	18,140.18	5 – 60
5500.90	10	25 IIA		18,173.81	3 – 43
5498.21	200	150 rII	3	18,182.70	2 – 38
5493.72	300	200 rII	3	18,197.56	3 – 44
5485.42	150	100 rII	2	18,225.09	1 – 33
5466.72	250	125 rII	3	18,287.44	4 – 53
5453.00	300	150 rII	3	18,333.45	6 – 68
5433.82	30	20 II	2	18,398.16	3 – 47
5421.57	80	30 I	2	18,439.73	5 – 61
5411.39	100	50 II	1	18,474.42	6 – 69
5411.15	10	40 IIA	1	18,475.24	1 – 38
5405.23	200	125 rII	3	18,495.47	2 – 40
5403.70	200	80 I	3	18,500.71	4 – 54
5368.352	150	80 II	2	18,622.52	7 – 76
5353.701	1	5 IIA		18,673.49	4 – 57
5349.116	15	40 IA	2	18,689.49	3 – 50
5348.067	10	30 IA	2	18,693.16	2 – 43
5341.265	100	50 I	3	18,716.96	2 – 44
5320.575	100	100 I	4	18,789.75	5 – 64
5299.21	4	15 IA		18,865.50	3 – 51
5282.891	100	50 I	2	18,923.78	4 – 60
5271.388	200	125 I	3	18,965.07	3 – 53
5269.96	5	10 IA	1	18,970.21	5 – 66
5265.646	20	25 I	2	18,985.75	1 – 43
5251.912	150	100 I	5	19,035.40	5 – 67
5210.738	10	10 I		19,185.81	5 – 68
5200.592	200	100 I	3	19,223.24	4 – 61
5187.131	10	15 I	2	19,273.13	4 – 62
5185.550	2	6 IA	1	19,279.00	3 – 55
5175.443	150	80 I	3	19,316.65	
5172.750	80	40 I	2	19,326.71	5 – 69
5157.260	20	30 I	2	19,384.75	2 – 51
5145.834	10	12 I	1	19,427.80	5 – 70
5122.159	125	60 I	3	19,517.60	6 – 76
5117.188	100	80 I	2	19,536.56	
5088.347	20	30 I	1	19,657.29	
5071.205	100	60 I	3	19,713.70	
5060.916	15	30 IIA	2	19,753.78	4 – 66
5049.503	10	30 IA	2	19,798.42	2 – 55
5044.275	80	40 I	2	19,818.95	4 – 67
5010.88	3	10 IA		19,951.02	3 – 62
4975.949	60	60 I	4	20,091.08	1 – 55
4946.305	40	60 II	2	20,211.49	4 – 70
4924.044	30	30 II		20,302.86	7 – 98
4918.994	125	100 I	2	20,323.71	4 – 71
4910.400	150	100 II	2	20,359.27	5 – 75
4907.81	2	2 III		20,370.02	5 – 76
4904.963	80	80 II	3	20,381.84	3 – 65
4883.971	200	100 II	4	20,469.44	6 – 87
4883.763	100	100 II	4	20,470.31	2 – 62
4848.309	100	100 I	2	20,620.01	5 – 78
4841.701	400	150 I	2	20,648.15	7 – 102
4789.977	50	50 II	1	20,871.11	6 – 93
4785.884	150	125 I	3	20,888.96	3 – 70
4783.125	300	200 I	3	20,901.01	2 – 65
4770.20	30	20 I	2	20,957.64	5 – 82
4760.291	300	150 rI	5	21,001.27	3 – 71
4760.033	50	60 II		21,002.40	4 – 74
4750.725	60	50 II	1	21,043.55	5 – 84
4728.433	300	100 I	2	21,142.76	4 – 75
4718.641	40	30 I	1	21,186.63	6 – 97
4717.071	150	125 I	1	21,193.68	1 – 65
4716.097	250	80 I	2	21,198.07	6 – 98
4688.733	150	100 I	2	21,321.78	5 – 87
4684.196	1	4 IIA		21,342.43	6 – 100
4681.551	50	40 II	1	21,354.48	4 – 77
4678.084	3	4 I		21,370.31	7 – 108
4670.834	60	80 I	3	21,403.48	4 – 78
4670.747	50	60 I	2	21,403.88	4 – 79
4664.509	2	10 IIA		21,432.50	7 – 109
4663.556	100	80 rI	1	21,436.86	5 – 89
4649.491	100	80 rI	3	21,501.73	3 – 73
4648.078	40	40 I	1	21,508.27	6 – 101
4645.405	100	100 rI	3	21,520.64	2 – 71
4640.518	3	8 IA		21,543.31	6 – 102
4632.770	1	8 IA		21,579.33	5 – 91
4629.430	5	20 IA	2	21,594.90	7 – 111
4618.228	2	10 IIA		21,647.28	6 – 103
4616.615	1	12 IIA		21,654.84	7 – 113
4611.248	20	50 IA	3	21,680.05	3 – 74
4602.024	1	10 IA		21,723.50	5 – 93
4598.285	4	8 IA	1	21,741.17	4 – 82
4596.743	60	100 rI	2	21,748.46	
4581.729	150	80 I	2	21,819.73	7 – 114
4581.581	100	100 rI	3	21,820.43	3 – 75
4580.188	1	12 IIA		21,827.07	4 – 84
4569.579	6	20 IA	2	21,877.74	5 – 95
4566.767	12	25 IA	1	21,891.21	4 – 85
4556.628	4	40 IA	2	21,939.92	6 – 106
4550.032	8	20 IA	2	21,971.73	5 – 96
4539.830	1	5 IIA		22,021.06	2 – 73
4537.570	2	10 IA	1	22,032.07	3 – 77
4536.161	1	20 IA	1	22,038.91	5 – 97
4534.869	1	20 IA		22,045.19	7 – 117
4533.799	50	50 I	1	22,050.39	5 – 98
4532.444	8	40 IA	3	22,056.99	4 – 86
4527.418	5	15 IA	2	22,081.47	3 – 79
4523.182	30	30 I	2	22,102.15	3 – 80
4522.546	20	30 I	2	22,105.26	4 – 87
4511.327	40	40 I	2	22,160.23	7 – 137
4504.321	1	6 IIA		22,194.70	5 – 100
4503.378	80	125 rI	3	22,199.35	2 – 74
4499.108	100	150 RI	3	22,220.42	4 – 89
4490.758	1	10 IIA		22,261.73	6 – 107
4490.019	4	30 IIA	1	22,265.40	6 – 108
4480.316	30	60 IA	2	22,313.61	1 – 73
4477.505	6	15 IA	1	22,327.62	6 – 109
4471.504	1	8 IIA		22,357.59	4 – 90
4470.886	100	100 rI	2	22,360.68	5 – 101
4470.475	1	4 IIA		22,362.73	4 – 91
4463.897	3	15 IIA	1	22,395.69	5 – 102
4459.290	80	60 I	1	22,418.82	3 – 82
4456.708	3	40 IA	2	22,431.81	3 – 83
4452.953	60	50 I	2	22,450.72	7 – 120
4445.153	80	125 rI	2	22,490.12	6 – 111
4443.270	6	15 IA	2	22,499.65	5 – 103
4442.276	80	100 rI	1	22,504.68	3 – 84
4441.812	100	150 RI	1	22,506.94	4 – 93
4433.344	3	50 IIA		22,550.03	6 – 113
4433.076	15	30 IA	1	22,551.39	2 – 77
4429.664	60	80 rI	2	22,568.76	3 – 85
4423.383	10	20 IA	1	22,600.81	2 – 79
4419.332	80	150 RIA	2	22,621.52	2 – 80
4411.585	30	60 rIA	2	22,661.25	4 – 95
4405.224	1	8		22,693.97	5 – 104
4403.116	100	150 RI	2	22,704.83	5 – 105
4401.174	100	60 I	2	22,714.85	6 – 114

TABLE I—(*Continued.*)

I.A.	Int. and Temp. Class Arc	Fur.	Abs.	ν(vac)	Designation
4397.341	60	60 I	2	22,734.65	3−86
4393.354	60	30 II	1	22,755.28	4−96
4393.170	1	20 IIA		22,756.23	7−122
4386.219	40	60 I	2	22,792.30	5−106
4381.257	1	8 IIA		22,818.11	3−88
4380.423	100	100 rI	2	22,822.45	4−97
4365.954	4	25 IA	1	22,893.09	3−89
4362.912	150	150 RI	2	22,914.05	1−80
4357.896	2	40 IIA	1	22,940.42	6−117
4355.835	2	40 IA	2	22,951.28	2−83
4350.815	6	50 IA	2	22,977.76	4−99
4339.924	5	20 IIA	2	23,035.42	3−90
4338.965	25	60 IA	3	23,040.52	3−91
4336.137	150	125 RI	2	23,055.54	6−137
4331.447	40	50 I	3	23,080.51	
4330.016	125	150 RI	3	23,088.13	2−85
4326.145	4	30 IIA		23,108.79	7−124
4325.163	2	30 IIA	2	23,114.07	5−107
4324.460	60	60 rI	1	23,117.80	5−108
4319.530	100	100 rI	2	23,144.18	4−101
4313.871	3	30 IIA	2	23,174.54	3−92
4312.854	60	30 I	2	23,180.00	5−109
4301.275	8	15 IIA	1	23,242.41	3−94
4299.141	20	40 IA	2	23,253.94	2−86
4296.743	300	300 RI	2	23,266.92	$^3F-{}^3G$
4293.743	4	15 IIA	1	23,283.18	4−103
4290.832	1−	8 IIA		23,298.97	5−110
4283.772	5	8 I		23,337.37	2−88
4283.500	80	80 rI	2	23,338.85	3−95
4282.833	80	80 rI	1	23,342.49	5−111
4282.208	100	100 rI	2	23,345.89	6−120
4274.011	2	12 IIA		23,390.66	5−112
4271.862	40	40 I	2	23,402.43	5−113
4266.309	30	20 I	2	23,432.89	3−96
4258.168	1	6	1	23,477.69	4−104
4256.209	2	12	1	23,488.50	4−105
4244.246	3	12 IA	1	23,554.70	2−90
4240.450	6	40 IA	1	23,575.79	4−106
4230.727	4	10 IA	1	23,629.97	1−88
4226.858	2	10 IIA		23,651.60	6−122
4226.178	50	60 rI	5	23,655.30	3−99
4219.306	8	40 IA	2	23,693.93	2−92
4207.250	1	6 IIA		23,761.72	2−94
4205.779	40	40 I	4	23,770.13	
4201.766	1	4		23,792.83	5−117
4183.333	60	50 rI	4	23,897.67	4−107
4164.790	1	8 IIA		24,004.07	6−124
4151.213	4	8 IA		24,082.58	4−110
4151.135	1	5 IA		24,083.03	
4147.974	1	6 IA	1	24,101.38	
4146.636	1	4 IA	1	24,109.16	3−119
4145.594	1	6 IA		24,115.22	
4145.239	20	30 I	3	24,117.28	
4142.969	1	4 IIA		24,130.50	6−125
4138.734	3	12 IIA	1	24,155.19	3−104
4135.505	10	20 IA	3	24,174.05	4−112
4106.284	1	8 IIA		24,346.07	5−121
4087.505	1	10 IIA		24,457.92	6−128
4079.834	20	40 IIA	2	24,503.91	5−122
4069.751	1	8 IIA		24,564.62	4−116
4062.320	15	40 IIA	2	24,609.55	6−131
4051.822	1	6 IIA		24,673.31	7−136
4016.111	2	4 IIA		24,892.70	4−119
4001.612	1	5 IIA		24,982.89	5−125
3998.350	40	15 I	1	25,003.27	
3991.019	30	15 I	1	25,049.20	
3990.025	300	50 rI	2	25,055.44	6−132
3978.244	5	10 IA	1	25,129.64	4−121
3974.665	150	80 RI	3	25,152.27	5−127
3972.272	1	8 IIA	1	25,167.42	3−115
3962.136	20	12 I	1	25,231.80	
3960.501	1	8 IIA	1	25,242.21	3−116
3951.887	100	60 rI	3	25,297.23	
3949.849	4	10 IA	1	25,310.29	5−128
3945.252	1	8 IIA		25,339.78	6−134
3926.325	20	20 II	1	25,461.92	5−131
3925.216	400	60 rI	2	25,469.12	3−118
3909.946	50	12 I	1	25,568.58	6−136
3901.046	3	4		25,626.92	6−138
3891.955	8	8 II	1	25,686.78	2−115
3877.486	200	?II	2	25,782.62	7−142
3858.737	200	100 r?II	4	25,907.90	5−132
3858.517	80	40 ?II	1	25,909.37	4−126
3854.556	150	?II	2	25,936.00	4−127
3853.295	200	50 r?II	1	25,944.49	6−139
3846.761	30	15 II	2	25,988.56	2−118
3834.945	5	8		26,068.63	7−144
3834.476	300	80 rII	3	26,071.81	7−145
3832.808	150	20 III	3	26,083.16	5−133
3824.811	8	8 III	1	26,137.69	4−129
3822.972	100	15 ?III	3	26,150.27	3−123
3818.363	80	20 III	3	26,181.83	4−130
3816.846	8	8 III		26,192.23	5−134
3813.827	150	30 III	3	26,212.97	7−147
3809.954	100	30 III	4	26,239.61	6−140
3806.467	60	20 III	1	26,263.68	7−148
3803.942	300	100 RII	4	26,281.09	1−118
3783.804	30	20 III	1	26,420.95	5−136
3775.459	10	15 III		26,479.35	5−138
3773.331	150	80 rII	3	26,494.28	
3766.923	20	20 III	1	26,539.35	7−150
3760.169	60	15 III	2	26,587.02	3−126
3756.411	600	100 RII	3	26,613.62	3−127
3748.521	100	80 rII	3	26,669.64	2−123
3747.360	20	15 III		26,677.90	6−142
3745.465	100	80 rII	3	26,691.40	4−132
3730.737	100	25 III	2	26,796.76	5−139
3728.162	50	20 III	2	26,815.27	3−129
3722.026	60	40 III	3	26,859.48	3−130
3721.028	150	50 III	3	26,866.68	4−133
3707.850	150	40 III	4	26,962.16	1−123
3707.629	10	12 III		26,963.77	6−144
3707.167	100	30 III	3	26,967.13	6−145
3705.995	1	10 IIIA		26,975.66	4−134
3690.084	300	50 III	2	27,091.98	5−140
3688.129	30	10 III	2	27,106.33	2−126
3687.878	200	20 III	1	27,108.17	6−147
3680.983	100	15 III	2	27,158.95	6−148
3668.887	20	10 III	2	27,248.49	7−158
3666.972	2	6 IIIA		27,262.82	4−138
3657.312	100	15 III	2	27,334.73	2−129
3651.825	4	8 III		27,375.80	5−141
3643.997	30	15 III	1	27,434.61	6−150
3636.106	30	8 III		27,494.14	6−151
3629.480	80	40 III	3	27,544.33	3−133
3604.714	4	8 III		27,733.57	7−161
3594.508	2	4 III		27,812.31	6−155
3594.004	20	12 III		27,816.21	5−144
3592.894	10	8 III		27,824.80	3−135
3586.360	80	40 III	3	27,875.40	4−140
3562.224	15	15 II	1	28,064.36	5−149
3552.206	8	10 III		28,143.51	6−158
3550.216	50	40 II	1	28,159.29	4−141
3530.07	1	4		28,319.98	7−164
3527.066	15	12 III		28,344.11	2−135
3526.779	15	15 III	1	28,346.41	5−151
3524.108	2	6 III		28,367.89	6−159
3510.15	1	4		28,480.70	5−152
3491.995	2	6 III		28,628.76	6−161
3491.040	6	8 III		28,636.59	1−135
3490.705	2	6 III		28,639.34	4−146
3487.612	4	8 III		28,664.74	5−155
3481.523	4	10 III		28,714.87	7−166
3466.796	30	20 III		28,836.85	3−141
3465.466	60	30 III		28,847.92	4−149
3457.788	1	2		28,911.47	5−156
3447.790	20	15 III		28,995.81	5−158
3446.58	1	4		29,005.99	3−143
3431.890	20	20 III		29,130.14	4−151
3427.855	2	6		29,164.44	6−163
3421.903	1	5		29,215.16	6−164
3421.304	5	8 III		29,220.27	5−159
3416.198	20	12 III		29,263.94	4−152
3411.22	1	5		29,306.65	4−153
3410.037	20	12 III		29,316.82	3−146
3408.049	4	6 III		29,333.92	4−154
3394.815	5	6		29,448.26	4−155
3391.024	3	5 III		29,418.18	5−161
3385.970	8	12 III		29,525.19	2−143
3376.246	1	2		29,610.22	6−166
3366.522	1	4		29,695.75	4−156
3352.727	6	8		29,817.93	1−143
3350.664	12	10 III		29,836.28	2−146
3338.864	8	8		29,941.72	3−152
3334.119	3	2		29,984.34	3−153
3331.935	4	4		30,003.98	4−159
3331.074	6	6		30,011.75	3−154
3330.508	4	4		30,016.85	5−163
3324.872	2	4		30,067.73	5−164
3309.885	1	3		30,203.87	7−171
3307.346	1	3		30,227.05	4−160
3291.429	15	10 III		30,373.22	3−156
3287.693	2	3		30,407.73	3−157
3283.728	2	3		30,444.45	4−162
3281.775	5	4		30,462.57	5−166
3277.354	5	6 III		30,503.66	2−153
3274.430	1	4		30,530.90	2−154
3245.802	30	10		30,800.17	4−163
3234.850	1	3		30,904.45	3−160
3232.489	6	6		30,927.01	2−157
3218.260	2	2		31,063.75	6−170
3217.706	1	2		31,069.10	4−165
3214.613	2	4		31,098.99	6−171
3212.224	1	3		31,122.12	3−162
3205.636	6	1		31,186.92	6−172
3202.201	3	4		31,219.53	1−157
3181.386	2	2		31,423.78	2−160
3177.748	3	3		31,459.76	5−169
3159.497	1	2		31,641.48	2−162
3157.688	1	1		31,659.61	7−174
3149.027	1	2		31,746.67	3−165
3135.985	2	2		31,878.70	6−173
3132.751	10	5		31,911.61	7−175
3132.288	1	1		31,916.32	5−170
3128.864	1	2		31,951.25	5−171
3120.254	2	2		32,039.41	5−172
3118.862	2	2		32,053.71	3−167
3102.867	2	2		32,218.94	3−168
3100.500	1	1		32,243.54	4−169
3098.328	1	1		32,266.14	2−165
3070.874	3	3		32,554.59	6−174
3069.144	1	1		32,572.94	2−167
3057.229	2	2		32,699.88	4−170
3054.313	2	2		32,731.10	5−173
3053.634	6	5		32,738.37	2−168
3047.254	2	2		32,806.91	6−175
3045.759	2	2		32,823.02	4−172
3041.817	3	2		32,865.55	1−167
3036.682	3	2		32,921.13	3−169
3026.588	3	3		33,030.92	1−168
2992.521	3	2		33,406.93	5−174
2982.897	2	1		33,514.71	4−173
2970.098	12	2		33,659.13	5−175

The present knowledge of the normal configurations, either definite or indicated, for the rare earths is presented in Table VI.

The data presented in Table VI show the same type of variation of relative binding between the 4*f* and 5*d* electrons as exists between the *d* and *s* electrons[11] in the long periods. In the rare earth group the 5*d* electron is most tightly bound at the beginning and middle of the group and has a minimum just before the middle and at the end of the group.

[11] R. C. Gibbs and H. E. White, Proc. Nat. Acad. Sci. **14**, 559 (1928); W. E. Albertson, Phys. Rev. **45**, 304 (1934).

TABLE II. *Energy levels of* Sa I.

Symbol	Level	J	Symbol	Level	J	Symbol	Level	J	Symbol	Level	J	Symbol	Level	J	Symbol	Level	J
1	0.00	0	30	17,959.28	4	59	20,396.67	4, 5	90	23,847.25	2	118	26,281.09	1	148	30,284.37	6
2	292.58	1	31	18,075.57	2	60	20,413.30	3, 4	91	23,852.43	3	119	26,382.25	3, 4	149	30,337.45	3, 4
3	811.92	2	32	18,209.04	3	61	20,712.80	3, 4	92	23,986.48	1, 2	120	26,471.36	6	150	30,560.04	6
4	1,489.55	3	33	18,225.13	1	62	20,762.84	2	93	23,996.55	4	121	26,619.18	3, 4	151	30,619.60	4
5	2,273.09	4	34	18,298.29	6	63	21,055.79	6	94	24,054.32	1, 2	122	26,776.98	5	152	30,754.57	3
6	3,125.46	5	35	18,328.64	3	64	21,062.82	5	95	24,150.80	3	123	26,962.19	1	153	30,796.23	2
7	4,020.66	6	36	18,350.40	4, 5	65	21,193.68	1	96	24,244.52	3	124	27,129.49	6	154	30,823.54	2
8	13,999.43	1	37	18,416.62	2	66	21,243.27	4	97	24,312.03	4	125	27,255.97	4, 5	155	30,937.80	4
9	14,380.44	2	38	18,475.28	1	67	21,308.50	3, 4	98	24,323.51	5	126	27,398.92	2	156	31,185.17	3
10	14,863.85	1	39	18,503.49	4	68	21,458.89	5	99	24,467.27	2, 3	127	27,425.54	3	157	31,219.59	1
11	14,915.83	3	40	18,788.08	2	69	21,599.84	5	100	24,467.84	4, 5	128	27,583.38	4, 5	158	31,269.01	5
12	15,039.59	2	41	18,811.11	5	70	21,700.89	3	101	24,633.74	4	129	27,627.25	2	159	31,493.41	4
13	15,507.35	3	42	18,948.80	3	71	21,813.22	2	102	24,668.79	5	130	27,671.39	2, 3	160	31,716.41	2
14	15,567.32	2	43	18,985.74	1	73	22,313.63	1	103	24,772.74	4	131	27,735.01	6	161	31,754.24	5
15	15,579.11	4	44	19,009.52	2	74	22,491.94	2	104	24,967.14	3	132	28,180.95	5	162	31,934.03	2
16	15,650.55	1	45	19,174.84	4	75	22,632.34	3	105	24,977.99	3, 4	133	28,356.24	4	163	32,289.85	4
17	16,131.53	4	46	19,161.62	4, 5	76	22,643.12	5	106	25,065.37	4	134	28,465.26	4	164	32,340.69	5
18	16,211.04	3	47	19,210.10	3	77	22,844.00	2	107	25,387.19	4	135	28,636.67	1	165	32,558.65	2
19	16,690.76	1	48	19,254.29	6	78	22,893.07	3, 4	108	25,390.91	5	136	28,694.02	5	166	32,735.62	5
20	16,859.31	5	49	19,264.60	5	79	22,893.40	2	109	25,453.11	5	138	28,752.40	4	167	32,865.57	1
21	16,890.59	4	50	19,501.27	3	80	22,914.07	1	110	25,572.10	3, 4	139	29,069.90	4, 5	168	33,030.91	1
22	17,190.19	2	51	19,677.38	1, 2	82	23,230.73	3	111	25,615.57	5	140	29,365.03	4	169	33,733.00	3
23	17,462.31	2	52	19,712.44	6	83	23,243.80	1, 2	112	25,663.67	3, 4	141	29,648.83	3	170	34,189.35	4
24	17,504.63	3, 4	53	19,776.97	3	84	23,316.62	3	113	25,675.50	5	142	29,803.32	6	171	34,224.44	5
25	17,565.84	3, 4	54	19,990.25	4	85	23,380.72	2	114	25,840.31	6	143	29,817.92	1	172	34,312.48	4
26	17,587.44	5	55	20,091.03	1	86	23,546.54	2	115	25,979.35	1, 2	144	30,089.27	5	173	35,004.21	4
27	17,654.03	6	56	20,153.47	5	87	23,594.86	4	116	26,054.15	2, 3	145	30,092.53	6	174	35,680.11	5
28	17,769.68	1	57	20,162.99	4	88	23,629.98	1	117	26,065.88	5	146	30,128.83	2	175	35,932.29	5
29	17,830.80	3	58	20,183.36	4, 5	89	23,709.98	3	137	26,181.95	6	147	30,233.63	6			

TABLE III. *Typical* ^7FG *multiplet in samarium.*

^7F / ^7G	0 0.00	1 292.58	2 811.92	3 1,489.55	4 2,273.09	5 3,125.46	6 4,020.66
1 22,914.07	22,914.05 150 2 150 RI 4362.912	22,621.52 80 2 150 RIA 4419.332	22,102.15 30 2 30 I 4523.182				Wave number Arc abs. Fur. Wavelength
2 23,380.72		23,088.13 125 3 150 RI 4330.016	22,568.76 60 2 80 rI 4429.664	21,891.21 12 1 25 IA 4566.767			
3 24,150.80			23,338.85 80 2 80 rI 4283.500	22,661.25 30 2 60 rIA 4411.585	21,877.74 6 2 20 IA 4569.579		
4 24,633.74				23,144.18 100 2 100 rI 4319.530	22,360.68 100 2 100 rI 4470.886	21,508.27 40 1 40 I 4648.078	
5 25,615.57					32,342.49 80 1 80 rI 4282.833	22,490.12 80 2 125 rI 4445.153	21,594.90 5 2 20 IA 4629.430
6 26,471.36						23,345.89 100 2 100 rI 4282.208	22,450.72 60 2 50 I 4452.953
7 27,287.58							23,266.92 300 2 300 RI 4296.743

TABLE IV. *Classified lines of* Gd I.

I.A.	Int. and Temp. Class Arc	Fur.	(vac)	Designation	I.A.	Int. and Temp. Class Arc	Fur.	(vac)	Designation	I.A.	Int. and Temp. Class Arc	Fur.	(vac)	Designation
4680.04	40	150 II	21,361.38		4286.127	100	60 II	23,324.55	5 – 23	4023.154	80	100 I	24,849.12	
4658.60	6	40 IIA	21,459.69		4274.167	40	60 II	23,389.81	1 – 15	4019.739	12	40 IIA	24,870.23	3 – 27
4654.765	4	20 IIIA	21,477.39	5 – 12	4267.010	80	80 II	23,429.04	2 – 16	4015.592	6	10 III	24,895.92	5 – 35
4647.650	30	50 II	21,510.25	5 – 14	4266.601	125	100 II	23,431.29	4 – 18	4008.339	25	50 IIA	24,940.96	4 – 30
4608.583	8	30 IIIA	21,692.59	3 – 6	4260.123	125	100 II	23,466.92	3 – 17	4006.975	6	30 IIIA	24,949.46	2 – 34
4602.932	40	60 II	21,719.22	4 – 9	4225.846	300	300 rI	23,657.26	5 – 25	3992.696	20	40 IIA	25,038.67	
4581.294	100	100 II	21,821.80	4 – 10	4225.028	20	50 IIA	23,661.84	5 – 26	3987.840	50	50 II	25,069.17	
4542.034	125	100 II	22,010.42	2 – 6	4191.628	125	100 I	23,850.38	4 – 21	3979.346	60	80 IIA	25,122.68	2 – 24
4537.820	200	150 I	22,030.86	3 – 8	4190.779	200	200 I	23,855.21	4 – 22	3974.819	30	40 II	25,151.29	4 – 33
4519.661	200	150 I	22,119.37	2 – 7	4175.539	200	150 I	23,942.28	5 – 28	3972.713	30	40 I	25,164.62	1 – 34
4506.226	200	125 I	22,185.32	3 – 9	4167.271	12	30 IIA	23,989.78	4 – 32	3969.004	60	50 I	25,188.14	2 – 27
4503.803	8	30 IIA	22,197.25	4 – 12	4157.781	15	50 IIA	24,044.53	4 – 23	3966.279	60	60 II	25,205.44	
4497.133	150	100 I	22,230.17	4 – 14	4148.864	20	40 IIA	24,096.21		3953.372	80	40 I	25,287.73	3 – 29
4486.908	125	100 II	22,280.83	5 – 17	4134.169	100	100 I	24,181.81	3 – 20	3945.548	150	100 I	25,337.88	1 – 24
4485.484	8	30 IIA	22,287.90	3 – 10	4127.3	2	4 IIIA	24,221.0	5 – 30	3943.244	30	20 II	25,352.68	
4476.144	300	150 I	22,334.41	1 – 7	4111.251	2	3 IIIA	24,316.66	3 – 21	3942.643	60	30 I	25,356.55	
4473.282	20	40 IIA	22,348.70	2 – 8	4100.269	60	50 I	24,381.79	4 – 26	3941.802	40	25 II	25,361.95	
4430.631	300	150 I	22,563.83	1 – 8	4092.718	100	80 ?I	24,426.77	5 – 31	3935.393	40	30 II	25,403.25	1 – 27
4422.409	300	150 I	22,605.78	2 – 10	4091.966	2	3 III	24,431.26	5 – 33	3934.790	200	50 I	25,407.18	3 – 30
4414.741	200	100 I	22,645.04	4 – 16	4090.418	40	30 I	24,440.55	2 – 19	3905.653	30	25 II	25,596.69	
4411.160	150	80 I	22,663.43	3 – 12	4087.847	2	10 IIIA	24,455.87	3 – 32	3904.293	20	25 II	25,605.60	2 – 29
4401.849	300	150 I	22,711.33	5 – 18	4080.534	15	30 IIA	24,499.70	2 – 20	3902.718	30	25 II	25,615.94	4 – 35
4373.831	300	150 I	22,856.85	3 – 15	4078.705	300	200 I	24,510.69	3 – 23	3874.476	8	6 II	25,802.66	
4346.624	200	150 I	22,999.92	2 – 13	4058.222	250	200 I	24,634.40	2 – 21	3867.62	8	6 ?II	25,848.40	
4346.460	400	250 I	23,000.78	4 – 17	4054.731	80	75 I	24,655.61	1 – 19	3811.989	30	15 ?I	25,852.61	
4327.106	250	200 I	23,103.66	1 – 11	4053.643	200	150 I	24,662.23	4 – 28	3843.275	40	10 I	26,012.13	
4325.691	200	200 I	23,111.21	3 – 16	4045.013	60	100 I	24,714.84	1 – 20	3840.264	6	5 II	26,032.52	
4321.202	100	100 II	23,135.23	5 – 22	4035.396	20	60 IIA	24,773.74	2 – 32					
4313.851	200	200 I	23,174.65	2 – 15	4027.613	12	30 IIIA	24,821.61	4 – 29					
4306.348	200	150 I	23,215.02	1 – 13	4023.355	60	100 I	24,847.88	3 – 26					

TABLE V. *Energy levels of* Gd I.

Symbol	Level	J	Symbol	Level	J	Symbol	Level	J	Symbol	Level	J	Symbol	Level	J	Symbol	Level	J
1	0.00	2	7	22,334.40	2	13	23,215.03	2	19	24,655.64	2	34	25,164.60		29	25,820.73	4
2	215.12	3	8	22,563.83	3	14	23,229.32	6	20	24,714.82	3	24	25,337.89	2	30	25,940.14	5
3	532.99	4	9	22,718.33	3	15	23,389.81	3	21	24,849.52	4	25	25,376.37	7	31	26,145.86	
4	999.14	5	10	22,820.91	4	16	23,644.18	4	22	24,854.34	6	26	25,380.93	5	33	26,150.43	
5	1,719.09	6	11	23,103.66	1	17	23,999.92	5	32	24,988.88		27	25,403.24	3	35	26,615.05	
6	22,225.57	2	12	23,196.43	5	18	24,430.42	6	23	25,043.67	5	28	25,661.37	6			

TABLE VI. *Normal configurations of spectra in the rare earths.*

Atomic number	Element	Normal configuration
62	Samarium	$4f^{6}6s^{2}$
63	Europium	$4f^{7}6s^{2}$
64	Gadolinium	$4f^{7}5d6s^{2}$
69	Thulium	$4f^{13}6s^{2}$
70	Ytterbium	$4f^{14}6s^{2}$
71	Lutecium	$4f^{14}5d6s^{2}$

ACKNOWLEDGMENTS

The author is especially indebted to Dr. A. S. King of the Mt. Wilson Observatory for his kindness in supplying the unpublished material both for samarium and thulium; to Mr. F. W. Paul, of this laboratory for making a special exposure to the absorption spectrum of samarium; and to Professor G. R. Harrison, under whom this work was done.

Absorption Spectrum of Lead Oxide

E. N. SHAWHAN AND FRANK MORGAN, *Mendenhall Laboratory of Physics, Ohio State University*

(Received January 16, 1935)

The spectrum of PbO has been photographed in absorption. A new system, designated as the *E* system, has been found. It is nearly coincident with the *D* system. A number of previously unclassified bands together with some new bands are assigned to a new system, replacing Mecke's *C* system. The *D* system has been extended and the new values require that $x_e\omega_e'$ be changed from 1.05 to 3.13. All three systems have the same lower level in common with the *A* and *B* systems.

INTRODUCTION

EDER and Valenta[1] photographed the band spectrum of lead oxide (PbO) and measured the wavelengths of the heads to four figures. Lamprecht[2] and Grebe and Konen,[3] using higher dispersion, repeated and extended the observations. Mecke[4] on the basis of Lamprecht's data gave a partial vibrational quantum analysis. Bloomenthal[5] made a new series of measurements of the wavelengths of these band heads on moderate dispersion spectrograms and revised and extended the vibrational analysis which had been given by Mecke. The fine-structure analysis of the bands in the *A* and *D* systems has been given by Christy and Bloomenthal.[6]

Since all observations on these bands seem to have been made in emission, it is of interest to study them in absorption in order if possible to extend them and improve the accuracy of the vibrational analysis.

EXPERIMENTAL

Chemically pure yellow lead oxide (PbO) was heated in an iron tube about 50 cm long and 2 cm in internal diameter. The tube was open at both ends so that the oxide was exposed to the air at atmospheric pressure. The tube containing the oxide was heated by means of a compressional ring Hoskins electric furnace operated at 25 volts a.c. and 400 amperes. The temperature of the tube and oxide was maintained at about 1200°C.

Light from an underwater spark with magnesium electrodes, arranged as used by Smith and Muskat,[7] was used as a source of continuous radiation in the ultraviolet. In the visible region of the spectrum continuous radiation was obtained from an ordinary incandescent lamp.

The spectrograms were taken with a Hilger Littrow mounted E-1 quartz spectrograph having a dispersion of about 5A/mm at 3100A and 14A/mm at 4200A. An iron arc provided a standard of wavelengths.

RESULTS

To the *A* and *B* systems which were analyzed by Mecke[4] and by Bloomenthal[5] nothing has been added by this investigation. It may be of interest to state that we observed these systems in absorption and also in emission from the vapor of the lead oxide in the furnace. They are more completely developed in emission.

The *D* system, which was first observed by Bloomenthal,[5] is strongly developed in absorption, making an extension of the system possible. The positions of the heads of the bands of this system are shown in Table I, together with their vibrational quantum numbers. Those marked with an (*) have been previously observed by Bloomenthal.[5] The others are reported for the first time. The heads are represented within observational error by the formula

$$\nu = 30{,}195.0 + 532.0(v'+1/2) - 3.13(v'+1/2)^2 - 722.5(v''+1/2) + 3.75(v''+1/2)^2$$

which is essentially the same as that given by Bloomenthal[5] except that it is necessary to

[1] Eder and Valenta, *Atlas Typischer Spectra*.
[2] Lamprecht, Zeits. f. wiss. Phot. **10**, 16, 33 (1911).
[3] Grebe and Konen, Physik. Zeits. **22**, 546 (1921).
[4] Mecke, Naturwiss. **17**, 122 (1929).
[5] Bloomenthal, Phys. Rev. **35**, 34 (1930).
[6] Christy and Bloomenthal, Phys. Rev. **35**, 46 (1930).
[7] Smith and Muskat, Phys. Rev. **29**, 663 (1927).

TABLE I. *Band heads in the D system.*

ν observed	v'	v''	$\nu_{obs.}-\nu_{calc.}$	ν observed	v'	v''	$\nu_{obs.}-\nu_{calc.}$
27287.7	0	4	−0.1	30234.0	3	2	−2.7
27811.3*	1	4	−2.2	30432.0	2	1	2.0
27979.3	0	3	0.0	30624.8*	1	0	−0.7
28314.3	6	7	1.5	30747.5	4	2	3.8
28480.9	5	6	−7.5	31036.0	6	3	−3.8
28679.4*	0	2	2.1	31102.5	9	5	−7.6
28843.9	3	4	0.7	31145.3*	2	0	0.3
29028.3*	2	3	3.8	31316.3	8	4	−2.1
29161.3	5	5	−8.6	31441.7	4	1	−8.5
29385.8*	0	1	1.0	31658.3	3	0	0.1
29725.2	2	2	1.7	32166.0	4	0	0.8
29909.8*	1	1	−0.7	32230.0	7	2	3.0
30100.8*	0	0	1.0	29857.0	5	4	3.1

* Reported by Bloomenthal.

raise the value of $x_e\omega_e'$ from 1.05 to 3.13 in order accurately to represent our data.

In addition to the *A*, *B* and *D* systems, a new system of bands has been observed. These bands, which are weaker than those of the *D* system, are degraded toward the red. The origin of the system is slightly farther toward the violet than that of the *D* system. The band heads of this system are represented by the formula:

$$\nu = 30{,}899.0 + 425.8(v'+1/2) - 1.48(v'+1/2)^2 - 722.5(v''+1/2) + 3.75(v''+1/2)^2.$$

Table II gives a comparison of observed and calculated frequencies together with the assignment of vibrational quantum numbers. Additional bands of this system were observed which were either too weak to measure or were obscured by stronger bands of the *D* system.

TABLE II. *Band heads in the E system.*

ν observed	v'	v''	$\nu_{obs.}-\nu_{calc.}$	ν observed	v'	v''	$\nu_{obs.}-\nu_{calc.}$
27668.0	1	5	−5.6	30463.8	1	1	5.2
27932.8	0	4	−3.0	30585.7	3	2	−2.2
27979.3	5	7	−7.5	30752.3	0	0	1.5
28247.1	4	6	0.3	30887.3	2	1	8.8
28767.9	2	4	10.6	31172.8	1	0	−0.8
29193.9	3	4	−1.5	31232.6	8	4	1.4
29747.3	1	2	−3.8	31590.5	2	0	−3.5
29883.0	3	3	−4.9	31711.7	4	1	2.4
30037.2	0	1	1.4	31809.6	6	2	−9.1
30173.8	2	2	2.8	32425.0	4	0	−0.7

In the vicinity of λλ3600–4200 Lamprecht[2] reported a number of weak bands which have not been analyzed. Bloomenthal[5] states that the bands in this region were too weak to measure on his plates. These bands are fairly strong in absorption. It has been possible to measure them with an accuracy greater than that claimed by Lamprecht[2] and to add two additional bands not recorded by him. The heads of this system are represented by the formula

$$\nu = 24{,}871.6 + 516.0(v'+1/2) - 3.5(v'+1/2)^2 - 722.5(v''+1/2) + 3.75(v''+1/2)^2.$$

The origin of this system lies between the origins of the *B* and *D* systems. It may therefore be referred to as the *C* system. It must not, however, be confused with the *C* system proposed by Mecke[4] although the origin is approximately the same. Bloomenthal[5] was able to include in his *B* system nearly all the bands originally attributed to Mecke's *C* system. The bands left out are included in the *C* system proposed here. The new values of the bands in this system are given in Table III. The bands in this table marked (*) were reported by Lamprecht[2] but not observed by us. Those marked (**) are reported for the first time.

TABLE III. *Band heads in the C system.*

ν observed	v'	v''	$\nu_{obs.}-\nu_{calc.}$	ν observed	v'	v''	$\nu_{obs.}-\nu_{calc.}$
23351*	0	2	5	25565.2	3	1	5.9
24052.6	0	1	−0.7	25780.8	2	0	1.5
24352.9	2	2	−3.9	26038.0	4	1	−9.3
24558*	1	1	−4	26278.9	3	0	4.6
24765.7	0	0	−2.6	26753.2	4	0	−9.1
25070.0	2	1	5.7	27244.8**	5	0	1.5
25278.2	1	0	0.9	27716.7**	6	0	−0.6

* Not observed by authors.
** Not previously reported.

The authors wish to express their appreciation for the many essential suggestions and helpful advice which Professor Alpheus W. Smith and Dr. R. V. Zumstein have given in the course of this work.

The Elastic Scattering of Electrons in Argon and Krypton

GLENN M. WEBB,* *Wayman Crow Laboratory of Physics, Washington University, St. Louis, Mo.*

(Received January 7, 1935)

Scattering coefficients have been experimentally determined for the elastic scattering of electrons in argon and krypton for the angular range 5° to 150° and incident electron energies 25 to 950 volts. In argon it was found that one maximum and two minima are present up to 150 volts. In the scattering by krypton maxima of two different orders are observed, the first being prominent from 25 to 100 volts, the second appearing at 100 volts for large angles. With increasing energies the first order maximum changes position progressively to smaller angles and merges with the main body of the scattering at about 200 volts in argon and 350 volts in krypton. From 300 to 800 volts one minimum only occurs in argon. There is a single maximum in the range 350 to 950 volts in krypton. The experimental results are compared with theoretical curves. At low voltages (for A) the agreement is only qualitative when Henneberg's phases are used, while (for Kr), using Holtsmark's phases, the agreement is excellent. At higher voltages (500 to 800 volts in A, and 700 to 900 volts in Kr) the scattering is given quite accurately by the Born approximate equation for a limited angular range.

INTRODUCTION

THE elastic scattering of electrons by the rare gases has been investigated experimentally by several physicists. Accurately determined scattering coefficients[1] for these gases are now available for certain angular and primary electron energy ranges. The following Table I summarizes the experimental results obtained up to the present. Only those researches are here mentioned which contain results in tabulated form.

A glance at this table indicates that for the rare gases He and Ne the scattering has been investigated over sufficiently extensive a range of both angles and primary electron energies to enable one to check the curves computed theoretically. As regards argon and krypton there is a definite lack of information at large angles (above 100°) and at small angles (below 20°) throughout the range of primary electron energies 25 to 900 volts. For this reason it was thought advisable to determine the scattering for these two gases over the range of angles 5° to 150° and incident electron energies of 25 to 900 volts.

EXPERIMENTAL PROCEDURE

The experimental method used will not be discussed in detail since the apparatus has been described in a previous report.[5] The argon and krypton were used directly from the manufac-

TABLE I. *Summary of experimental results on the scattering of electrons by rare gases.*

Gas	Angular range	Voltage range	Ref.
Helium	10°–150°	25–700	2
	20°–140°	4–50	3
	15°–167°	1.8–19.2	4
Neon	10°–150°	15–800	5
	10°–120°	29–412	6
	10°– 40°	813	6
	30°–130°	6–30	3
	15°–167°	0.99–15.9	4
	20°–155°	50–150	7
Argon	15°–120°	42–780	6
	20°–130°	6–30	3
	40°–160°	30–150	7
	15°–167°	0.6–12.5	4
Krypton	15°–120°	41–800	6
	15°–167°	0.83–10.6	4
Xenon	15°–120°	42–800	6
	15°–167°	0.61–8.1	4

* This article is part of a dissertation to be presented to the Board of Graduate Studies of Washington University in partial fulfilment of the requirements for the degree of Doctor of Philosophy.

[1] The scattering coefficient is defined as the number of electrons scattered in a direction θ to the original beam, through unit solid angle, per unit length of path of the original beam, per single electron in the beam, per single atom in unit volume.

[2] A. L. Hughes, J. H. McMillen and G. M. Webb, Phys. Rev. **41**, 154 (1932).

[3] E. C. Bullard and H. S. W. Massey, Proc. Roy. Soc. **A133**, 637 (1931).

[4] C. Ramsauer and R. Kollath, Ann. d. Physik **9**, 756 (1931); **12**, 529 (1932).

[5] A. L. Hughes and J. H. McMillen, Phys. Rev. **43**, 875 (1933).

[6] F. L. Arnot, Proc. Roy. Soc. **A133**, 615 (1931).

[7] C. B. O. Mohr and F. H. Nicoll, Proc. Roy. Soc. **A138**, 469 (1932).

turer's containers; the labels thereon stated the gases were better than 99 percent pure.

In the experiments with argon the gas was allowed to leak out of the container through a small capillary tube continuously; the rate of pumping was so adjusted that the proper pressure (to insure single electron collisions only) was maintained. In the work with krypton this method could not be used due to its comparative rarity and high cost. The method was to seal the pumps off from the apparatus after it had been baked out for two hours at about 250°C, allow a small quantity of gas to enter the collision chamber and then circulate the gas by means of a fast pump in series with a trap cooled with solid CO_2 to remove impurities. The increase in pressure under these conditions with the electron gun operating was less than three percent over a period of four hours. A single run required, on the average, about an hour.

Experimental Results

(1) Argon

The results obtained for argon are tabulated in Table II in arbitrary units and illustrated graphically in Figs. 1 and 2.[8] The most prominent feature is a maximum occurring at about 90° for the lower voltages. It is very small at 150 volts and at 240 volts is perceptible only in the form of a kink in the scattering curve. A very

Table II. *Elastic scattering of electrons in argon.* (Arbitrary units.)

θ \ V	25	50	100	150	240	360	510	780
5							620	602
10		146	118	172	414	1840	262	207
15		98.5	64.8	92.2	144	940	121	86.0
20	45	67.5	40.1	48.0	78.0	520	48.5	37.1
25		46.8	24.8	27.2	39.2	301	27.9	17.0
30	31	33.3	15.8	17.8	24.6	184	16.9	9.91
40	18.0	18.4	6.80	7.80	12.8	89.1	7.8	4.32
50	11.4	8.4	3.38	4.82	8.7	47.2	4.72	2.21
60	6.22	3.0	2.50	3.41	6.2	30.1	2.86	1.24
70	2.95	2.01	2.62	3.02	4.3	19.9	1.85	.763
80	2.57	3.22	3.02	3.17	3.2	14.6	1.32	.565
90	3.09	5.55	3.35	2.69	2.2	10.2	1.20	.455
100	3.91	6.02	2.95	1.50	1.0	9.3	1.09	.400
110	3.69	5.20	2.01	0.83	1.2	10.2	1.26	.378
120	2.69	3.50	1.25	0.93	1.81	12.3	1.36	.400
130	2.19	1.42	1.35	2.42	2.95	15.5	1.70	.431
140	2.12	1.30	2.87	4.68	5.70	20.9	2.26	.525
150	2.30	2.61	5.70	8.61	1.12	28.4	3.02	.660

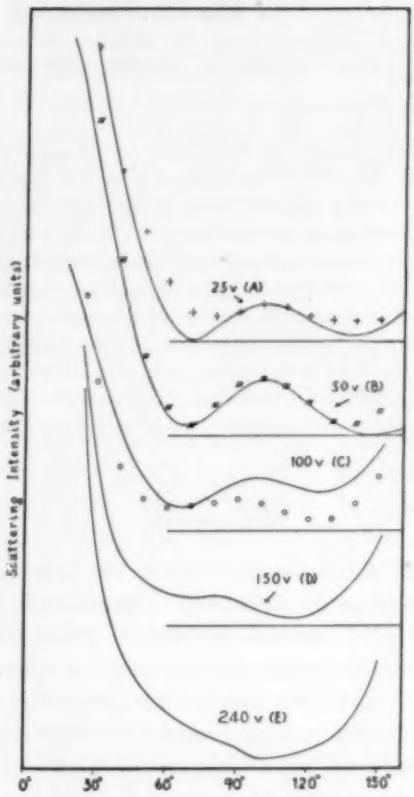

Fig. 1. Elastic scattering of electrons in argon. *A*, *B* and *C*, comparison of experimental points with theoretical curves; *D* and *E*, experimental curves.

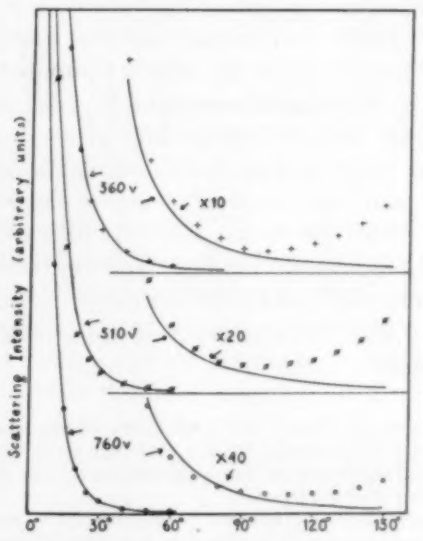

Fig. 2. Elastic scattering of electrons in argon. *Solid lines*, Born's approximate curves (Hartree field); *points*, experimental values.

[8] On these same graphs are plotted theoretical curves which will be discussed later.

prominent minimum is also present throughout the whole range of electronic velocities investigated. It shifts its position steadily from 145° at 25 volts to 96° at 760 volts.

The agreement of these results with those previously obtained by other investigators is good. Arnot's 240 volt curve is in excellent agreement with the present corresponding curves. Mohr and Nicoll's results at 150 volts are checked except for a very slight maximum which is not present in their curve. The general angular shift of maxima and minima is in agreement with Arnot's observations.

(2) Krypton

The experimental results obtained for krypton are given in Table III in arbitrary units; Figs. 3 and 4 illustrate the results graphically.[8] The main feature of this set of curves is the occurrence of a single maximum at low energies which merges with the main body of the scattering above 250 volts. Above 55 volts a second maximum appears which, as the energy of the colliding electrons is increased, retreats into smaller angles. This second maximum is present up the the highest voltage used (950 volts).

The general nature of these curves is the same as found by Arnot. His 54 and 820 volt curves, for example, agree very well with the present 55 and 780 volt curves, respectively, at large angles.

In view of the good agreement of the present results with those obtained by other investigators, it is believed that they are free from serious error due to peculiarities of the apparatus used and accurately represent the true scattering.

TABLE III. *Elastic scattering of electrons in krypton.* (Arbitrary units.)

θ \ V	25	55	100	250	350	510	780	950
°								
5		3210	7560	(835)	342			790
10		1950	4220	341	286	262	230	192
15		1160	2410	142	960	121	92.3	85.3
20	92.5	657	1310	65.0	45	64.5	48.1	40.1
25	62.8	455	613	31.8	21.5	37.1	26.7	18.6
30	43.3	242	233	13.8	14.5	23.3	16.8	12.4
40	20.6	53.4	20.1	10.1	8.23	9.35	7.32	5.90
50	10.2	15.8	22.5	11.1	4.55	3.87	3.77	2.47
60	4.02	29.2	55.2	6.50	2.55	2.08	2.07	1.10
70	1.92	40.8	53.0	2.1	1.31	1.42	1.26	1.03
80	2.65	32.9	29.2	1.1	1.35	1.60	.917	1.55
90	4.48	18.6	12.8	2.8	2.42	2.74	1.53	1.54
100	5.62	2.43	8.31	4.9	3.35	2.93	1.54	1.15
110	4.37	2.41	8.92	6.5	2.33	1.85	.693	.49
120	2.85	1.45	21.8	4.7	.91	.58	.713	.58
130	1.69	2.88	27.3	2.0	.58	.88	1.56	1.50
140	.79	5.20	16.2	1.4	2.36	2.90	3.05	2.31
150	.43	10.7	2.95	5.3	5.52	7.35	5.22	2.85

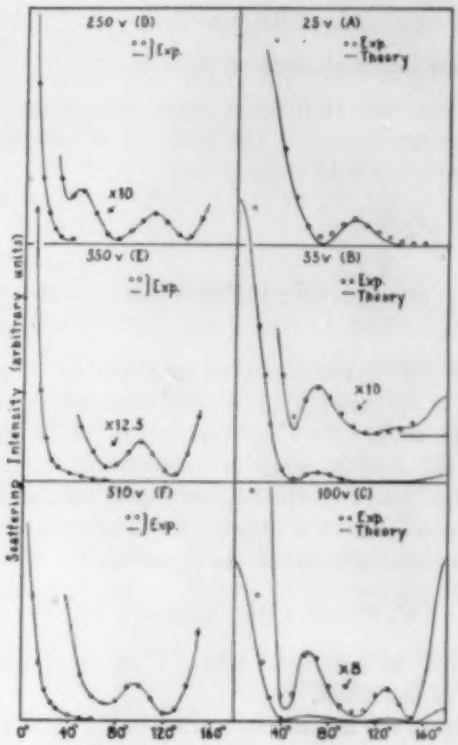

FIG. 3. Elastic scattering of electrons in krypton. *A*, *B* and *C*, comparison of experimental points with theoretical curves; *D*, *E* and *F*, experimental curves.

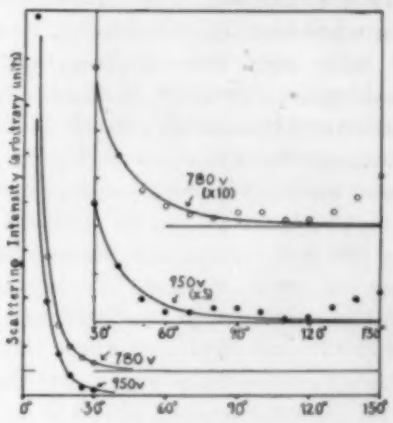

FIG. 4. Elastic scattering of electrons in krypton. *Solid lines*, Born's approximate equation (Thomas-Fermi field); *points*, experimental values.

Discussion

A. Low incident electron energies

Faxen and Holtsmark have shown that the elastic scattering of electrons by a spherically symmetrical field is given by [9]

$$I(\theta)=|F(\theta)|^2 =\frac{1}{4E}\left|\sum_{l=0}^{\infty}(2l+1)P_l(\cos\theta)(e^{2i\delta_l}-1)\right|^2, \quad (1)$$

where $I(\theta)$ is the scattered intensity at an angle θ, E is the energy of the incident electrons in atomic units ($E=1$ corresponds to 13.54 volts), l is the orbital angular momentum quantum number, and P_l is the Legendre polynomial of the lth degree. δ_l is the phase difference between the asymptotic solution of the equation

$$[d^2/dr^2+E+2V-l(l+1)/r^2]\psi=0, \quad (2)$$

when V is zero, and when V is the potential field of the atom.

Before the actual evaluation of Eq. (1) can be carried out, it is necessary to determine the phase differences. Holtsmark[10] has computed exact phase shifts for argon and krypton for values of E from 0 to 4 using the self-consistent field given by Hartree's method. His calculations also include a correction for polarization. Arnot and Baines[11] have very recently computed phase shifts for krypton ($E=0, 1, 4, 9$) using Jeffry's approximation and Holtsmark's atomic field values.

To compute theoretical curves for krypton in the present work, Holtsmark's exact phase shifts (for $l=0, \cdots, 4$) for 25 and 55 volts were used. For the 100 volt curve, the phase shifts (for $l=0, \cdots, 6$) were obtained by interpolating between the values given by Arnot and Baines for 55 and 121 volt electrons. These three theoretical curves are shown in Fig. 3, and the agreement with the experimental points is seen to be exceptionally good.

Since the phase-shifts have not yet been computed for argon using the Hartree field at moderate voltages, a method developed by Henneberg,[12] using the W-K-B approximation and the Thomas-Fermi field was used. The phase shifts are determined by the equation

$$\delta_l=\int_R^{\infty}\left[E+2V-\frac{l(l+1)}{r^2}\right]^{1/2}dr -\int_{R_0}^{\infty}\left[E-\frac{l(l+1)}{r^2}\right]^{1/2}dr, \quad (3)$$

where R and R_0 are the roots of the respective integrands, E is the incident electron energy and V is the potential field of the atom under consideration, given by

$$V=(Z/r)\varphi(r/\mu); \quad \mu=0.885/Z^{1/3}. \quad (4)$$

Upon substituting equation (4) in (3) we note that the resulting formula for $\delta_l Z^{-1/3}$ remains invariant if we place

$$EZ^{-4/3}=E_1Z_1^{-4/3}; \quad l(l+1)Z^{-1/3} =l_1(l_1+1)Z_1^{-1/3}, \quad (5)$$

where E, Z and E_1, Z_1 are corresponding values of the incident electronic energy and atomic number of the scattering atom. If we define a quantity, q, such that

$$q=(Z_1/Z)^{1/3},$$

it is seen that

$$\delta_Z(E)=q^{-1}\delta_{Z_1}(q^4E),$$

and the value of l is changed according to the relation

$$l_Z=q^{-1}(l_{Z_1}+\tfrac{1}{2})-\tfrac{1}{2}.$$

Henneberg has computed the phase shifts for mercury ($Z_1=80$) by graphical integration of Eq. (3) for $l=0, \cdots, 10$ and $E=0$ to 50. Hence we can immediately compute from his results the phase shifts for any atom of atomic number Z sufficiently large to make the use of the Thomas-Fermi field valid. Thus the phase shifts for argon have been determined by this method for primary electron energies from 25 to 100 volts.

Henneberg points out that for low velocity electrons (but not so low that exchange effects are appreciable) one can get an accurate picture of the shape of the angular distribution curves by using in the evaluation of Eq. (1) only those

[9] H. Faxen and J. Holtsmark, Zeits. f. Physik **45**, 307 (1927).
[10] J. Holtsmark, Zeits. f. Physik **55**, 437 (1929); **66**, 49 (1930).
[11] F. L. Arnot and G. O. Baines, Proc. Roy. Soc. **A146**, 651 (1934).
[12] W. Henneberg, Zeits. f. Physik **83**, 555 (1933).

terms for which $\delta_l \geq \pi/2$. The reason for this is that the products $(2l+1)\sin 2\delta_l$ and $(2l+1)(1-\cos 2\delta_l)$, being the coefficients of the lth Legendre polynomial P_l, determine the relative contributions of the various P's. Obviously, since δ_l decreases monotonically with increasing l (for large l, roughly as l^{-3}) that value of δ_l nearest to $\pi/2$ will have most effect in determining the shape of the scattering curve.

To test this out for argon, the theoretical curves for 25, 50 and 100 volts are plotted in Fig. 1 on the same graphs as the experimental points. For each of these curves the first three values of δ_l (for $l=0, 1, 2$) were used. The agreement is best for 50 volts, good for 25 volts and only fair for 100 volts. In this last curve, the shape (i.e., the positions of maxima and minima) is predicted quite accurately, but the absolute magnitude of the scattered intensity is considerably in error. Thus we see that as the incident electron energy increases we must include in our evaluation of Eq. (1) a correspondingly greater number of terms.

This lack of complete agreement between theory and experiment at 100 volts may also be partially explained by the following factors: (1) Use of the Thomas-Fermi rather than the Hartree field; (2) neglect of polarization which, according to Massey and Mohr,[13] is of considerable importance, and (3) neglect of exchange. The excellent agreement of the low voltage krypton experimental results with theory substantiates these conclusions when it is remembered that there the Hartree field was used and polarization was taken into account. In an attempt to get better agreement with experiment, phases for argon are being calculated using the Hartree field as given by Holtsmark.

B. High incident electron energies

When the incident electron energy is sufficiently high, it is of interest to compare the experimental results with Born's approximate equation. Mott[14] has put this equation in a convenient form by making use of the F-factors calculated from the self-consistent field:[15]

$$I(\theta) = (e^4/4m^2v^4)(Z-F)^2 \operatorname{cosec}^4 \theta/2. \quad (6)$$

When the Thomas-Fermi field is used, an integral equation connecting the scattered intensity and scattering angle is obtained which can only be solved by numerical integration. Mitchell[16] and Bullard and Massey,[17] carrying out this integration, have tabulated $I(\theta)Z^{-2/3}$ as a function of $Z^{-1/3}v \sin \theta/2$.

For heavy atoms the Born approximate equation obtained with either of the above atomic fields should be valid; but as the atomic number decreases the Hartree field can be expected to give better results than the Thomas-Fermi field.

In Fig. 2 Eq. (6) has been plotted for 760, 510 and 360 volt electrons in argon. The agreement at the highest voltages is good to angles up to about 100 degrees, while at 360 volts the experimental curve rises above the theory curve below 10° and at large angles.

In Fig. 4 the Born approximate equation has been plotted using the Thomas-Fermi field for krypton at 950 and 780 volts. It is seen that for both curves the experimental results fit the theory up to about 40°; beyond this point the experimental curve oscillates about it.

In order to obtain better agreement between theory and experiment at these high energies, it appears that only one additional factor need be taken into account: distortion. The general effect of including distortion is to introduce maxima and minima in the angular distribution curves. Since the Born approximate equation is valid at small angles we should expect excellent agreement between theory and experiment throughout the complete angular range if distortion were included. The effect of exchange and polarization are undoubtedly small at these energies.

Conclusion

It is a pleasure for the writer to acknowledge his indebtedness to Professor A. L. Hughes, who suggested and directed this research, for his continued interest throughout the course of the work.

[13] H. S. W. Massey and C. B. O. Mohr, Proc. Roy. Soc. **A146**, 880 (1934).
[14] N. F. Mott, Proc. Roy. Soc. **A127**, 658 (1930).
[15] R. W. James and G. W. Brindley, Phil. Mag. **12**, 81 (1931).
[16] A. C. G. Mitchell, Proc. Nat. Acad. Sci. **15**, 520 (1929).
[17] E. C. Bullard and H. S. W. Massey, Proc. Camb. Phil. Soc. **26**, 556 (1930).

The Elastic Scattering of Electrons in Molecular Hydrogen

GLENN M. WEBB, *Wayman Crow Laboratory of Physics, Washington University, St. Louis, Mo.*

(Received January 7, 1935)

The distribution-in-angle of electrons scattered elastically by molecular hydrogen has been investigated throughout the angular range 5° to 150° with incident electron energies varying from 30 to 912 volts. At low energies (30 to 100 volts) a single minimum occurs at about 90°. At the higher energies (200 to 912 volts) the curves all fall monotonically with angle. The experimental results are compared with theory. At low velocities of impact the agreement is excellent up to 100° when the Born formula is altered to take into account polarization. At the higher velocities the Born formula gives quite accurately the scattering up to about 60°. Beyond 60° the experimental points all fall consistently above the theoretical curves. A comparison of the theoretical atomic and molecular curves with the 100 volt experimental values is made. The curve for the molecule agrees best with the experimental data. In an attempt to detect the diffraction pattern in the experimental H_2 curves, the experimental molecular scattering coefficients were divided by the theoretical atomic scattering coefficients; this ratio was then plotted as a function of $2\pi mva_0 \sin \frac{1}{2}\theta/h$ and compared with the predicted curve. Agreement is good to about 70° for 912 volt incident electrons.

INTRODUCTION

THIS paper is an account of an investigation of the angular distribution of electrons scattered elastically by molecular hydrogen. The problem is of considerable fundamental importance because of the comparative simplicity of the hydrogen molecule. This molecule is the only one for which extensive theoretical calculations have been made.

Much work has been done on the problem of electrons elastically scattered by hydrogen. Arnot[1] determined the scattering coefficient[2] over a range of angles of 10° to 120° and voltages of 29 to 205 volts, and from 10° to 40° for 412 and 820 volts. Bullard and Massey[3] working with electrons in the low energy region 4 to 30 volts give values of the scattered intensity for angles from 20° to 120°. Ramsauer and Kollath[4] investigated the scattering at very low energies (1.15 to 11.0 volts) over the angular range 15° to 165°. Hughes and McMillen[5] have worked with 35 to 200 volt electrons (50° to 170°), checking the general characteristics of the scattering curves in this region observed by others. As yet no extended results have been published which have been obtained with a single apparatus and which might be used to check adequately existing theories. Hence, it was thought to be desirable to determine the scattered intensity accurately over a wide range of angles and voltages. The angular and voltage ranges investigated in the present research were 5° to 150° and 30 to 912 volts respectively.

EXPERIMENTAL METHOD

The apparatus used in this work is the same as was used in the study of argon and krypton.[6] The hydrogen was made by electrolyzing a dilute solution of H_2SO_4; the wet gas was dried and purified by allowing it to run slowly through three traps in series immersed in liquid air. (The last one contained outgassed activated charcoal.) The gas was collected in a Pyrex liter flask which had been previously baked out at 400°C.

Since the scattering from H_2 is so small, difficulty was experienced in getting rid of the background scattering. However, by baking the apparatus at 250°C just before using, the background scattering was reduced to a minimum. At angles above 90° it varied from two to eight percent of the total scattering. The final read-

* This article is part of a dissertation to be presented to the Board of Graduate Studies of Washington University in partial fulfilment of the requirements for the degree of Doctor of Philosophy.

[1] F. L. Arnot, Proc. Roy. Soc. **A133**, 615 (1931).

[2] The scattering coefficient is defined as the number of electrons scattered in a direction θ to the original beam, through unit solid angle, per unit length of path of the original beam, per single electron in the beam, per single atom in unit volume.

[3] E. C. Bullard and H. S. W. Massey, Proc. Roy. Soc. **A133**, 637 (1931).

[4] C. Ramsauer and R. Kollath, Ann. d. Physik. **12**, 529 (1932).

[5] A. L. Hughes and J. H. McMillen, Phys. Rev. **41**, 39 (1932).

[6] See preceding paper of this journal.

ings were corrected by the proper amount in each case.

Experimental Results

The experimental results are tabulated in arbitrary units in Table I and illustrated graphically in Figs. 1 and 2. On these same graphs are plotted theoretical curves to be discussed later. It will be noticed that at 30, 50 and 100 volts there is a pronounced minimum in the region 100°–120°. At 200 volts and above, the minimum disappears and the curves all fall monotonically with angle.

Table I. *Elastic scattering of electrons in molecular hydrogen.* (Arbitrary units.)

θ \ V	30	50	100	200	350	600	912
5	203	215			4140	(7270)	(3910)
10	170	141.5		502	750	1530	915
15	135	95.8	337	208	180	377	337
20	111	51.3	228	121	72	198	161
25	85.2		150.5	79.4	26.5	113	90
30	63.7	26.5	96.9	48.2	15.4	63.3	49
40	33.0	11.7	44.7	18.6	7.20	29.9	21.3
50	19.0	5.53	23.4	11.4	4.63	17.8	7.30
60	11.2	3.23	14.3	8.01	2.90	9.0	4.00
70	6.68	1.99	10.4	5.44	1.80	5.13	3.06
80	4.28	1.33	7.37	4.30	1.42	4.01	2.42
90	3.45	1.12	5.57	3.62	1.11	3.35	1.96
100	3.40	1.09	4.62	3.32	.93	2.71	1.60
110	3.87	1.17	4.72	3.20	.83	2.31	1.31
120	5.34	1.41	4.98	3.03	.74	2.20	1.01
130	7.28	1.69	6.15	2.68	.67	1.91	.72
140	8.79	1.97	7.75	2.51	.63	1.72	.63
150	9.87	2.42	10.1	2.06	.59	1.61	.53

The agreement with previous works is good as regards the general characteristics of the curves. In Fig. 1, Arnot's 29 and 200 volt points are shown. Bullard and Massey's 30 volt results (not shown) agree with the present 30 volt curve better than do Arnot's or Hughes and McMillen's. The latter's 100 volt curve is in good agreement with the present curve.

The values of the scattering coefficients obtained are believed to be free from serious error because they agree closely with those obtained by other investigators in the overlapping regions. Since the apparatuses used were of widely different types, we are justified in saying then that these results really represent the true scattering.

Discussion

The theory of the scattering by molecules is a much more complicated phenomenon than the scattering by atoms. The atomic field is spherically symmetrical while the molecular field (for H_2) is axially symmetrical. The method of the self-consistent field has not yet been applied to this type of field, but for the hydrogen molecule Wang[7] and Rosen[8] have applied variational methods to the problem and obtained approximate wave functions.

Using these approximate wave functions, Massey and Mohr,[9] assuming the applicability of Born's approximation, have shown that the scattering by a number of independent axially symmetrical fields will be a function only of v sin $(1/2)\theta$ (v is the velocity of the incident electrons and θ the angle of scattering) when the axes of these fields are oriented at random. The final result obtained by Massey and Mohr is that

$$I(\theta)=(1+\sin x/x)(I_1+I_2)^2 \\ +\text{higher order terms}, \quad (1)$$

where $I(\theta)$ is the scattered intensity per unit solid angle at an angle θ, "I_1 gives the scattering by the two atoms considered separately, but with effective nuclear charge 1.166; I_1 gives the effect of the molecular binding in producing a concentration of charge between the nuclei, and $(1+\sin x/x)$ is the diffraction factor due to the two scattering centers."[10] In this equation $x=4\pi mvd \sin (1/2)\theta/h$ where d is the equilibrium nuclear separation ($\leqq 0.80\times10^{-8}$ cm).

In order to evaluate the Eq. (1), I_1 was calculated from the expression

$$I_1=\pi^2Z^{-3}(2Z^2+K^2)(Z^2+K^2)^{-2}, \\ Z=1.166/a_0;\ K=2\pi mv \sin \tfrac{1}{2}\theta/h, \quad (2)$$

where a_0 is the radius of the first Bohr orbit ($\leqq 0.53\times10^{-8}$). I_2 is given in the form of an integral equation which is not amenable to direct calculation. However, Massey and Mohr have computed the ratio $(I_1+I_2)/I_1\equiv\lambda$ for hydrogen. Hence, after obtaining I_1 from Eq. (2), and using these values of λ, we can compute the sum (I_1+I_2).

In this manner complete scattering curves for molecular hydrogen have been computed for

[7] H. Wang, Phys. Rev. **31**, 579 (1928).
[8] N. Rosen, Phys. Rev. **38**, 2099 (1931).
[9] H. S. W. Massey, Proc. Roy. Soc. **A129**, 616 (1930); Massey and Mohr, ibid. **A135**, 258 (1932).
[10] See Mott and Massey, *Theory of Atomic Collisions*, Oxford University Press, page 205.

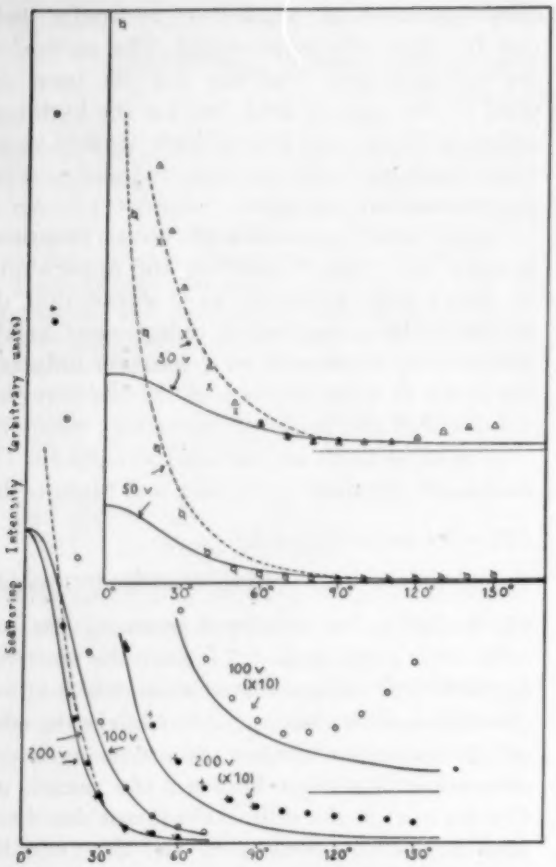

FIG. 1. Elastic angular distributions in hydrogen. *Solid line*, calculated using Born's approximate equation; *dashed line*, calculated taking polarization and distortion into account also. *Crosses*, Arnot's 29 volt experimental values; *plusses*, Arnot's 205 volt experimental values. *All others:* Author's observed values.

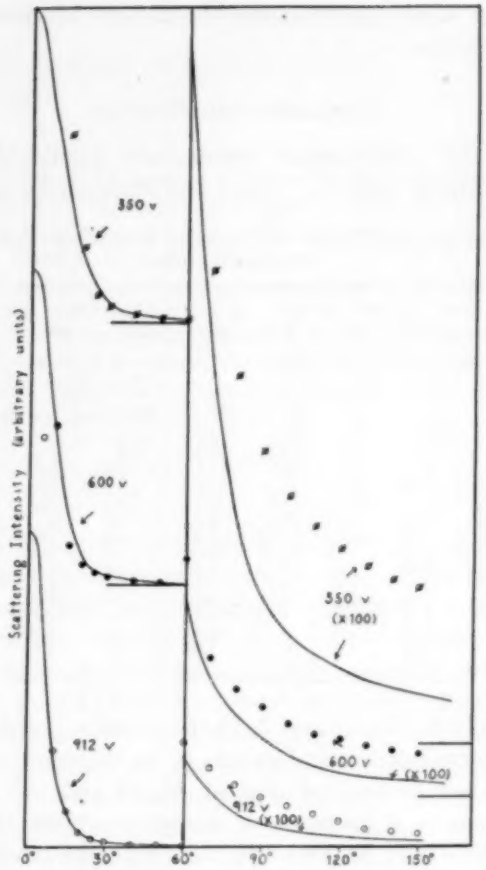

FIG. 2. Elastic angular distributions in hydrogen. *Solid lines*, Calculated using Born's approximate equation; *points*, Experimental values.

primary electron energies 30–912 volts. These have been reproduced in Figs. 1 and 2 in solid lines along with the experimental points. Each set of experimental points has been fitted arbitrarily to its corresponding theoretical curve. We see that at intermediate angles (10° to 70°) the Born approximate equation appears valid from about 100 to 912 volts. But even at 912 volts for large angles the experimental points fall consistently above the curve predicted by the theory. At the lower voltages (30–100 volts) the experimental curves rise much more rapidly at small angles than do the theoretical curves; further, at large angles, the increase in scattering observed experimentally is not present in the calculated curves.

To explain the departures of the observed curves from the theoretical curves it is necessary to recall the approximations made in the theoretical development. Born's approximation assumes that the atomic field is undisturbed by the incident electrons and that the effect of the atomic field on the colliding electron is small. This approximation takes into account neither distortion (disturbance of the incident and scattered electron waves by the field of the atom) nor exchange nor polarization (disturbance of the atomic field by the incident electron).

The effect of distortion is best studied by the method of Faxen and Holtsmark.[11] In order to

[11] See Mott and Massey, *Theory of Atomic Collisions*, Chapter X, for detailed discussion.

apply this method to the scattering of electrons by molecules, however, it is necessary to take a much simplified form for the molecular field. Stier[12] has done considerable work on the problem, and using a field suggested by Allis and Morse's[13] simplified atomic field, has arrived at a formula very similar to Eq. (1) of the preceding paper yet more complicated. As far as the writer knows this formula has not been evaluated for hydrogen, but the general result expected would be the appearance in the angular distribution curves of maxima and minima in analogy with the scattering by atoms. (Probably for H_2 a single minimum would be predicted, since that alone is observed experimentally).

The effect of exchange has been studied by several theoretical physicists. Massey and Mohr[14] state that this effect is quite negligible in atomic hydrogen when the incident electron energy is greater than 70 volts; Morse and Allis[15] give a lower value (30 volts) to the energy at which exchange effects seriously begin to affect the angular distribution curves. Hence, we are certain that the lack of agreement of the present experimental and theoretical curves will not be appreciably improved by inclusion of exchange considerations.

A recent paper by Massey and Mohr[16] has to do with a detailed study of the polarization effect in hydrogen (atomic) and helium. They point out that the scattered amplitude can be considered as comprising the sum of three terms: That given by Born's first approximation plus terms due to the polarization and distortion effects. They have calculated, for atomic hydrogen, scattering curves (5° to 100°) for 205, 54, 29 and 83 volts. The first three of these were compared with experimental curves for 200, 50 and 30 volts respectively. These calculated curves are shown in Fig. 1 (dotted lines). The agreement with experiment is seen to be excellent.

Thus we see that over the angular range 10° to 100° the experimental results are adequately explained only when terms arising from polarization and distortion are added to the Born approximate equation. Since these two effects become rapidly less prominent as the voltage is increased, it is not yet clear why the experimental curves at high voltages and large angles lie above those calculated from the Born equation. Perhaps the effect of molecular binding is larger at these energies and angles than has previously been thought to be the case. Also, the use of a better wave function, such as that of James and Coolidge,[17] might give better agreement between theory and experiment.

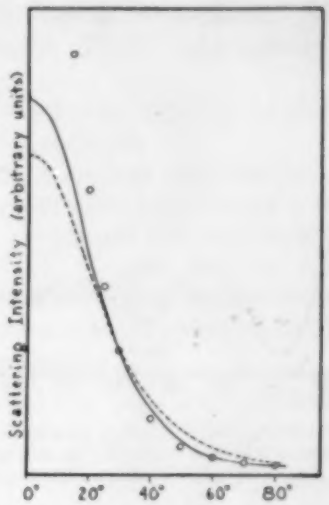

FIG. 3. Comparison of observed values (100 volts) with theoretical atomic and molecular curves. *Solid line*, Theoretical molecular curve; *dashed line*, Theoretical atomic curve; *circles*, Observed values.

It is of interest to compare the experimental curves for H_2 with those calculated from the Born approximate equation for the atom and molecule. In Fig. 3 this comparison has been made for 100 volt electrons. The solid curve is for molecular hydrogen, the dashed curve for atomic hydrogen and the circles are the experimental points. All three curves have been fitted at 30°. It is seen that the experimental points agree most closely with the curve computed for molecular hydrogen.

It is also of interest to detect, if possible, the existence of a diffraction pattern in the scattering curve. Because of the $(1+(\sin x)/x)$ factor this is to be expected; however, owing to the rapidity

[12] H. Stier, Zeits. f. Physik **76**, 439 (1932).
[13] W. P. Allis and P. M. Morse, Zeits. f. Physik **70**, 567 (1931).
[14] H. S. W. Massey and C. B. O. Mohr, Proc. Roy. Soc. **A132**, 605 (1931); **A136**, 289 (1931); **A139**, 187 (1932).
[15] P. M. Morse and W. P. Allis, Phys. Rev. **44**, 269 (1933).
[16] H. S. W. Massey and C. B. O. Mohr, Proc. Roy. Soc. **A146**, 880 (1934).
[17] H. M. James and A. S. Coolidge, J. Chem. Phys. **1**, 825 (1933).

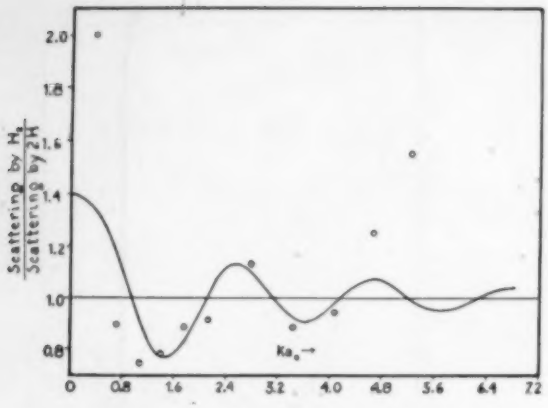

FIG. 4. Illustrating the diffraction pattern in hydrogen. *Ordinates*, Ratio of the scattering by H_2 to the scattering by 2H; *solid line*, Theoretical; *circles*, Observed values.

with which the experimental curve decreases with angle, its actual observation in H_2 is difficult. If, however, we calculate the ratio of the scattering by H_2 (experimental) to the theoretical scattering by two hydrogen atoms and plot the result as a function of Ka_0, we should get a curve which oscillates about the value unity. This has been done for 912 volts, and the result is shown in Fig. 4. The solid line is the theoretical ratio, the circles the experimental points. We note that the agreement is about as good as could be expected. At large values of Ka_0 the experimental points lie far above the value unity. The reason for this is that in the angular distribution curve the experimental values fall above the theoretical curve.

CONCLUSION

The writer takes this opportunity to express his appreciation to Professor A. L. Hughes who proposed this problem and whose suggestions were invaluable aids throughout the investigation.

MARCH 1, 1935 PHYSICAL REVIEW VOLUME 47

Isotope Effect in Acetylene

WALTER F. COLBY, *University of Michigan*

(Received January 8, 1935)

The normal frequencies of the linear acetylene molecule have been computed for infinitesimal vibrations with the generalization that the masses of the two hydrogen atoms are different. Constants of the potential energy have been determined by using the well-known frequencies of normal acetylene. Numerical calculations have then been carried through for the molecules C_2HD and C_2D_2 and the results compared with observed frequencies.

RECENT measurements in the infrared of the absorption bands of acetylene in which one or both of the hydrogen atoms has been replaced by deuterium makes it desirable to calculate at least in first approximation the normal frequencies for this molecular model. It is well known that the four atoms of acetylene lie in one line and the consequent symmetry makes the problem of infinitesimal vibrations comparatively simple. If one takes as provisional coordinates, displacements of the atoms in their own line and perpendicular to it, a general expression for the energy containing only quadratic terms will contain squares of these coordinates and likewise products with the exception of those which involve the perpendicular displacements linearly. This is obvious from the symmetry of the model. The energy expression, therefore, separates into two parts each of which contains only one type of displacement and one may solve for the frequencies in two distinct calculations. The longitudinal displacements involve three normal coordinates and the transverse involves four coordinates which are degenerate in two pairs.

We shall first consider the longitudinal displacements choosing as coordinates the relative displacements of the particles $H-x_1-C-x_2-C-x_3-H$. The potential energy may then be

written

$$2V=K_1(x_1^2+x_3^2)+K_2x_2^2 +2K_3(x_1x_2+x_2x_3)+2K_4x_1x_3.$$

Only four constants are involved since the displacements x_1 and x_3 are symmetrical. Both K_3 and K_4 may be considered small since they record the interaction of nonadjacent atoms. K_4 is doubtless too small to influence these calculations appreciably.

Calling the change of coordinates of the four atoms taken in the same order, y_1, y_2, y_3, y_4,

$$2T=m_1\dot{y}_1^2+M\dot{y}_2^2+M\dot{y}_3^2+m_2\dot{y}_4^2.$$

Where m_1 and m_2 are the masses of the two hydrogens and M that of the carbon atom.

Four equations may be written of which three interrelate the x's and y's and the fourth states the condition for stationary centroid. With the help of these the kinetic energy may be written as follows:

$$2\Sigma T=m_1(m_2+2M)\dot{x}_1^2+(M+m_1)(M+m_2)\dot{x}_2^2 +m_2(m_1+2M)\dot{x}_3^2+2m_1(m_1+M)\dot{x}_1\dot{x}_2 +2m_1m_2\dot{x}_1\dot{x}_3+2m_2(m_1+M)\dot{x}_2\dot{x}_3,$$

where $\Sigma=m_1+m_2+2M$, the total mass of the molecule.

Setting up the determinant in $\lambda(=(2\pi\nu)^2)$ one obtains a cubic equation which for the case $m_1=m_2=m$ may be factored into the two equations

$$\lambda^2-\lambda\left[\frac{\Sigma}{M(m+M)}K_2+\frac{\Sigma}{2mM}(K_1+K_4) -\frac{2\Sigma}{M(m+M)}K_3\right]+\frac{\Sigma^2}{Mm(m+M)^2} \times\left[\frac{K_2(K_1+K_4)}{2}-K_3^2\right]=0,$$

$$\lambda-\frac{K_1-K_4}{2mM}\Sigma=0.$$

The linear equation does not contain K_3 and is therefore to be identified with a vibration which involves no relative motion of the two carbons. This frequency has been called ν_3 by Dennison. It will be seen that for this vibration the dependence of the frequency on m is given by the factor $(\Sigma/m)^{\frac{1}{2}}$, independent of the force constants.

This gives a ratio of $(13/7)^{\frac{1}{2}}$ for the frequencies ν_3 for C_2H_2 and C_2D_2.

For the remaining longitudinal frequencies which Dennison has called ν_1 and ν_2 the situation is not so simple and it is necessary to solve for the constants K. This may be done in close approximation by using the three known parallel frequencies of normal acetylene which are given by Sutherland[1] as

$$\nu_1=1974, \quad \nu_2=3372, \quad \nu_3=3288.$$

The equations contain four constants and with only three frequencies it will be necessary to set $K_4=0$. We thus obtain

$$K_1=\ 5.850\times10^5 \qquad \text{dynes/cm}$$

$$\left.\begin{aligned}K_2&=15.587\\K_3&=\ 0.0279\end{aligned}\right\} \text{ or } \left\{\begin{aligned}&27.432\times10^5\\&5.896\times10^5.\end{aligned}\right.$$

The double values of K_2 and K_3 arise from the quadratic equations in which they appear and for this calculation it is immaterial which pair is used since the results will be the same. It may be noted that the first pair in which K_3 is much smaller than K_1 is the more plausible.

Setting these constants into the quadratic equation for λ, one obtains, together with ν_3 the following frequencies for C_2D_2:

$$\nu_1=1750, \quad \nu_2=2690, \quad \nu_3=2414.$$

For the molecule C_2HD it is necessary to return to the cubic in λ in which have been substituted $m_1=1$, $m_2=2$, $M=12$ and the above values of K. This yields

$$\nu_1=1840, \quad \nu_2=3335, \quad \nu_3=2560.$$

To set up the potential energy expression for transverse displacements it is most convenient to choose as coordinates the angles made between the line connecting the two carbons and the lines connecting each hydrogen with its adjacent carbon. Calling these angles α_1 and α_2,

$$V=\tfrac{1}{2}K_1(\alpha_1^2+\alpha_2^2)+K_2\alpha_1\alpha_2.$$

For the kinetic energy

$$T=\tfrac{1}{2}(m_1\dot{x}_1^2+M\dot{x}_2^2+M\dot{x}_3^2+m_2\dot{x}_4^2).$$

Where x indicates the displacement of an atom

normal to the axis of the molecule. These coordinates are related through the equations

$$\alpha_1=(x_2-x_1)/a+(x_2-x_3)/b,$$
$$\alpha_2=(x_3-x_4)/a+(x_3-x_2)/b.$$

Where a is the normal distance from H to C and b from C to C.

Translation and rotation may be removed with the equations

$$m_1x_1+Mx_2+Mx_3+m_2x_4=0,$$
$$aMx_2+(a+b)Mx_3+(2a+b)m_2x_4=0.$$

The determinant in λ is now of second order and yields the following equation:

$$\lambda^2a^4+\lambda^2a^2\left[-\frac{K_1}{M}\left(2+4c^2+4c+\frac{M}{m_1}+\frac{M}{m_2}\right)+\frac{K_2}{M}(4c^2+4c)\right]$$
$$+\frac{K_1^2-K_2^2}{M^2}\left[\frac{M^2}{m_1m_2}+\left(\frac{M}{m_1}+\frac{M}{m_2}\right)(1+2c+2c^2)+1+4c+4c^2\right]=0,$$

where $c=a/b$. It contains besides the two force constants K_1 and K_2, the two lengths a and b. For $m_1=m_2=m$, it may be factored into

$$\lambda_5a^2=(1+4c+4c^2+M/m)/M(K_1-K_2),$$
$$\lambda_4a^2=[(M+m)/Mm](K_1+K_2).$$

That frequency in which K_1 and K_2 enter symmetrically has been identified with ν_4 in which the two carbon atoms move in the same direction. Since one may write

$$\lambda_4a^2=A_1(1+M/m),$$

the dependence on m is very simple and one has the ratio of frequencies ν_4 for C_2H_2 and C_2D_2 equal to $(13/7)^{\frac{1}{2}}$.

Even in the case of ν_5 which may be written

$$\lambda_5a^2=A_2(1+4c+4c^2+M/m),$$

the ratio of frequencies is independent of K and may be evaluated by assuming a value for $c=a/b$.

By using the values given by Mecke $a=1.08\times10^{-8}$ and $b=1.19\times10^{-8}$, the ratio of the frequencies ν_5 for C_2H_2 and C_2D_2 is $(19.92/13.92)^{\frac{1}{2}}$.

For the molecule C_2HD it is necessary to evaluate the force constants with the help of the frequencies ν_4 and ν_5 for normal acetylene which are given by Sutherland[1] as $\nu_4=730$, $\nu_5=605$. By using Mecke's values for a and b

$$K_1=2.442\times10^{-12},$$
$$K_2=0.922\times10^{-12} \quad \text{dyne cm/rad.}$$

Returning to the second order determinant with $m_1=1$ and $m_2=2$ we get $\nu_4=669$, $\nu_5=523$. The frequencies are thus as presented in Table I. Observations of absorption bands of C_2HD and C_2D_2 have been made in the infrared by Randall and Barker.[2] These bands are fundamentals and low order combinations and are therefore best suited for identification by this calculation which has not considered higher powers than the second in the potential energy. There is some difficulty in placing the center of the observed bands because of these perturbations but the agreement with calculation leaves little doubt as to the classification. Table II shows the data now available. It will be seen that the agreement between observation and calculation is good. The differences are of the magnitude 10 cm^{-1} which may easily be due to the anharmonic terms in the potential energy which have not been included in this calculation. In order to determine how these terms should transform, a much more detailed analysis would be necessary.

TABLE I. *Frequencies of acetylene molecule.*

	C_2H_2	C_2HD	C_2D_2
ν_1	1974	1840	1750
ν_2	3372	3335	2690
ν_3	3288	2560	2414
ν_4	730	669	535
ν_5	605	523	505

TABLE II. *Data on vibrational frequencies of acetylene molecule.*

Molecule	Assignment	Character	Freq. obs.	Freq. calc.
C_2D_2	ν_4	$\perp$	539.2	535
C_2D_2	$\nu_4+\nu_5$	$\parallel$	1043	1040
C_2DH	ν_4	$\perp$	679	669
C_2DH	ν_5	$\perp$	518.9	523
C_2DH	$\nu_4+\nu_5$	$\parallel$	1202	1192
C_2DH	ν_3	$\parallel$	2585	2560

[1] Sutherland, Phys. Rev. **43**, 883 (1933).

[2] Randall and Barker, Phys. Rev. **45**, 124 (1934).

Magnetoresistance of Liquid Sodium-Potassium Alloy

J. E. ARMSTRONG, *Rice Institute*

(Received January 17, 1935)

The liquid alloy, Na-K, has been investigated for change of resistance in a magnetic field. The use of very fine containing tubes is believed to have minimized spurious effects due to motions in the liquid. The results of Fakidow and Kikoin are confirmed and in addition it is found that a longitudinal magnetic field produces a larger effect than a transverse field. For fields of over 2000 gauss there is a straight line relationship between magnetoresistance and field.

IT has recently been found by Fakidow and Kikoin[1] that the liquid alloy of sodium and potassium shows the phenomenon of magnetoresistance. This observation is of considerable importance because the effect in this alloy is so large that there can be little doubt as to its being genuine. It represents, therefore, the first distinct instance of magnetoresistance in liquids. The present paper describes further experiments on the alloy, in which the effect of a longitudinal field has been investigated.

The Na-K alloy was prepared and its composition determined by observation of the freezing point and reference to data given in the *International Critical Tables*. The sodium content was approximately 35 percent. The liquid alloy was then distilled in a vacuum through a series of bulbs and finally forced into a capillary tube by air pressure in a manner similar to that used by Fakidow and Kikoin. Platinum wires were sealed into bulbs at the ends of the capillary tube. These wires extended through each bulb and into each end of the capillary tube for a short distance. They fitted snugly into the capillary but allowed sufficient space for the alloy to flow through the bulb into the tube during the filling process. Two types of capillary tubes were used. In the first type, a straight tube about 20 cm long was bent back and forth so as to form a grid of parallel bars about 3 cm long connected at alternate ends by sharp bends. The second type was a straight tube, about 3 cm long, with no bends or turns.

The magnetic field was produced by a Weiss electromagnet, with pole pieces 10 cm in diameter and 3 cm apart.

The conventional type of Wheatstone bridge was used in measuring the resistance of the specimen. High sensitivity was secured by making the arms of the bridge as nearly equal as possible and by using a galvanometer of high sensitivity. This galvanometer was of the astatic needle type, equipped with a triple iron shield. A change of resistance of 5×10^{-7} ohms could be measured in a total resistance of 3 ohms.

The curves of Fig. 1 agree as well as could be expected with the results of Fakidow and Kikoin. The curve which they give, using a transverse field, is, in fact, almost coincident with curve III of Fig. 1.

In Fig. 1, the magnetoresistance is considerably smaller than in Fig. 2. This difference is probably due in part to the fact that different samples of the alloy were used in getting data for the two figures. Apparently the magnitude of the magnetoresistance is quite sensitive to the composition of the alloy. Another reason for the difference may be inaccurate determinations of R in dR/R. In correcting for the resistance of the fine platinum wires leading into the Na-K alloy it was difficult to get an accurate estimate of the correct length of these wires; they extended some distance into the alloy. The resistance of the wires being comparable with the resistance of the alloy an appreciable error could easily be introduced.

It will be noticed in Figs. 1 and 2 that there is an apparent dependence of the magnitude of dR/R on the diameter of the capillary tube. There are two reasons for this dependence. First, when different tubes are used, comparison of absolute values of dR/R cannot be made with a high degree of accuracy because of errors in allowing for lead resistances when R is determined. Second, a spurious, secondary effect due to motions of the liquid in the tube may arise.

[1] Fakidow and Kikoin, Physik. Zeits. d. Sowjetunion **3**, 381 (1933).

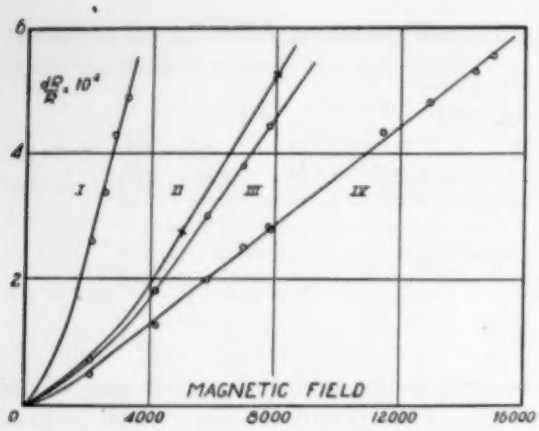

FIG. 1. Magnetoresistance of Na-K alloy contained in bent tubes. (I) Longitudinal field, tube diameter, 0.024 cm. (II) Transverse field, tube diameter, 0.024 cm. (III) Longitudinal field, tube diameter, 0.009 cm. (IV) Transverse field, tube diameter, 0.009 cm.

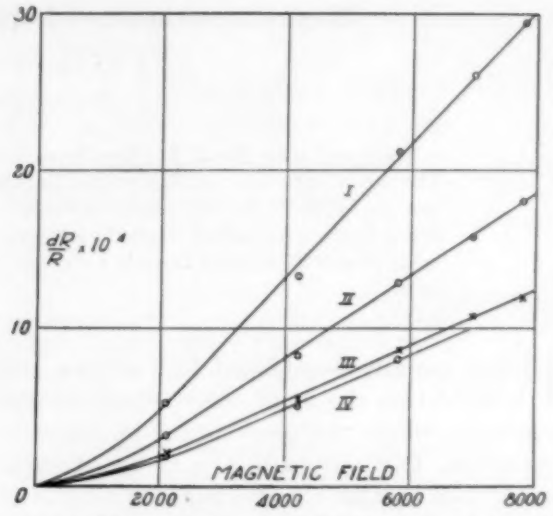

FIG. 2. Magnetoresistance of Na-K alloy contained in straight tubes. (I) Longitudinal field, tube diameter 0.008 cm, bridge current, 2.5 m.a. (II) Transverse field, tube diameter, 0.014 cm, bridge current, 2.5 m.a. (III) Transverse field, tube diameter, 0.008 cm, bridge current, 2.5 m.a. (IV) Transverse field, tube diameter, 0.008 cm, bridge current, 5.0 m.a.

This secondary effect appears as an increase of resistance which is dependent on tube diameter, —the resistance increase having been found by Jones[2] to be proportional to the diameter for the case of mercury in large tubes.

It is believed that the spurious effect is very small in the present experiments and that differences in magnitude of dR/R for different tubes are due to errors in determining R. The reason for believing the spurious hydrodynamic effect to be small is because the capillary tubes in the present experiments were of such small diameter. Fakidow and Kikoin found only about 8 percent decrease in the effect when they changed the tube diameter from 1 mm to 0.5 mm. The tubes in the present experiment were considerably smaller than those used by Fakidow and Kikoin, hence there should be a considerably smaller dependence of the effect on tube diameter. Furthermore, a separate series of measurements was made on mercury in these fine tubes, and the resistance change was found to be negligibly small. If the spurious hydrodynamic effect is negligible in the case of mercury in these tubes we should expect it to be negligible for the alloy also.

In Fig. 2 curves III and IV show that when the current through the specimen is cut in half there is a slight increase in dR/R. Jones has found for mercury that the resistance increase due to hydrodynamic action is proportional to the current raised to the power -0.4, using a tube 5 mm in diameter and currents between 0.5 and 5.0 amperes. He suggests that for very small currents the resistance change would be independent of the current. In the present experiments it appears that the current is still large enough to produce a small effect, and therefore the spurious hydrodynamic effect has not been completely eliminated.

There are certain general conclusions which may be drawn in spite of the possibility of errors of the kind discussed above. (1) An intrinsic magnetoresistance exists in the liquid alloy apart from any effect due to motions in the liquid. (2) A longitudinal magnetic field produces a larger effect than a transverse field. (3) Above 2000 gauss there is a straight line relation between dR/R and the field strength.

The second conclusion is a matter of some interest because in nonferromagnetic, polycrystalline solids the converse is true. The third conclusion states a relation which has been found to hold in solid metals for very large fields. The liquid state appears to make possible the straight line relation in much smaller fields.

This research was suggested by Professor C. W. Heaps who also gave much helpful advice during the progress of the work. The writer is also indebted to Mr. F. T. Rogers for measuring the magnetoresistance of mercury specimens.

[2] T. J. Jones, Phil. Mag. **50**, 46 (1925).

On the Effect of Slight Impurities on the Elastic Constants, Particularly the Compressibility of Zinc

P. W. BRIDGMAN, *Research Laboratory of Physics, Harvard University*

(Received January 8, 1935)

The conclusion of Hanson that the elastic constants and particularly the compressibility of different grades of pure zinc differing only slightly in purity may differ by relatively large amounts is subjected to direct experimental test by compressibility measurements on the same grades of zinc as used by Hanson. Measurements on virgin material show no measurable difference. Apparent differences, both in compressibility and in the other elastic constants, are probably to be explained by small internal strains. Improved values are found for the compressibility of zinc as follows:

$$\begin{aligned} &90^\circ \text{ orientation}, && -\Delta l/l_0 = 1.57\times10^{-7}p - 0.75\times10^{-12}p^2, \\ &0^\circ \text{ orientation}, && -\Delta l/l_0 = 13.50\times10^{-7}p - 7.68\times10^{-12}p^2, \\ &\text{Volume compression}, && -\Delta V/V_0 = 16.64\times10^{-7}p - 9.62\times10^{-12}p^2, \end{aligned}$$

at 30°C, p in kg/cm².

IN the *Physical Review* for March 1, 1934, Hanson has published a careful determination by the method of the bending and twisting of cylindrical rods of the five elastic constants of zinc crystals from two different sources, both of purity higher than 99.99 percent, and has calculated from these constants the linear and cubic compressibilities. Considerable differences were found in some of these constants; for example, the calculated linear compressibility parallel to the axis of one grade of zinc was 40 percent higher than that of the other, and the cubic compressibility was 30 percent higher. These results were quite unexpected to me, both because of the opinion which seems to be quite widely held by experimenters on phenomena in crystals that the elastic constants are not "structure sensitive," and also because of my own personal experience. I had made measurements of the elastic constants by a more direct method and had found nothing to suggest as great a variability as found by Hanson. This was in particular true of my direct measurements of the linear compressibilities, which gave more clean cut results than for the other constants. Furthermore, all my experience with the compressibility of other materials indicated that it is not sensitive to slight impurity.

The matter seemed important to me, since our opinions on "structure sensitive" properties of crystals are still hardly out of the controversial stage, and it would be desirable to get this matter correct in the beginning if possible. I therefore suggested to Professor Tyndall, under whose direction Hanson's work was done, the desirability of checking by direct experiment on the identical specimens some of Hanson's calculated compressibilities. Professor Tyndall cooperated in the readiest way by immediately placing at my disposal all of Hanson's samples of suitable orientation. Nine sets of measurements in my regular pressure apparatus were made on these samples. On consulting with Professor Tyndall as to the form which the results should take for publication, considerable difference of opinion developed as to the proper interpretation, and it eventually appeared after considerable correspondence that conclusions satisfactory to both of us could be obtained only by the execution of fresh experiments. The main point at issue hinged on the effect of the handling which the specimens had received, since they were known in some instances to have been strained beyond the elastic limit. The effect of this strain was removed as far as possible by a process of annealing which at that time was believed to be effective in restoring the electrical properties to the original condition, although there was no proof that the elastic properties were similarly restored, and it has developed later that even the electrical properties are not equally well restored at all orientations. Professor Tyndall therefore undertook the preparation of fresh samples of zinc especially for this work, and every

precaution has been taken to avoid all possibility of overstrain.

The freshly prepared zinc crystals were from three sources: (1) Evanwall "Rod" (E. R.) zinc made from material left by Hanson, originally obtained from the Evans Wallower Zinc Company; (2) Evanwall "Block" (E. B.) zinc from a fresh 50 pound block of zinc from the Evans Wallower Zinc Company, the same as the zinc used by Cinnamon[1] in a recent paper, and (3) Horsehead Special (H. H.) zinc, from the same 50 pound block as used by Hanson. Another sample of zinc from Evans Wallower showed by direct chemical analysis: Fe 0.0004 percent, Cd 0.0008 percent, Pb 0.0047 percent, Cu 0.0002 percent, As, Co, Ni, Al, 0.0000. Spectroscopic comparison of this with the E. R. zinc showed no detectible difference. Spectroscopic comparison with the H. H. zinc indicated somewhat more iron and somewhat less copper than the E. R. zinc. Spectroscopic comparison between E. R. and E. B. showed no iron at all in E. B. and slightly more copper. There were three samples of E. R. of orientations 5°, 90° and 8°, the angle being measured between the hexagonal axis of the crystal and the length of the rod. The 8° specimen had been strained in removing from the mold, and slip bands could be seen on the central portion, but the ends appeared free from slip bands. There were two samples of E. B. of orientations 9.5° and 85°. There were four samples of H. H. of 5°, 8°, 21°, and 89° orientations. The 21° orientation was really not pertinent for the present purpose, and was measured more or less by way of curiosity. These all were cast by methods already fully described[2] into crystals about 8 cm long and of slightly trapezoidal section about 5 mm on the side. For the compressibility measurements it was necessary to form these into pieces about 2.7 cm long for the more incompressible orientation and 1.3 cm long for the other more compressible orientation, with accurately flat and parallel ends. In order to perform the small amount of necessary machining, the specimens were first embedded in wax in a heavy brass tube of internal diameter just sufficient to admit the rod freely. The wax was cast around the rod by slowly lowering the mold containing the crystal surrounded by molten wax into cold water by a process very similar to my method for making single crystals. Pieces were then cut out of the mold of the requisite length with a fine jeweller's saw; the ends of the specimen were faced off in the lathe while still embedded in the wax, taking a very fine chip and using a keen tool, and finally the completed specimen was freed from the mold by melting the wax. In a few cases there were longitudinal ridges left from the casting that had to be removed; this was done with a fine file, after part of the mold had been filed away, and while as much of the crystal as possible was still embedded in the wax.

TABLE I. *Summary of linear compressibility measurements on fresh samples of zinc.*

Grade of zinc	Orientation	Linear compression at 30° $-\Delta l/l_0$		$-\Delta l/l_0$ at 10,000 kg/cm²	Width of hysteresis loop	Average deviation from smooth curve
E. R.	90°	$1.57\times10^{-7}p$	$-0.75\times10^{-12}p^2$	0.00149		1.90%
E. B.	85°	1.66	− 0.75	.00159		.83
H. H.	89°	1.58	− 0.75	.00151		.83
E. R.	5°	13.39	− 6.75	.01270	0.83%	.14
E. B.	9.5°	13.03	− 5.98	.01243	1.36	.50
H. H.	8°	13.56	−10.65	.01249	.75	.18
H. H.	5°	13.18	− 6.01	.01258	.83	.21
E. R. Strained	8°	12.71	− 7.45	.01197	1.27	.35
H. H.	21°	11.77	−10.35	.01073	1.40	.24

The results of the measurements of linear compressibility of these fresh samples are given in Table I. The method was the same as in all my previous work and has been fully described.[3] The measurements were made at 30°C, over a pressure range of 12,000 kg/cm², readings being made at equal pressure intervals with both increasing and decreasing pressure, making in all fourteen readings. The pressures in the tables are in kg/cm² units. In addition to the regular pressure run, an initial seasoning application of 2000 kg/cm² was made in all cases; this initial application was followed by no permanent change of zero within the regularity of the other readings, showing that there was no perceptible porosity in the specimen. The results could in practically all cases be represented within the regularity of the readings by a second degree expression in the pressure. Space does not permit a reproduction of all the individual readings, which repay careful

[1] C. A. Cinnamon, Phys. Rev. **46**, 215 (1934).
[2] W. J. Poppy, Phys. Rev. **46**, 815 (1934).
[3] P. W. Bridgman, Proc. Am. Acad. **58**, 166 (1923).

study. The results were never entirely regular within the limits of error of the method, but there were irregularities greater than would be shown under similar conditions by harder materials. The most important feature was that there was always perceptible hysteresis between pressure and change of length for the most compressible orientation, that is, parallel to the axis, while the other and relatively incompressible orientation showed no appreciable hysteresis. In order to indicate the character of the results as fully as possible Table I contains, in addition to the two power expression in pressure which best represents the results, the maximum width of the hysteresis loop expressed as a fractional part of the total displacement at the maximum pressure, and the mean departure from a smooth curve of the individual points similarly expressed. This latter gives an idea of the regularity of the results; it will be seen that the average deviation is of the order of a few tenths of one percent. It is significant that by far the greater part of the average irregularity was contributed by the initial points at atmospheric pressure. A result of this would be that measurements made in only a small pressure range would show much greater irregularity, both relatively and absolutely, than measurements over a wider range. In order to eliminate as far as possible the effect of small local irregularities, I have chosen as giving the best comparative indication of the true com-compressibility the fractional change of length under 10,000 kg/cm². This change of length should be a linear function of $\cos^2\theta$. The results are plotted in Fig. 1 against $\cos^2\theta$ giving only the parts of the diagram on a much enlarged scale in the neighborhood of $\cos^2\theta=0$ and $\cos^2\theta=1$.

The diagram will leave no room for doubt, I believe, but that the linear compressibilities of these different grades of zinc are as close to the same value as could be expected in view of the experimental irregularity, and that no difference exists within experimental error which can be correlated with a difference in origin of the samples and therefore with minute differences in purity. The extreme discrepancy between any two samples is 1.2 percent, which is to be contrasted with a discrepancy of 40 percent in Hanson's averaged final results. This is the main

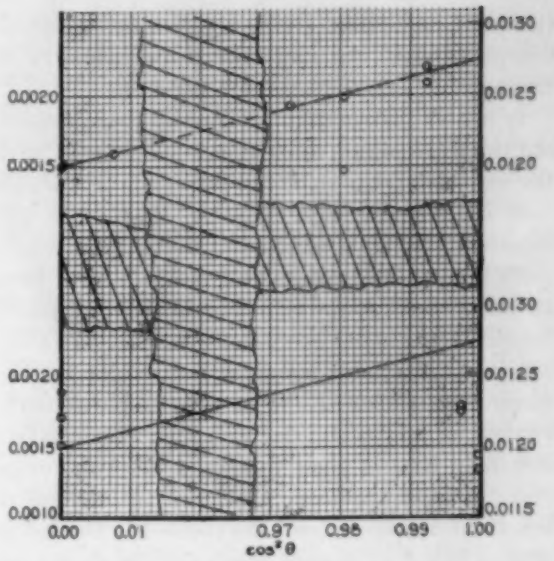

FIG. 1. Shows in the upper part of the diagram the fractional changes of length at 10,000 kg/cm² plotted against $\cos^2\theta$ for the freshly prepared zinc crystals. In the lower part of the diagram are shown similar data for the elasticity samples of Hanson. Elasticity theory demands that the relation be linear in $\cos^2\theta$.

point of this paper, and I believe establishes the fact that there is at present no reason to believe that at any rate the compressibilities are sensitive to small impurities.

It is instructive that the compressibility of the one sample known to have been strained in the mold, which is also plotted in Fig. 1 and which may be identified by comparison with Table I, definitely does not fall in line with the others, in spite of the fact that the sample was cut from what appeared to be an undamaged part of the crystal. This suggests the extreme sensitiveness of these effects to strain. Doubtless the fact that the individual readings for all the other samples were not as regular as those given by many other mechanically harder materials is to be explained as an effect of slight strains introduced in spite of the greatest care in handling.

The results listed in Table I for the 21° sample should be given no consideration in comparison with the others because the method is not adapted to measuring the linear compressibility of such an orientation. The thickness of this sample was about one-half its length; calculation will show that under hydrostatic pressure there is a change of angle for this orientation which in specimens of these proportions produces an effect

far from negligible, giving too low an apparent compressibility. In fact, the compressibility of this sample was too low by 5 percent.

It is now instructive to compare these results, obtained on virgin unstrained specimens, with the measurements made on the specimens which had been previously used by Hanson in determining the five elastic constants, and which were known in at least some cases to have been strained before the compressibility measurements. The results are given in Table II. They are distinctly more irregular than those for the virgin material in Table I. This is particularly evident in the second degree terms which in two instances have a positive sign, a very abnormal state of affairs indeed. The relative changes of length at 10,000 kg/cm² are plotted in the lower part of Fig. 1. The very much greater scattering of the points is in the first place striking and also the fact that at the high orientations all the points lie above the line for the unstrained material and at the low orientations all, with one exception, lie below it. The obvious interpretation of this is that small strains act effectively like the introduction of other orientations; at 90° the only other orientations possible are nearer 0°, and at 0° the only possible other orientations are nearer 90°.

Going back now to the results on the unstrained specimens, the present values of compressibility are much to be preferred to those which I previously published;[4] not only is the present material purer than mine, which we have seen to be of comparatively minor importance, but the specimens were doubtless freer from strain. The average values given by the new measurements, weighting measurements on different specimens inversely as their average deviations from a smooth curve, and correcting for orientation, are at 30°C pressure expressed in kg/cm²:

$$\text{At } 90°,\ -\Delta l/l_0 = 1.57\times10^{-7}p - 0.75\times10^{-12}p^2.$$
$$\text{At } 0°,\ -\Delta l/l_0 = 13.50\times10^{-7}p - 7.68\times10^{-12}p^2.$$

From these the volume compressibility may be computed to be:

$$-\Delta V/V_0 = 16.64\times10^{-7}p - 9.62\times10^{-12}p^2.$$

My previous results were:

$$\text{At } 90°,\ -\Delta l/l_0 = 1.95\times10^{-7}p - 1.11\times10^{-12}p^2.$$
$$\text{At } 0°,\ -\Delta l/l_0 = 12.98\times10^{-7}p - 5.32\times10^{-12}p^2.$$
$$\text{Cubic},\ -\Delta V/V_0 = 16.87\times10^{-7}p - 8.08\times10^{-12}p^2.$$

It will be noticed that the difference between the two determinations is in exactly the direction that would be expected, that is, the linear compressibility of the strained 90° specimen is greater than that of the unstrained specimen, because of the effective introduction by the strain of other orientations, all of which have a greater compressibility, while for the 0° orientation the relations are reversed. The result is a comparatively large change in the ratio of the compressibilities in the two directions, the ratio being 8.6 for the unstrained specimen and only 6.65 for the strained specimen. It is also to be noticed that the effect of strain is much larger on the 90° orientation, measured in percent, than on the 0° orientation; the absolute magnitudes of the effects are not greatly dissimilar.

Interesting questions suggest themselves as to the mechanism by which strain simulates the effect of a change of orientation. The cleavage planes seem to be unchanged in orientation and as easily produced in strained as in virgin specimens. Perhaps the possibility is to be considered of a partial rotation of the atoms in position in the lattice; it is probable that the atoms cannot have complete spherical symmetry in a lattice as strongly anisotropic as zinc. The fact that annealing is comparatively successful in restoring electrical properties is not incon-

TABLE II. *Summary of linear compressibility measurements on Hanson's elasticity samples.*

Grade of zinc	Orientation	Linear compression at 30° $-\Delta l/l_0$		$-\Delta l/l_0$ at 10,000 kg/cm²	Width of hysteresis loop	Average deviation from smooth curve
E. R. *b.a.*	90°	$1.38\times10^{-7}p$	$+ 3.38\times10^{-12}p^2$	0.00172		1.18%
E. R. *a.a.*	90°	1.96	− 0.70	.00189		1.86
H. H. *a.a.*	90°	1.49	+ 0.33	.00152		.68
E. R. *b.a.*	3°	13.91	−16.55	.01225	1.7%	.13
E. R. *a.a.*	3°	13.60	−13.1	.01229	2.1	.25
H. H. *b.a.*	1°	13.40	− 4.22	.01298	.45	.00
H. H. *a.a.*	1°	12.98	−10.40	.01194	2.1	.28
H. H. *a.* 2nd *a.*	1°	12.91	−10.72	.01184	1.8	.29

b.a., before annealing, or "as received."
a.a., after annealing, 380° for 8 to 10 hours.
a. 2nd *a.*, second annealing, 400° for 24 hours.

[4] P. W. Bridgman, Proc. Am. Acad. **60**, 338 (1925).

sistent with an asymmetry in the atoms because the wave mechanics picture of electrical conduction represents the electron distribution as much more uniform than the atomic distribution. This is also suggested by the fact that the ratio of the electrical conductivities for the two independent perpendicular directions is only 1.055, against 8.6 for the ratio of the elastic constants.

Leaving now the question of compressibility and passing to the other elastic constants as determined by Hanson, it seems to me that one may well question whether there is any longer ground to believe seriously that the other constants are sensitive to minute impurities. For I think it may be taken as now established that there is no such variation in the compressibility as Hanson calculated from his other constants and this of course means an error in those constants. There are two factors which I think should be especially considered in appraising the situation. There is in the first place the consideration that slight permanent strains may introduce *systematic* errors, changing the elastic properties for orientations near one extreme all in one direction, and those near the other extreme in the other. In the second place, there is the consideration that slight errors in the observational data may, because of the nature of the mathematical relationships, introduce very serious errors into some of the computed elastic constants. Thus it can be shown that by making a change of only 1 percent in the direct observational data from which S_{11}, S_{33} and S_{44} are computed, a change of 18 percent may be thereby introduced into S_{12}, 22 percent into S_{13}, 35 percent into the parallel linear compressibility, 81 percent into the perpendicular linear compressibility, and 47 percent into the cubic compressibility. If one examines the regularity of the experimental points in Hanson's diagrams, and further considers the possibility of systematic errors just mentioned and the fact that all the bending specimens consistently showed distinct hysteresis, I believe that the danger of an accumulation of errors like that just suggested must appear to be a very real one.

The possibility of systematic errors arising from small strains offers the possibility of understanding how Hanson could have arrived at his conclusion that very small differences in purity produce comparatively large differences in elastic constants. For the elastic limit is known to be sensitive to very slight impurities so that one grade of zinc may have been more susceptible to permanent strain than the other, and therefore more sensitive to systematic error. Something of this sort is definitely suggested by a study of the irregularities of the data. The spectroscopic analysis suggests that the H. H. zinc was slightly less pure than E. R. or E. B. and therefore less likely to receive permanent strains. Tables I and II both show a distinct tendency for the H. H. points to deviate less from smooth curves than the others which is what would be expected. There is also the fact that the compressibilities calculated by Hanson for the H. H. zinc are distinctly nearer the values directly determined above than are the others.

In view of the various possibilities of error in the method of determination of elastic constants by bending and torsion, particularly when applied to substances with low elastic limits, it is pertinent to urge the great superiority of "direct" methods, that is, methods in which the specimen is subject to a homogeneous stress and strain corresponding to the constant to be determined. The constants S_{11} and S_{33} can be measured "directly" in terms of the shortening under compressive load, and so determined can be given more confidence than can be given to a determination by bending which involves a strain varying from positive to equal negative values across the section of a slender specimen. Similarly S_{12} and S_{13} can be determined by direct measurements of the lateral contraction of suitably oriented specimens, and so determined are not susceptible to the possibility of large accumulated errors already indicated in the indirect method. Finally there can be no doubt but that directly measured compressibilities are to be preferred to compressibilities calculated by a combination of other constants.

In a note following this Professor Tyndall presents the values of the elastic constants of zinc which he now thinks may be deduced with greatest probability from Hanson's data in view of these results on linear compressibility.

Note on the Probable Values of the Elastic Constants of the Zinc Crystal

E. P. T. TYNDALL, *Physical Laboratory, University of Iowa*

(Received January 8, 1935)

In consideration of the compressibility data in the preceding paper by Bridgman a somewhat different interpretation is given to the measurements of Hanson. A satisfactory set of constants for the zinc crystal may be based on Bridgman's measurements and on those obtained by Hanson on one of his lots of zinc. These are: $S_{11}=7.70$, $S_{12}=0.83$, $S_{13}=-6.93$, $S_{33}=27.66$, $S_{44}=24.40$, all $\times 10^{-13}$ cm²/dyne.

THE results set forth in Table I of the preceding paper undoubtedly disprove Hanson's[1] hypothesis that slightly different kinds of very pure zinc differ markedly in their compressibilities. The earlier data (Table II) appeared to the writer inconclusive and when combined with Hanson's independently measured constants, for the E.W. zinc particularly, still led to exactly the same inconsistencies[2] which had originally guided Hanson to his hypothesis. It seems worth while now, however, to reexamine Hanson's data with a view to determining just what are the best values of the elastic constants and whether a real difference in constants for the two sorts of zinc can be maintained.

The Horsehead special zinc is considered first. Using the values of three constants determined independently[3] by Hanson, $S_{11}=7.70$,[4] $S_{33}=27.66$, $S_{44}=24.40$, and the compressibility data of Bridgman given in the preceding paper, $(\Delta l/l)_0=13.80=2S_{13}+S_{33}$, $(\Delta l/l)_{90}=1.60=S_{11}+S_{12}+S_{13}$, one may compute $S_{12}=0.83$ and $S_{13}=-6.93$, values not greatly different[5] from those proposed by Hanson. The consistency of these new constants with Hanson's further data on this zinc is excellent. Thus the computed reciprocal of the rigidity modulus for a 90° crystal is given by $(1/T)_{90}=S_{11}-S_{12}+\frac{1}{2}S_{44}=19.07$, which may be compared with 19.40 and 19.50, experimental values (Hanson's Fig. 4) for two 90° crystals. Likewise for orientation 75°, the computed value of $1/T$ is 22.55 as compared with 22.76 observed experimentally.[6] Thus the data on the H.H. crystals are not only self-consistent but are in good agreement with Bridgman's latest data.[7] This set of constants, however, shows marked differences from other determinations, as may be observed in Hanson's Table II. S_{11} and S_{44} are noticeably lower and S_{33} higher than for the E.W. zinc.

Hanson's data for the E.W. zinc, treated in the same fashion as above, yield $S_{11}=8.08$, $S_{33}=26.28$, $S_{44}=25.15$ (Hanson's values) and $S_{12}=-0.24$, $S_{13}=-6.24$ (new values). Also computation gives $(1/T)_{90}=20.89$ and $(1/T)_{75}=23.90$. These values are distinctly unsatisfactory as S_{12} should almost certainly be positive and the $1/T$ values are too high.[8] Thus the data on the E.W. zinc cannot in this fashion be made at the same time self-consistent and satisfy the compressibility data. It is quite true that, by slightly modifying S_{11}, S_{33} and S_{44}, the other constants and the three compressibilities can be made to go through large changes and the data could perhaps be made self-consistent, etc., though this is not easy to do.[9] Moreover the three

[1] A. W. Hanson, Phys. Rev. **45**, 324 (1934).

[2] See Hanson, footnote 24.

[3] i.e., values of reciprocal of Young's modulus, or rigidity modulus, for a single suitable orientation.

[4] Throughout this note all elastic constants and compressibilities are expressed in c.g.s. units$\times 10^{13}$, i.e., $S_{11}=7.70\times 10^{-13}$ cm²/dyne.

[5] Considering the insensitivity of his method for determining S_{12} and S_{13}, Hanson's values are: $S_{12}=0.45$ and $S_{13}=-6.39$. It must be noted further that S_{12} is still open to considerable error due to the method of computation.

[6] Interpolated between 23.20 and 22.10 for 73° and 78°, respectively.

[7] This was to be expected as the values of compressibilities computed from Hanson's original constants were already in fair agreement with the correct values.

[8] Hanson's data on torsion of crystals of orientations between 65° and 90° certainly indicate values of $1/T$ for 90° and 75° crystals of about 19.0 and 22.2, respectively, for unstrained crystals. Strained crystals gave higher values.

[9] Adopting for E.W. zinc the values of S_{33} and S_{44} obtained for H.H. zinc does the trick at once, since the two zincs agree within experimental error in the results for torsion of 60°–90° crystals and possibly for the bending of 90°. The difference for the two zincs between S_{33} (or S_{44})

constants just mentioned are in much better agreement with Bridgman's earlier values[10] than are the corresponding ones for the H.H. zinc. It must be noted here that the values of $1/T$ for 90° and 75° crystals, computed from these constants of Bridgman are also high, being 20.39 and 23.56, respectively, so that the behavior of his crystals is very similar to that of the E.W. crystals, except naturally in regard to the compressibilities.

If now one assumes that the elastic constants, like the compressibilities, are unaffected by the presence of small amounts of impurities, then the best[11] set of constants for the zinc crystal appears to be the one derived above from the measurements on H.H. zinc by Hanson combined with Bridgman's latest data. Such a conclusion is entirely in line with Professor Bridgman's idea that the Evanwall crystals were more sensitive to disturbing effects of some sort. Perhaps a hint of this behavior is given by the fact that some of the circular section E.W. crystals used in the torsion measurements by Hanson were strained during growth and had to be annealed[12] before measurements were made. Aside from this there was no indication in Hanson's work of any difference in behavior of the two materials. The same amount and type of hysteresis were found in the bending tests for both zincs. The two sets of crystals were grown by the same method, handled with equal care, etc. Nor should there be any implication that the set of crystals recently prepared for Professor Bridgman was in any way superior to those crystals of Hanson's which had a trapezoidal section. Actually these crystals were smaller in cross section than Hanson's, had the additional handling incident to packing and mailing, and therefore had much more probability of being strained than did Hanson's crystals which were measured immediately after growth with a minimum of handling.

The necessary modification of Hanson's conclusions in the light of new data must not be considered to detract from the general reliability of his experimental observations, the main purpose of which was not a determination of elastic constants. Further, his work combined with Bridgman's has led to a much more satisfactory set of constants than any previously proposed.

---

is, however, definitely greater than the experimental difference between separate crystals of the same sort of zinc. See Hanson's Fig. 4.

[10] P. W. Bridgman, Proc. Am. Acad. **60**, 305 (1925); also quoted in Hanson's Table II.

[11] The data of Grüneisen and Goens and of Goens are not specifically considered here because their measurements were made in part by a dynamic method. The set of constants recommended by Goens, although each constant is numerically greater than those of the set recommended above, yields not only good values of the three compressibilities but also gives nearly the correct ratio for the two linear compressibilities, 7.55 as compared with 8.60. The $(1/T)_{78}$ is, however, high.

[12] The question of the efficacy of this anneal has formed the subject of considerable discussion with Professor Bridgman. I should say now that in the case of high orientation crystals it seems to have been effective as judged by agreement with unstrained E.W. and H.H. crystals. For the low orientation crystals one cannot be so sure, although the hysteresis was completely removed by the anneal and this criterion seemed entirely satisfactory at the time Hanson's paper was written.

The Theoretical Constitution of Metallic Lithium

FREDERICK SEITZ, *Palmer Physical Laboratory, Princeton University*

(Received January 15, 1935)

On the basis of previous theoretical developments concerning the nature of cohesion in metals which were applied to sodium, a treatment of metallic lithium is presented. As before, the system of Fock equations are solved by an indirect procedure as a start. These solutions differ appreciably from those for sodium in several important respects and account for a greater percentage of the observed binding energy than in the latter case. The modification of the exchange energy of the electrons arising from these differences is computed. Finally, the work of Wigner on correlation energies of metal electrons is applied directly to obtain a final binding energy of 34 kg.cal. as compared with the observed value of 38.9. The lattice constant is found to agree with the observed one to within about three percent. Some general remarks concerning the applicability of the present development to solids other than metals are made.

INTRODUCTION

IN previous work[1] a basis for an investigation of the constitution of metals was laid and applied to sodium. In this work a completely self-consistent solution of Fock's equation for the lattice was found and this result was then employed in finding an additional approximation to the problem of minimizing the total energy.[2] The final results of this work yielded a binding energy of 22.3 kg.cal. per mole, to be compared with the observed value of 26.9 kg.cal.

The solution to Fock's equation was undertaken under the guiding principles afforded by the free electron picture of metals, and it was found that the results yielded 4.7 kg.cal. Since this discrepancy was many times larger than the computational errors could allow it was concluded that the simple Slater determinant was inadequate to handle the complexity of the problem and an effort was made to find a more general solution based upon the one-electron one.

An attempt in this direction was presented in II of the previously mentioned papers and this met with partial success. Upon this basis, however, Wigner[1] was able to establish a much more rigorous method and succeeded in solving a set of equations which were the counterpart of the Fock equations in an extended minimal problem, namely, that of minimizing the energy integral by use of a function of the form

$$\Psi=\begin{vmatrix} \psi_1(x_1; y_1\cdots y_n)\cdots\psi_1(x_n; y_1\cdots y_n) \\ \cdot \qquad\qquad \cdot \\ \cdot \qquad\qquad \cdot \\ \cdot \qquad\qquad \cdot \\ \psi_n(x_1; y_1\cdots y_n)\cdots\psi_n(x_n; y_1\cdots y_n) \end{vmatrix} \begin{vmatrix} \psi_1(y_1)\cdots\psi_1(y_n) \\ \cdot \qquad \cdot \\ \cdot \qquad \cdot \\ \cdot \qquad \cdot \\ \psi_n(y_1)\cdots\psi_n(y_n) \end{vmatrix}, \tag{1}$$

in which the variables x and y refer to the three position coordinates of electrons of upward and downward spin, respectively, $\psi_r(y_1)$ are the one-electron solutions of Fock's equations and $\psi_r(x, y_1\cdots y_n)$ are functions of the variable x and parameters $y_1\cdots y_n$. The last set of functions are to be determined in such a way as to minimize the energy. The final energy value obtained was 22.3 kg.cal. for the observed lattice-constant of 4.23A. The remaining discrepancy is regarded as arising principally from a conservative computation of the gain given by (1).

After assuming an ion-core field the work on sodium was considerably lightened by the fact that the solutions of Hartree's equations for the lattice were almost exactly of the form

$$\psi_\kappa=(1/V^{\frac{1}{2}})e^{i\kappa\cdot\mathbf{r}}, \tag{2}$$

where $\mathbf{r}$ is the position vector of the particle, κ is a lattice vector in the inverse-lattice space and V is the total volume of the crystal. This had as

[1] Wigner and Seitz, Phys. Rev. **43**, 804 (1933); **46**, 509 (1934) (I and II). Wigner, Phys. Rev. **46**, 1002 (1934). This work is closely connected with the following papers of J. C. Slater, Phys. Rev. **45**, 794 (1934); Rev. Mod. Phys. **6**, 209 (1934).

[2] A complete account of the equations of Hartree, Fock and Dirac and their interconnection has been given by L. Brillouin, *Actualités Scientifiques et Industrielles*, Nos. 71, 159, 160.

its first important consequence the fact that the solutions of Hartree's equations were practically identical with those of Fock[2] so that the best one-electron solution was obtained with an ease not met in any atomic problem involving more than one electron. In the second place, this gave a definite analytic form to the ψ (y)'s in (1) and allowed an analytic solution of the problem outlined in the previous paragraph. Since (2) are the wave functions for perfectly free electrons, it is to be expected that this simplicity will not generally be met with even in simple metals, for the probability distribution function of each electron will usually be greater inside the unit cell surrounding each ion than on its boundary.

In order to investigate the possibility of applying the scheme employed for sodium to more general cases, the corresponding solution for lithium was undertaken from a similar viewpoint, and these results are presented in the following sections. This work begins with the development of an effective ion core field which reproduces the atomic energy values and follows with a solution of Hartree's equations using this field. The connection between Hartree's and Fock's equations is not as well defined as in the case of sodium but it is found that the energies determined by both are practically identical. In the present paper the work of Wigner on the correlation hole is applied without additional modification.

§1. The Effective Ion-Core Field

The problem of determining a coulomb field $V(r)$ which when placed in an equation of the simple Schroedinger type

$$(\hbar^2/2\mu)\Delta\psi+(V(r)-E)\psi=0 \qquad (3)$$

will yield eigenvalues that are identical with the term values of a single electron series and yet be physically plausible, may not be expected to possess even an approximate solution in any but the simplest of practical cases. The correctness of this assertion follows from consideration of the extensive work of Hartree when viewed in the light of Fock's equations. For the best one-electron solution of any atomic problem is given by the system of equations

$$((\hbar^2/2\mu)\Delta_i+\sum_{i\neq j} V_i(x_j)+\mathbf{A}_i-E_i)\psi_i=0, \qquad (4)$$

in which i and j range over all electrons of the atom, $V_i(x_j)$ is the coulomb potential arising from the ith electron wave function when regarded as an electron charge distribution, and $\mathbf{A}$, is a linear integral "exchange" operator of the form

$$\mathbf{A}_i\psi_i(x_j)=\sum_{i\neq j}e^2\int(1/|x_j-x_i|)(j|\rho|i)\psi_j(x_i)d\tau_i, \qquad (5)$$

in which $(j|\rho|i)$ is the ijth matrix component of the density matrix

$$(j|\rho|i)=\sum_k\psi_k^*(x_j)\psi_k(x_i). \qquad (5a)$$

That $\mathbf{A}_i$ is not completely negligible is shown by the fact that in the case of a single valence electron, Hartree's energy parameters E_j do not agree exactly with the term values of the one-electron states. Because of the form of the exchange operator it is not to be expected that it can be replaced by a central field term, but it may be hoped that in the case of one-electron outside closed shells, its effect on the terms E_j may be roughly approximated by such a field. In the case of Na this was found to be the case, for the Prokofjew field employed in reference 1 gave very good results from the standpoint of energy levels, all of the values agreeing with the observed ones to within one percent.

If this were true for Na, it might be expected that similar results would be true for Li so an attempt was made to find such a field. Prokofjew[3] employed the Wentzel-Kramers-Brillouin approximation in his work, but I found that the field obtained by this method is not a very definitely determined one since all terms in a given series cannot be fitted with equal accuracy in the manner prescribed by Prokofjew. As a result the following device was used.

For a coulomb field of the form Ze^2/r, the W.K.B. approximation gives energy values that are determined by an equation of the Balmer type, namely $E=hcZ^2R/n^2$ in which R is the Rydberg constant in wave numbers per cm, n is an integer, and E the energy in ergs. Since only that portion of r for which

$$\left(E-\frac{Ze^2}{r}+\frac{\hbar^2(l+\frac{1}{2})^2}{2\mu r^2}\right)^{\frac{1}{2}} \qquad (6)$$

[2] Prokofjew, Zeits. f. Physik **58**, 255 (1929).

is real is of importance in using the W.K.B. approximation, where l is the modern angular momentum quantum number and μ the reduced electron mass, the effective field was taken to be of the form e^2/r from ∞ to the value r_m given by the smallest allowable root of (6) for the series of smallest l in which the terms are hydrogen-like. The value of 3.24 Bohr units was taken to be a safe estimate of this quantity, r_m, and will be employed in all of the following work. The problem reduces itself to that of determining a $V(r)$ within this radius which shall join the function e^2/r continuously and with continuous first derivative at this point, be of the form $3e^2/r$ near the nucleus, and reproduce the energy spectrum of the s, p and d series. Other series will automatically be given because of the choice of e^2/r outside of $3.24a_h$.

Now the form of the wave functions for regions beyond r_m may be found for each of the observed energy values because the boundary condition at infinity entirely determines the form of the function in any region excluding the sphere of radius r_m. Hence the ratio $\psi'(r_m)/\psi(r_m)$ may be determined by use of an asymptotic series, for example. This was done for five of the lowest energy values of the Li spectrum and the results for $R'r/R$ at r_m, where $R=r\psi$, are shown in Table I. $V(r)$ is to be chosen so that the functions

TABLE I. *Values of $R'r/R$ at r_m.*

Term	Energy (Ryd. units)	rR'/R (calc.)	Original V	Final V
$2s$	0.3963	−0.1331	−0.06931	−0.122
$3s$	0.1484	−1.646	−1.538	−1.642
$4s$	0.07723	−2.255	−2.126	−2.2570
$2p$	0.2605	0.2422	2.192	0.2428
$3d$	0.1111	1.92	1.91	1.92

derived using it satisfy the proper boundary conditions at the origin and have the same ratio of rR'/R at r_m for the given energies. An initial field V_I was selected on the basis of reasonableness and its solution yielded the ratio shown in the fourth column of Table I. $Z_p=rV_I$ is given in Table II in which Rydberg units are employed. From knowledge of the change of wave functions, it was concluded that V was to be made more negative in the neighborhood of the nucleus to bring the s ratios into agreement and more positive in the neighborhood of the boundary,

TABLE II. *Values of rV_I and rV_{II}.*

r	rV_I	rV_{II}	r	rV_I	rV_{II}
0.00	6.000	6.000	0.84	2.528	2.490
0.04	5.512	5.481	1.00	2.384	2.392
0.08	5.294	5.236	1.16	2.284	2.322
0.12	5.078	4.998	1.32	2.214	2.262
0.20	4.652	4.540	1.64	2.122	2.172
0.28	4.232	4.102	1.96	2.066	2.100
0.36	3.810	3.672	2.28	2.034	2.038
0.44	3.408	3.274	2.60	2.012	2.012
0.52	3.118	2.994	2.92	2.004	2.004
0.68	2.748	2.660	3.24	2.000	2.000

r_m, to improve the p ratios. The correction adopted was of the form

$$-0.4(1.2-r)^2-0.05(0.8-r)(2.5-r)^2 \quad 0\leq r\leq 1.2,$$

$$-0.05(0.8-r)(2.5-r)^2, \quad 1.2\leq r\leq 2.5.$$

This brought about the agreement shown in the last column of Table I and yields the second column of Table II.

The full significance of the procedure employed here is probably best shown by Fig. 1 in which curves A correspond to the ratio $R'r/R$ at $r_m=3.24$ plotted against the energy parameter for the system of functions in which the proper boundary condition is satisfied at infinity and the field $-e^2/r$ is employed. This system is a highly singular one, of course, since $R(r_m, E)$ will have an infinite number of roots in the range between -1 and 0 on the Rydberg scale of units. Only two branches of this curve are shown. Curves B_I and B_{II} represent plots of the same ratio derived

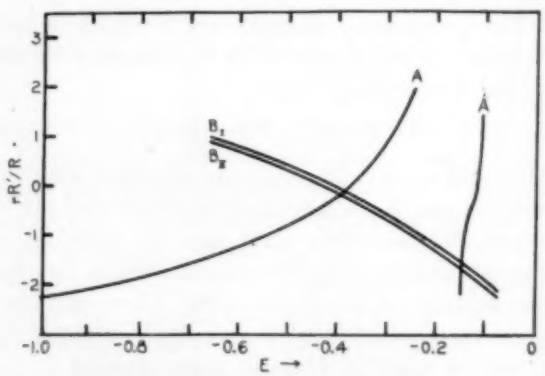

FIG. 1. Plot showing the ratio rR'/R for $r_m=3.24$ as a function of energy. The curve A corresponds to solutions satisfying the proper boundary conditions at infinity, while curves B_I and B_{II} correspond to solutions which satisfy the proper condition at the origin for the initial and final fields, respectively. The abscissas are in Rydberg units and the ordinates in Bohr units.

for the system of functions which satisfy the proper conditions at the origin and for which V_{I} and V_{II} have been employed. The points at which either B_{I} and B_{II} cross the system A yield the eigenvalues of the corresponding fields. Our endeavor has been to make these points be identical with the observed term values and the degree of success is illustrated by the fact that on the scale of this plot the curve B_{II} completely overlaps the curve C drawn through the intercepts of A and the observed term values.

Similar considerations for the Prokofjew field for Na show that the corresponding B curve is not nearly so good a fit of the corresponding curve C and that it would be difficult to find a better field.[4]

§2. Solution of Hartree's Equations

The procedure to be employed in solving Hartree's equations for the lattice will be very similar to that used in the case of Na. On the basis of an approximate Hamiltonian H_i^0 which is the same for each electron, and possesses the proper symmetry properties for the lattice set of "starting functions" are determined by numerical integration of the Schroedinger equation arising from H_i^0. Using these solutions, a Hamiltonian H_i^H may be written down which contains the interaction terms of the ith electron with each ion in the lattice and the Hartree field of interaction between the ith electron and all others, assuming that their charge distribution is determined by the solutions of H_i^0. This field will be the same for all electrons since it is the potential arising from all electrons minus that arising from the electron under consideration and the ratio of the latter to the form will generally be of the order $1/N$, where N is the total number of electrons, that is a very large number. Regarding $H_i^H - H_i^0$ as a perturbation on H_i^0, we may apply the perturbation scheme of Schroedinger or of Brillouin-Wigner[5] and if this perturbation does not appreciably alter the wave functions the solution will be self-consistent in the Hartree sense. Since the perturbation is symmetric (i.e., possesses the same symmetry group as the unperturbed problem) we know at once that no states in the lowest band will enter in the new functions and but one from each of the higher bands, namely that which belongs to the same representation as the unperturbed function.

The Hamiltonian H_i^0 is taken to be of the form

$$-\frac{\hbar^2}{2\mu}\Delta_i + \sum_{\alpha\beta\gamma}{}^{*} V_{\alpha\beta\gamma} = -\frac{\hbar^2}{2\mu}\Delta_i + V^{*}, \qquad (7)$$

in which $V_{\alpha\beta\gamma}$ represents the potential arising from the ion situated at the position $\alpha\tau_1+\beta\tau_2+\gamma\tau_3$ where α, β, γ are integers, τ_1, τ_2, τ_3 are the primitive translations of the group, and $\sum^{*}$ indicates that the sum is to be carried out in such a way that $V_{\alpha\beta\gamma}$ is regarded as being zero outside of the rhombic dodecahedron surrounding the α, β, γ-th ion. In other words the potential at a given point is to be taken as that arising from the ion in the polyhedron within which the point is situated, so that it will generally be a function with discontinuous derivative. That (7) is a good starting operator arises from the fact that it regards the ion-ion interaction as just balancing the interaction of the given electron with all other electrons and ions outside of the polyhedron, in which the electron is, and the interaction of outer electrons with the ion in this polyhedron which would be true if the other electrons formed a constant charge distribution outside of the polyhedron containing the given electron. The results for Na show that this is a rough description of affairs for all simple metals.

Using H_0 and the fact that all wave functions are to be of the form $\eta_\kappa e^{i\kappa\cdot r}$ in which η_κ is invariant under the translation-group and κ is a lattice vector in the inverse-lattice space, the Schroedinger equation for η_κ may be written

$$-(\hbar^2/2\mu)\Delta\eta_\kappa - (\hbar^2/\mu)i\kappa\cdot\nabla\eta_\kappa + V^{*}\eta_\kappa = E_\kappa'\eta_\kappa, \quad (8)$$

where $E_\kappa' = E_\kappa - (\hbar^2/2\mu)\kappa^2$ may be regarded as being the energy of η_κ. If the operator $-(\hbar^2/\mu)i\kappa\cdot\nabla$ be viewed as a perturbation then as in reference 1 we have, using the Schroedinger perturbation theory

[4] As yet unpublished work of Dr. E. Gorin has shown that there is no satisfactory field for K, but that each series may be approximated to within several percent by means of separate fields. I wish to thank Dr. Gorin for the privilege of making this statement.

[5] Brillouin, J. de physique **1** (III), 373 (1932). Wigner, Bull. Hung. Acad. (to appear shortly). Brillouin first presented the perturbation scheme and Wigner later showed that various stages of approximation yield mean values of the Hamiltonian operator.

$$E_\kappa' = E_0 - \sum_\lambda \frac{|\int \eta_\gamma (\hbar^2/\mu)\kappa\cdot\nabla\eta_0|^2}{E_\lambda - E_0}, \qquad (9)$$

$$\eta_\kappa = \eta_0 + i\frac{\hbar^2}{\mu}\sum_\lambda \frac{\int \eta_\lambda \kappa\cdot\nabla\eta_0}{E_\lambda - E_0}\eta_\lambda, \qquad (9a)$$

where λ runs over all solutions of the unperturbed problem. If we consider any η to be expressed by a sum $\sum^*$ over each of the polyhedrons, it was previously shown that the polyhedron may be replaced by a sphere of equal volume for purposes of determining energies. The lowest η_0 is then that function for which the boundary condition $\psi' \equiv \eta' = 0$ is satisfied at the surface of the sphere, while the only η_λ's which need be considered are those p functions which satisfy the relation $\eta_\lambda = 0$ at the boundary of the sphere. For the observed lattice constant of Li, namely, 3.46A, the radius r_s of the equivalent sphere is $3.21a_h$. The energy-r_s curves are shown in Fig. 2.

If we employ the Hartree system of units for which the Bohr radius is the unit of length, e^2/a_h is the unit of energy and both $\hbar$ and the electron mass are 1, the values of the integrals $\int \eta_\lambda \partial\eta_0/\partial x = \alpha_\lambda$ are given in Table III for the

TABLE III. *Values of integrals* $\int \eta_\lambda \partial\eta_0/\partial x = \alpha_\lambda$.

	r_1	3.21	3.33	3.62	3.88
I	$E-E_0$	0.64	0.60	0.50	0.43
	α_λ	0.2402	0.2214	0.1720	0.1407
II	$E-E_0$	2.27	2.10	1.79	1.54
	α_λ	0.2718	0.2565	0.2317	0.2142
III	$E-E_0$	4.84	4.55	3.93	3.47
	α_λ	0.2045	0.1822	0.1568	0.1513

three lowest-energy p functions going with four values of r_s. The values of $E_\lambda - E_0$ are listed simultaneously in terms of Hartree's energy unit. The Roman numerals refer to each of the three sets of p functions of Fig. 2. Using these integrals and the same system of units, the sum in (9) reduces to the form $\beta\kappa^2/2$ for which β takes the values given in Table IV. In the perturbation scheme

TABLE IV. *Values of* β.

r_s	3.21	3.33	3.62	3.88
β	0.266	0.245	0.194	0.168

of Brillouin-Wigner the second approximation for the energy has a form much the same as (9),

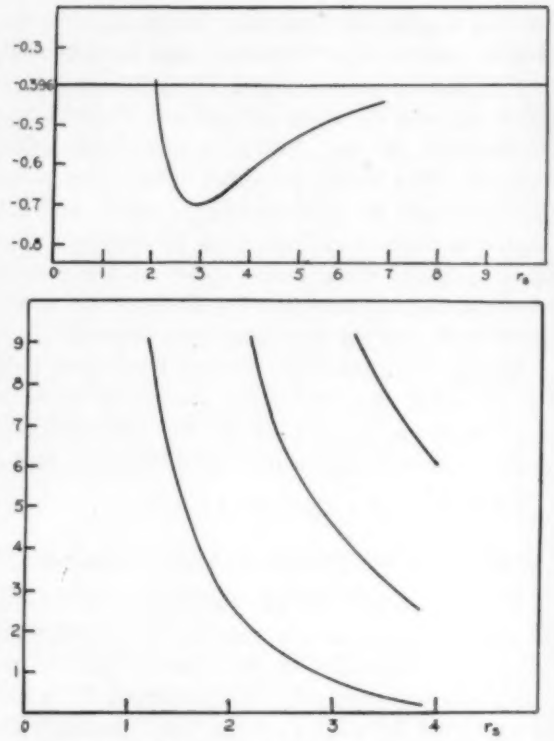

FIGS. 2a and 2b show the energy-r_s curves for s and p function, respectively. The ordinates are in Rydberg units and the abscissas in Bohr units.

with the exception that E_κ' replaces E_0 in the denominator of each term in the sum, so that one obtains an implicit equation for E_κ'. Since E_κ' is a function of κ^2, we may obtain a power series for E_κ' from this by means of a successive approximation method in which the solution obtained by placing $E_\kappa' = E_0$ in the denominator is regarded as the first-order solution. The next approximation is obtained by placing this in the denominator and expanding the fraction in terms of κ^2, etc. This series is of the form

$$E_\kappa' = E_0 - \tfrac{1}{2}\lambda_1\kappa^2 + \tfrac{1}{4}\lambda_2\kappa^4 - \tfrac{1}{8}\lambda_3\kappa^6,$$

in which λ_1 is just β of the Schroedinger approximation and

$$\lambda_2 = \lambda_1\left(\sum_\lambda \frac{2\alpha_\lambda^2}{(E_\lambda - E_0)^2}\right),$$

$$\lambda_3 = \lambda_2\sum_\lambda \frac{2\alpha_\lambda}{(E_\lambda - E_0)^2} + \lambda_1^2\sum_\lambda \frac{2\alpha_\lambda}{(E_\lambda - E_0)^3}.$$

The values of λ_2 and λ_3 for the values of r_s previously listed are given in Table V. The value

TABLE V. *Values of* λ_2, λ_3 *and* k.

r_s	λ_2	λ_3	k
3.21	0.0829	0.0745	0.5978
3.33	0.0747	0.0509	0.5754
3.62	0.0482	0.0319	0.5301
3.88	0.0423	0.0251	0.4946

$\sqrt{\kappa^2}=k$ corresponding to the uppermost electrons of the filled band of levels is given by $k=(9\pi/4)^{\frac{1}{3}}/r_s$ and from the last column of Table V it is seen that the term in k^6 is practically negligible. The term in k^4 corresponds to part of the fourth order approximation of the Schroedinger scheme so that its order of magnitude is an indication of the error made in employing the second order approximation of either perturbation scheme. The mean energy per electron of the function $\psi_\kappa=\eta_\kappa e^{i\kappa\cdot r}$ will be $\overline{E}_\kappa=\overline{E_\kappa'+\frac{1}{2}\kappa^2}$ in Hartree units or

$$\overline{E}_\kappa=E_0+\frac{3}{10}(1-\lambda_1)k^2+\frac{3}{28}\lambda_2k^4-\frac{1}{24}\lambda_3k^6. \quad (10)$$

The corresponding energy for perfectly free electrons in a potential trough of depth E_0 is $E_0+3k^2/10$. The ratio of (10) to this, excluding E_0 in both cases, is given in Table VI along with the ratio $1-\beta$ for the Schroedinger perturbation scheme. As expected from the minimum-value viewpoint, the Brillouin-Wigner scheme yields a higher energy than the Schroedinger scheme in the same approximation although they differ by only about a percent. In the last column of Table VI, the equivalent Fermi energy of the former scheme is listed in terms of kg.cal. per mole.

In the second appendix of II, reference 1, it was shown that the electrostatic energy of a body-centered lattice of positive charges e surrounded by a uniform distribution of negative charge such that there are e units per s polyhedron, was practically the same as the energy

TABLE VI. $(1-\beta)$ *and the ratio of* $E_0+3k^2/10$ *to* $\overline{E}_k$ *for the Brillouin-Wigner scheme.*

r_s	$1-\beta$	Brillouin-Wigner	Difference	Energy (kg. cal.)
3.21	0.734	0.744	0.010	48.8
3.33	0.755	0.763	0.008	46.5
3.62	0.806	0.810	0.004	42.0
3.88	0.832	0.835	0.003	37.8

of a uniformly charged sphere with a point charge e at its center, so that the classical energy per electron of the lattice, when the actual distribution is present, will be that of the actual charge distribution in the s sphere. As a result of this, we shall assume that the proper Hartree field to employ in writing down H_i^{II} of the first paragraph of this section, is just $H_i^0+\sum_{\alpha\beta\gamma}{}^{*}V_{e,\,\alpha\beta\gamma}$, where $V_{e,\,\alpha\beta\gamma}$ is the Hartree potential arising from the electron charge distribution within the $\alpha\beta\gamma$th s polyhedron. $V_{e,\,\alpha\beta\gamma}$ will be a slowly varying positive function of position within a given polyhedron just as in the case of sodium, so that $\sum_{\alpha\beta\gamma}{}^{*}V_{e,\,\alpha\beta\gamma}$ will be slowly varying throughout the lattice. Hence the integrals $\int\psi_\kappa^*(\sum_{\alpha\beta\gamma}{}^{*}V_{e,\,\alpha\beta\gamma})\psi_\lambda$ will be small in all cases except when $\kappa=\lambda$ because of orthogonality, and the eigenfunctions of H_i^{II} will be practically identical with those of H_i^0. This is clearly seen if $\sum_{\alpha\beta\gamma}{}^{*}V_{e,\,\alpha\beta\gamma}$ is regarded as a perturbation on H_i^0 as in reference 1, II.

Thus the eigenfunctions of H_i^0 are the solutions of Hartree's equations for the lattice and we may now proceed with an investigation of Fock's equations.

§3. The Solution of Fock's Equations for the Lattice

For the case of perfectly free electrons, Fock's Eqs. (4) are reducible to the Schroedinger form since exponential functions are[6] eigenfunctions of the operator **A**, so that Fock's and Hartree's equations are identical. In the present case this will not be precisely true, but we may easily determine the order of magnitude of the difference in the mean energies of the total Hamiltonian of the crystal obtained from an anti-symmetric combination of each set of solutions.

We have found that the eigenfunctions of H_i^0 were approximately of the form

$$\psi_n=\sum_{\alpha\beta\gamma}{}^{*}(f_0(r_{\alpha\beta\gamma})+i\kappa\cdot\mathbf{r}_{\alpha\beta\gamma}f_1(r_{\alpha\beta\gamma}))e^{i\kappa\cdot r}, \quad (11)$$

where $r_{\alpha\beta\gamma}$ is the radial distance in the $\alpha\beta\gamma$th s polyhedron, f_0 is an s function normalized within an s polyhedron, and f_1 is $r_{\alpha\beta\gamma}$ times a

[6] L. Brillouin, J. de physique **5**, 413 (1934).

sum of the radial part of p functions. More explicitly, if we normalize the radial p functions $f_\lambda(r)$ so that

$$\int_{\vartheta_0} f_\lambda^2 r^2 dr = 3/4\pi, \quad \text{or}$$

$$\int_{\vartheta_0} [(\kappa\cdot\mathbf{r})^2/r^2] f_\lambda^2 r^2 dr \sin\theta d\theta d\varphi = \kappa^2,$$

where ϑ_0 is the volume of an s-sphere, (11) is of the form

$$\psi_\kappa = e^{i\kappa\cdot\mathbf{r}} \sum_{\alpha\beta\gamma}{}^{*} (f_0 + i\cdot\kappa\cdot\mathbf{r}_{\alpha\beta\gamma} \sum_\lambda \gamma_\lambda f_\lambda / r_{\alpha\beta\gamma}) \quad (11a)$$

with

$$\gamma_\lambda = (\hbar^2/\mu) \int_{\vartheta_0} \eta_\kappa (\partial/\partial x_\kappa) \eta_0 d\tau / (E_\lambda - E_0) = \alpha_\lambda/(E_\lambda - E_0), \quad (11b)$$

so that

$$f_1 = \sum_\lambda \gamma_\lambda f_\lambda / r_{\alpha\beta\gamma}. \quad (11c)$$

Table VII gives the γ's corresponding to the α's of Table III. In order to proceed further with the present discussion we shall assume that f_0 and f_1 are constants. Aside from the fact that both of these functions are slowly varying, this will not affect any conclusions concerning relative orders of magnitude of effects. Under this assumption (11) reduces to

TABLE VII. *Values of γ corresponding to the α's of Table III.*

r_s	3.21	3.33	3.62	3.88
I	0.375	0.369	0.344	0.313
II	0.120	0.123	0.130	0.140
III	0.042	0.040	0.040	0.044

$$\psi_\kappa = \sum_{\alpha\beta\gamma}{}^{*} (1 + i\gamma\kappa\cdot\mathbf{r}_{\alpha\beta\gamma})/\cdot\vartheta_0^{\frac{1}{2}}, \quad (12)$$

where

$$\gamma^2 = 5(\sum_\lambda \gamma_\lambda^2)/r_s^2. \quad (13)$$

The normalizing constant for (12) is then $1/A$ where

$$A^2 = N(1+\kappa^2\gamma^2), \quad (13a)$$

N being the total number of electrons in the metal. In the following work, integrations over the entire crystal may be replaced by integrations over the s-sphere if the factor N in (13a) is neglected.

The term containing the operator $\mathbf{A}_\kappa$ in Fock's equations for ψ_κ may, as is well known, be replaced by the summation

$$-\sum_\nu{}' g_\nu(x)\psi_\nu(x), \quad (14)$$

where ν is summed over all values except κ and

$$g_\nu(x) = [\int \psi_\nu^{*}(y)\psi_\kappa(y) d\tau_y]/|y-x|, \quad (15)$$

where y and x each refer to three coordinate variables and $d\tau_y$ is the corresponding volume element. For the functions (12), if we let

$$\psi_\nu = \sum_{\alpha\beta\gamma}{}^{*} (1 + i\gamma\nu\cdot\mathbf{r}_{\alpha\beta\gamma})/\vartheta_0^{\frac{1}{2}},$$

any term of (14) may be written

$$(1+i\gamma\nu\cdot\mathbf{x}) e^{i\nu\cdot\mathbf{x}} \int [(1+i\gamma\kappa\cdot\mathbf{y})(1-i\gamma\nu\cdot\mathbf{y})/|y-x|^2] e^{i(\kappa-\nu)\cdot\mathbf{y}} d\tau_y.$$

Or if we make the transformation $z = y - x$ this is identically

$$(1+i\gamma\kappa\cdot\mathbf{x}) e^{i\kappa\cdot\mathbf{x}} \int [(1+i\gamma\kappa\cdot\mathbf{z})(1-i\gamma\nu\cdot\mathbf{z}) e^{i(\kappa-\nu)\cdot\mathbf{z}}/|z|] d\tau_z \quad (16)$$

to within terms of the second order in $\gamma\nu$ and $\gamma\kappa$. The integral in (16) is a constant, however, and may be added directly to the energy parameter. Hence to within terms of the second order in the foregoing quantities, Hartree's and Fock's equations are identical for functions of the type (12). The energy terms of this order of magnitude which arise in the so-called "exchange integrals," will be found to be negligibly small.

§4. The Energy Resulting from the Solutions of Fock's Equations

We may now proceed with a computation of the mean value of the proper Hamiltonian for the metal based upon the previous one-electron solutions. This Hamiltonian will be of the form

$$H=\sum_i \frac{\hbar^2}{2\mu}\Delta_i+\frac{1}{2}\sum_{i,j}{}'\frac{e^2}{r_{ij}}+\frac{1}{2}\sum_{\alpha,\beta}{}'\frac{e^2}{r_{\alpha\beta}}+\sum_{i\alpha} V_{\alpha i}, \tag{17}$$

using the notation of §1 where $V_{\alpha i}$ is the potential of the ith electron in the field of the αth nucleus. The simple form of the third term arises from the fact that the nuclei are separated enough so that the closed shells do not overlap. It was shown in II, reference 1, that the mean values of the first and last two operators combine with the coulomb integrals of the second in such a manner that the result is simply the sum of the energy parameters of (8) plus N times the self-potential of the charge distribution within an s-sphere. From (9), this distribution, is simply the mean value over occupied states of

$$e(f_s^2+(\kappa\cdot\mathbf{r})^2 f_1^2(r))(1-\kappa^2\gamma'+\kappa^4\gamma'^2), \tag{18}$$

where $\gamma'=\sum_\lambda \gamma_\lambda^2$. The last factor is simply the normalizing constant. This mean value is

$$e\left(1-\gamma'\frac{3}{5}k^2+\gamma'^2\frac{3}{7}k^4\right)f_s^2+\left(\frac{k^2}{5}-\gamma'\frac{k^4}{7}\right)(\sum_\alpha \alpha_\alpha f_\alpha)^2, \tag{19}$$

which is illustrated in Fig. 3 for $r_s=3.21$. If we designate by χ the part of this which deviates from the constant mean value e/ϑ_0, that is, let (19) be replaced by $e/\vartheta_0+\chi$, the self-energy, may be written

$$\frac{6}{10}\frac{e^2}{r_s}+\int \chi\left(\frac{3}{2}\frac{e^2}{2r_s}-\frac{e^2r^2}{2r_s^3}\right)r^2dr, \tag{20}$$

in which the self-energy of χ has been neglected. The integral in (20) has been evaluated for four values of the lattice constant and in each case the results were $0.001e^2/a_h$ (0.6 kg.cal.).

It now remains to compute the total exchange energy of the electrons. In the previous work this was done by determining the so-called Fermi-hole which is a function describing the probability that another electron will be at a distance r from a given electron and then evaluating the decrease in interaction energy of electrons resulting from this correlation. This decrease is just the exchange

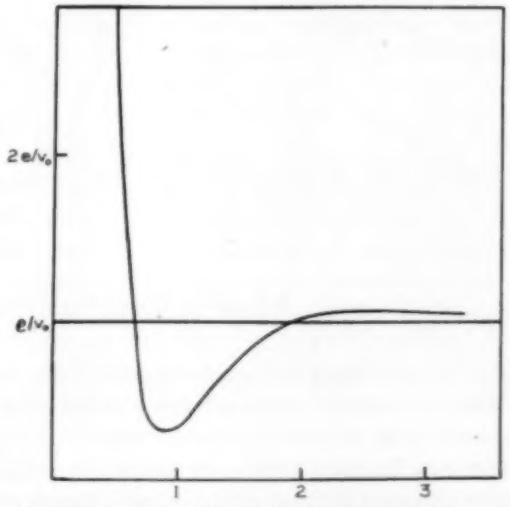

FIG. 3. Plot of mean charge distribution within a given s-sphere. The abscissas are in Bohr units.

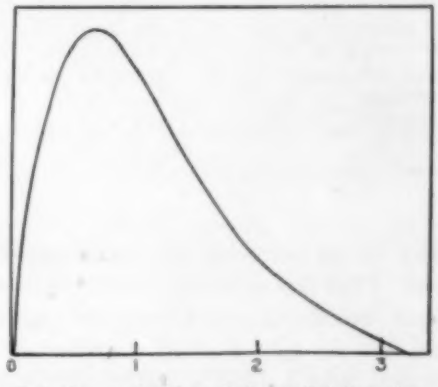

FIG. 4. Relative scale plot of the radial function f_1. The abscissas are in Bohr units.

energy and in the Fock approximation arises only for electrons of parallel spin. Explicitly, the energy is

$$\frac{e^2}{2}\sum_{\mu}\sum_{\nu}\int\frac{\psi_\mu^*(x_1)\psi_\nu^*(x_2)\psi_\mu(x_2)\psi_\nu(x_1)}{|x_1-x_2|}d\tau_1 d\tau_2, \tag{21}$$

in which ν and μ are to be summed over all occupied states of parallel spin. The factor $\frac{1}{2}$ enters in order that interactions are not counted doubly. If the order of summation and integration is interchanged the mean value of the summed numerator, when regarded as a function of x_1-x_2 is just the Fermi-hole.

In the case of the approximate eigenfunctions $e^{i\nu\cdot r}$ this function depended only upon $|x_1-x_2|$ so that the "exchange potential"

$$\int\psi_\mu^*(x_1)\psi_\nu^*(x_2)\psi_\mu(x_2)\psi_\nu(x_1)/|x_1-x_2|d\tau_{x_1-x_2}$$

of a given electron did not depend upon its position in the lattice. This statement is clearly identical with the previous one that the operator **A**, in (4) is constant for exponential functions.

In the case of lithium, the functions ψ_ν are of the form (11) so that the shape of the Fermi-hole and the exchange energy will differ from that of sodium. Any direct calculation of this change is made very difficult in comparison with the calculations of the coulomb energy because of the fact that the integral in (21) may not be split into integrals over single s-polyhedrons in any simple manner. For purposes of simplifying this computation, we shall assume a modified form of the function (11), namely, that in which both f_0 and f_1 are taken to be constants. The first function is very nearly constant, just as in the case of sodium, so that the error arising from this source will not be appreciable. The second has the form shown in Fig. 4, and though not constant, it varies smoothly and is small in comparison with f_0. An estimate of the error made in adopting this last assumption will be obtained from the magnitude of the energy terms arising from f_1 for it will be clear that these cannot undergo any great change if the actual f_1 is replaced by a constant.

We start, then, with functions

$$\psi_\nu=(e^{i\nu\cdot r}/\vartheta_0^{\frac{1}{2}})(1-i\vartheta_0^{\frac{1}{2}}\sum_\alpha{}^*\nu\cdot\mathbf{r}_\alpha f_1(r_\alpha)), \tag{22}$$

for which the normalizing constant is

$$\int_V|\psi_\nu|^2d\tau=N(1+\nu^2\gamma)=N\gamma_\nu'. \tag{22a}$$

The numerator of (21) is

$$e^{i(\nu-\mu)\cdot(r_1-r_2)}(1/\vartheta_0{}^2N^2\gamma_\mu'\gamma_\nu')[1+i\vartheta_0^{\frac{1}{2}}\sum_\alpha{}^*(\nu-\mu)\cdot\mathbf{r}_\alpha f_1(r_{1\alpha})+i\vartheta_0^{\frac{1}{2}}\sum_\beta{}^*(\mu-\nu)\cdot\mathbf{r}_{2\beta}f_1(r_{2\beta})$$

$$+i(\sum_\alpha{}^*(\mu-\nu)\cdot\mathbf{r}_{1\alpha}f_1(r_{1\alpha}))(\sum_\beta{}^*(\mu-\nu)\cdot\mathbf{r}_{2\beta}f(r_{2\beta}))+\vartheta_0\sum_\alpha{}^*(\nu\cdot\mathbf{r}_{1\alpha})(\mu\cdot\mathbf{r}_{1\alpha})f_1{}^2(r_{1\alpha}) \tag{23}$$

$$+\vartheta_0\sum_\beta{}^*(\mu\cdot\mathbf{r}_{2\beta})(\nu\cdot\mathbf{r}_{2\beta})f^2(r_{2\beta})]$$

in which terms involving the components of μ and ν to higher than the second power have been dropped. That this is allowable will be seen from the results below by comparing the order of magnitude of the effects arising from the term in the first power with those from the second.

If we now set $\mathbf{r}_{2\beta}=\mathbf{r}_{1\alpha}+\xi-\tau_{\alpha\beta}$ where ξ is to be regarded as being defined over the entire range of the crystal, and $\tau_{\alpha\beta}$ is the lattice vector connecting the αth and βth polyhedron, we obtain upon integrating over r_1 with $f_1=z\equiv(15\gamma/4\pi r_0^5)^{\frac{1}{2}}$

$$e^{i(\nu-\mu)\cdot\xi}(1/\vartheta_0^2 N^2\gamma_\mu'\gamma_\nu')\Big[N\vartheta_0+i\vartheta_0^{\frac{1}{2}}z\sum_a{}^*\int^*(\mu-\nu)\cdot(\xi-\tau_{a\beta})d\tau_1+N\vartheta_0(\mu-\nu)^2\gamma$$
$$+\vartheta_0 z^2\sum_a{}^*\int^*(\mu-\nu)\cdot\mathbf{r}_{1a}(\mu-\nu)\cdot(\xi-\tau_{a\beta})d\tau_1+2N\vartheta_0\nu\cdot\mu\gamma+\vartheta_0 z^2\sum_a{}^*\int^*\mu\cdot\mathbf{r}_{1a}\nu\cdot(\xi-\tau_{a\beta})d\tau_1$$
$$+\vartheta_0 z^2\sum_a{}^*\int^*\nu\cdot\mathbf{r}_{1a}\mu\cdot(\xi-\tau_{a\beta})d\tau_1+\vartheta_0 z^2\sum_a{}^*\int^*\mu\cdot(\xi-\tau_{a\beta})\nu\cdot(\xi-\tau_{a\beta})d\tau_1\Big]. \quad (24)$$

The integrals $\int^*$ are defined in such a way as to take the continuous nature of ξ into account. That is, in integrating r_1 over the range contained in a single polyhedron the discontinuous range associated with functions of r_2 must be kept clearly in mind. This may be done without difficulty if each integral $\int^*$ is regarded as being a sum of integral such that each one corresponds to a range of $\mathbf{r}_1$ for which $\mathbf{r}_1+\xi$ lies within a fixed polyhedron. It is clear that the integrals of $\mathbf{r}_1$ over different polyhedra are equal, so that we may restrict the discussion to just one and drop the N in the denominator of (24).

The results of this integration will be a continuous function of ξ and the variables ν and μ. If we average over the latter two the result will be simply the Fermi-hole for a given electron.

It is not convenient to carry out the integration over $\mathbf{r}_1$ for all orientations of ξ because of the complexity of the integrand and we shall restrict the discussion to the case in which ξ lies in the (100) direction. This will not alter the results arising from the constant term in the parenthesis of (24), since this gives rise to a spherically symmetric function of ξ, which was just the Fermi-hole in the case of sodium. Since there are fully forty-eight equivalent directions for a crystal having body-centered symmetry, the function arising from the remaining terms will be nearly spherically symmetric so that this restriction is not of major significance.

If we expand the normalizing constant $1/\gamma_\mu'\gamma_\nu'$ to second order terms in μ and ν and combine this with the parenthesis an important reduction is effected and the result is

$$e^{i(\nu-\mu)\cdot\xi}(1/\vartheta_0)\Big[1+i\vartheta_0^{\frac{1}{2}}z\int^*(\mu-\nu)\cdot(\xi-\tau_a)d\tau_1+z^2\int^*\mu\cdot\mathbf{r}_1\mu(\xi-\tau_a)d\tau_1$$
$$+z^2\int^*\nu\cdot\mathbf{r}_1\nu\cdot(\xi-\tau_a)d\tau_1+z^2\int^*\mu\cdot(\xi-\tau_a)\nu\cdot(\xi-\tau_a)d\tau_1\Big].$$

In performing the integration over $\mathbf{r}_1$, we shall replace the s-polyhedron by the equivalent sphere of radius r_s in the usual manner. Because of this, the vector ξ if fixed in direction will always lie within the cylinder generated by moving this sphere in the given direction. Since spheres do not form space-filling solids, we must adopt some reasonable arrangement of these within this cylinder corresponding to the different polyhedra. There are several reasonable configurations, but that which we shall adopt will be chosen in such a manner as to compensate in part the assumption that ξ lies in the (100) direction. We shall use the arrangement of Fig. 5 in which the spheres are placed tangentially on the axis of the cylinder. This is to be compared with Fig. 5b in which the actual polyhedron boundaries are shown on the corresponding scale for a plane normal to the (001) axis. There are several points to be noted in this comparison. First, the distance between sphere-centers does not correspond to the distance between polyhedron-centers, and this partly compensates the fact that neighboring polyhedra are farthest apart in the (100) direction. Second, since ξ lies in the (100) direction each of the integrands will be

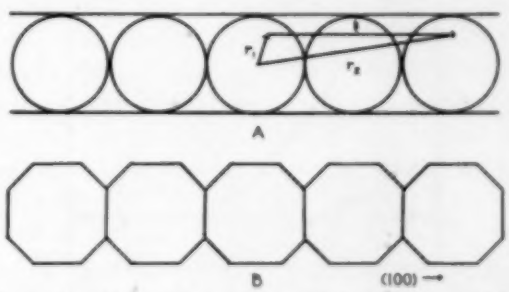

FIGS. 5a and 5b. A comparison of the relative positions of s-spheres and polyhedrons for a cut in the (100) direction of the crystal, orthogonal to the (010) direction.

the same function of $(\xi-\tau_{\alpha\beta})$ for polyhedra lying in the same vertical plane. Because of this, we shall take the integrand to be axially symmetric in the region of the cylinder outside of two neighboring spheres and assume that a node plane passes through the point of tangency. The volume outside of spheres is not equal to that contained in spheres, the ratio being 1 : 2, but this is not of great consequence. There are then three important regions of integration to be considered :

I. The region of $\mathbf{r}_1$ for which $\mathbf{r}_1+\xi$ is in the same sphere as when $\mathbf{r}_1=0$.
II. The region for which $\mathbf{r}_1+\xi$ lies in an adjacent sphere.
III. The region for which $\mathbf{r}_1+\xi$ lies outside of spheres.

Only in the case for which $\xi=nr_s$ with n an integer is the contribution from II and III zero. The correction to the Fermi-hole resulting from this integration is shown in Fig. 6 along with the Fermi-hole for free electrons. The exchange energy as a function of r_s is

$$-0.458e^2/r_s-1.05\gamma^{\frac{1}{2}}e^2/r_s^{\frac{1}{4}}+1.40\gamma e^2/r_s^{\frac{1}{2}}-2.49\gamma e^2/r_s^{\frac{1}{3}}.$$

The energy arising from each of these terms is given in Table VIII along with the sum. The energies are in kg.cal. As might have been expected, the energy arising from the linear term in ν of the parenthesis of (25) is larger than that arising from the quadratic terms by a factor of about 5. On the whole, however, the exchange energy is not greatly affected in spite of the presence of this linear term and we may conclude that f_1 in (11) causes a change in the shape of the Fermi-hole of such a type as to leave the energy almost unaltered.

TABLE VIII. *Energies arising from each term in the expression for the exchange energy.*

r_s	1	2	3	4	Sum
3.21	−88.5	−1.2	0.1	−0.3	−89.9
3.33	−85.3	−1.0	0.1	−0.3	−86.5
3.62	−78.4	−0.7	0.0	−0.2	−79.3
3.88	−73.2	−0.5	0.0	−0.1	−73.8

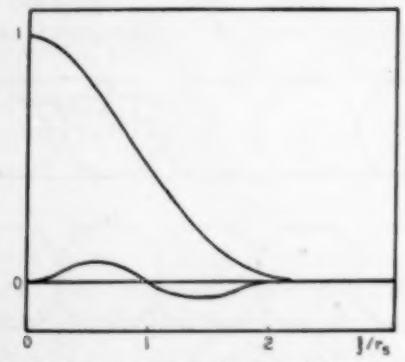

FIG. 6. The large curve is the Fermi-hole function for free electrons and the small curve represents the relative scale correction to this. Abscissas are in units of r_s.

We may now sum up the results of this investigation of the solution of Fock's equations with Table IX in which the mean value of the proper Hamiltonian when taken with an antisymmetric combination of the solutions is listed. The minimum value of the energy occurs for $r_s=3.38$ corresponding to a lattice constant of 3.65A.

TABLE IX. *Mean values of the proper Hamiltonian.*

r_s	3.21	3.33	3.62	3.88
Energy (kg. cal.)	13.9	14.5	14.0	12.6

§5. CONCERNING ADDITIONAL CORRELATIONS

As was pointed out in reference 1, II, the principal weakness of the Slater-Fock approximation lies in the fact that it does not give rise to correlations between electrons of antiparallel spin, that is, there is no analog of the Fermi-hole for electrons of antiparallel spin. That such a hole is of major importance from the standpoint of binding energy was a viewpoint adopted from the start and it was concluded that practically all of the discrepancy between the observed binding energy and that given by the solution to Fock's equations arises from this source. The process of introducing more general correlations is simply one of selecting a more general complete wave function than the Slater determinant, as discussed in the introduction, for the case in which the solutions to Fock's equations were practically of the form $e^{i\mathbf{k}\cdot\mathbf{r}}$, it was found possible to present another approximation which forms a natural sequel to the Fock approximation.

Strictly speaking, these results are valid only in the case of exponential eigenfunctions, but at the present time they will be taken over directly for the case of Li. The results on exchange energies indicate that the error introduced will probably not lie outside the computational error

of the work of Wigner so that until some future time when the entire work of correlation energies is gone over from a more rigorous standpoint, this will be considered adequate.

Using the work of Wigner directly, we obtain the results of Table X in which the upper row

TABLE X.

r_s	3.21	3.33	3.62	3.88	Obs.
Corr. energy (kg. cal.)	19.8	19.2	18.4	17.9	
Total	33.7	33.7	32.4	30.5	38.9

gives the correlation energies and the lower the final binding energies as functions of r_s. The final lattice constant is found to be 3.53A corresponding to $r_s = 3.27$ for which the binding energy is 33.8 kg.cal. The observed lattice constant of 3.46A corresponds to $r_s = 3.21$. The sources of these experimental values are the same as those used for sodium.

The fact that the results of the present work are in better accord with experimental results as far as the lattice constant is concerned, I believe to rest upon the increased accuracy of the computation for lattice constants other than the observed one. In the case of sodium most attention was paid to the computations for this value of r_s. For example, this was particularly true in the determination of the Fermi-energy. I hope that time permits a renewed investigation of this point in the near future.

§6. General Remarks Concerning the Solutions of Fock's Equations for Solids

There are several features of the preceding development that will be valid for crystals other than the monovalent metals lithium and sodium if slightly altered. It may be of interest to point these out at this time.

In the first place, the Hamiltonian (17) contains the explicit assumption that the full effect of closed shells and ions on the valence electrons may be included in the resultant field arising from the superposition of central fields which satisfy the conditions described in §1. This assumption is generally too stringent, for as discussed in the same section, these conditions may be satisfied only in the simplest cases. If the closed-shell electrons are not greatly affected by the precise form of the valence-electron functions, as Hartree's work shows to be the case for very many atoms, this ion-core field may be replaced by one of the Hartree type in which the classical potential of the core charge is employed. Then when Fock's equations have been solved for this field, the interaction energy of valence and core electrons may be treated as an additive constant to the binding energy. Such a procedure would be highly practicable in those cases in which the Hartree fields are known and probably represents the best approach to the theoretical solution of most solids for some time to come.

Next, in dealing with ion-ion interaction, it was assumed in the present case that the overlapping of closed shells was sufficiently small so that the interaction was purely classical and, as a consequence, the same as that arising from point centers. This is clearly the simplest possible case. The next degree of complexity of interaction is that in which overlapping occurs to such an extent that the interchange forces between neighboring ions are small but not negligible; that is, the magnitude of the interchange interaction energies is not negligible but the core eigenfunctions will not be altered enough to change the Hartree field arising from them. For most of the solids formed of atoms in the short periods of the periodic chart as well as the alkali and alkaline earth metals this will be the case, and the exchange interaction energy may be computed on the basis of the usual Heitler-London approximation for which a good deal of work has already been done.[7] In those cases in which the closed-shell electrons are considerably affected by ion-ion interaction, as may occur with certainty in the long series in which "unstable" closed shells are present in the free atom, the closed-shell electrons must be treated on an equal footing with the valence electrons. It is just in these cases that the clear-cut concept of valency breaks down from the chemist's viewpoint as well as that of the atomic spectroscopist. It is needless to say that although the formal procedure of solution may be well defined in such

[7] Heitler and London, Zeits. f. Physik **44**, 455 (1927); A. Unsöld, Zeits. f. Physik **43**, 563 (1927); L. Pauling, Zeits. f. Krist. **67**, 377 (1928); N. Bruck, Zeits. f. Physik **51**, 707 (1928); M. Born and J. Mayer, Zeits. f. Physik **75**, 1 (1932); J. Mayer and L. Helmholtz, Zeits. f. Physik **75**, 19 (1932); W. Bleick and J. Mayer, J. Chem. Phys. **2**, 252 (1934).

cases, the practical difficulty will be as great as it is in the case of Hartree's work. It is at this point that questions of ferromagnetism arise and quantitative treatment of this topic will probably be approached only after surmounting the difficulties outlined here, for the works of Heisenberg, and Bloch[8] give convincing indications that the source of ferromagnetism lies in strong ion-ion interaction rather than in the mere presence of free electrons of the type met with in lithium and sodium.

Next, in proceeding with the solution of Fock's equations for all electrons not in "fixed" closed shells we have assumed at start that the one-electron wave functions are of such a form that they extend throughout the entire crystal, or more exactly, that $|\psi|^2$ possesses the symmetry of the lattice in the space-group sense. This had as an extremely important consequence, from the practical computational standpoint, the fact that Fock's equation for each wave function is practically identical with all others because the effect on a given electron of an electron in the same state is negligible in comparison with the effect of all other electrons. As discussed in §2, the ratio of effects is $1 : N$, N being the total number of unit cells in the crystal. This rests directly upon the presence of translational symmetry, characteristic of the solid state in general, and is a primary point in which the Fock approximation for solids is simpler than for complex atoms or molecules. The importance of this lies not only in the fact that we need deal with but one equation of the form (4) in which $\sum_{i \neq j} V_i(x_j)$ and $\mathbf{A}_j$ are practically the same for all electrons, but that the different solutions are automatically orthogonal without introducing normalization parameters, or rather that these parameters may be taken to be zero.

As a final point, the neglect of magnetic interaction of electrons may be open to discussion. The general computational theory of atomic spectra shows that these forces are usually large only for tightly bound electrons that play an important role in the production of x-ray spectra and may be neglected for valence electrons. This neglect is unquestionably safe in the case of light atoms as the work of Hylleraas on He, Guillemin and Zener, Slater, and Wilson on lithium, and James and Coolidge on H_2 shows[9] to be the case.

In the present work it has been assumed that the so-called Brillouin discontinuities in the energy surface are not important. This was found to be true in sodium[1] and will probably be true in other alkali metals. In cases in which there are two or more valence electrons per atom, this neglect will not be permissible since electrons will occupy states outside of the first zone. At the present time the author is carrying on an investigation of these discontinuities from the standpoint of the representations of space-groups which it is hoped may clear up some uncertain points in connection with their existence.

[8] See Van Vleck, *The Theory of Electric and Magnetic Susceptibilities*, Oxford Press, Chapter XII.

[9] E. A. Hylleraas, Zeits. f. Physik **57**, 815 (1929); V. Guillemin and C. Zener, Zeits. f. Physik **61**, 199 (1930); J. C. Slater, Phys. Rev. **36**, 57 (1930); E. B. Wilson, J. Chem. Phys. **1**, 210 (1933); H. M. James and A. S. Coolidge, J. Chem. Phys. **1**, 825 (1933).

Structure, Ionization and Ultraviolet Spectra of Methyl Iodide and Other Molecules

ROBERT S. MULLIKEN, *Ryerson Physical Laboratory, University of Chicago*

(Received February 5, 1935)

A SYSTEMATIC and comparative study of a variety of molecular types (halogens, hydrogen halides, monovalent metal halides, methane, ammonia, and their halogen derivatives, ethane, ethylene, acetylene, hydrazine, hydrogen peroxide, CN compounds, etc.) has led to conclusions as to electronic structures in normal and low excited states and therefore as to the interpretation of observed ionization potentials and ultraviolet absorption spectra, for these molecules. A paper on the halogens has already appeared,[1] and papers on other molecular types are nearly finished. As a sample of the results, conclusions concerning methyl iodide (CH_3I) may be summarized.

The normal state (symmetry C_{3v}), omitting iodine inner electrons, may be described as

$$(1s_C)^2[sa_1]^2(5s_Ia_1)^2[\pi e]^4[\sigma a_1]^2(5p\pi_Ie)^4,\ {}^1A_1. \quad (1)$$

The orbitals $[sa_1]$, $[\pi e]$, etc., are given in probable decreasing order of term value (ionization potential). The orbitals $[sa_1]$, $[\pi e]$, $[\sigma a_1]$ may be regarded as belonging to the molecule as a whole, although $[\pi e]$ is completely, $[sa_1]$ largely, localized in the CH_3 radical. Symbols a_1 and e are systematic symbols, telling to what representation of the group C_{3v} the orbitals in question belong; the other symbols s, σ, π refer to more specific characteristics.

The orbital $[\sigma]$ is the chief C−I bonding orbital, but $[s]$ also helps a little in the C−I bonding. The chief C−H bonding orbitals are $[\pi]$ and $[s]$, especially the former, while $[\sigma]$ helps a little. $5s_I$ and $5p\pi_I$ (and others omitted in (1)) are non-bonding I atom orbitals. $5p\pi_I$ is especially important because its term value is lower than for any other orbital in (1). This means that the minimum I (I = ionization potential) of CH_3I corresponds to removal of a $5p\pi$ iodine electron.

In this and in other details of its electron configuration, a close analogy can be set up between CH_3I and ClI. The latter's normal state[1] (omitting inner electrons) may be written

$$(3s_{Cl}\sigma)^2(5s_I\sigma)^2(B\sigma)^2(3p\pi_{Cl})^4(5p\pi_I)^4,\quad {}^1\Sigma^+. \quad (2)$$

$B\sigma$ represents the Cl−I bonding orbital. Ionization by removal of a $5p\pi_I$ should give $\cdots(5p\pi_I)^3$, $^2\Pi$. This must have a $^2\Pi_{1\frac{1}{2}}$ (lower) and a $^2\Pi_{\frac{1}{2}}$ (higher) component; their separation $\Delta\nu$ should be[1] about 0.61 volt, which is 2/3 the separation 0.94 volt between $^2P_{1\frac{1}{2}}$ and $^2P_{\frac{1}{2}}$ of the ^2P normal state of the I atom.

Similarly in CH_3I, removal of one $5p\pi_I$ should leave a state $\cdots(5p\pi_Ie)^3$, ^2E. Since the gap in the structure (1) is localized in the I atom, and since the field in which the $5p\pi_I$ electrons move must be nearly the same in CH_3I as in ClI, even though technically the symmetry is different (C_{3v} instead of $C_{\infty v}$), it is reasonably clear that the ^2E of CH_3I^+ should have two components like those of the $^2\Pi$ of ClI^+, and with about the same $\Delta\nu$.

For ICl, no measurements of I exist, but a pair of absorption band-systems near λ1800 show a $\Delta\nu = 0.58$ volt, close to the value predicted for ClI^+. These systems have been interpreted[1] as having upper levels

$$[\cdots(5p\pi_I)^3,\ ^2\Pi_{1\frac{1}{2}}](C\sigma) \text{ and } [\cdots{}^2\Pi_{\frac{1}{2}}](C\sigma), \quad (3)$$

i.e., two levels for each of which a loosely attached electron in an orbital $C\sigma$ may be thought of as added to a ClI^+ core, respectively in the $^2\Pi_{1\frac{1}{2}}$ or $^2\Pi_{\frac{1}{2}}$ state. The observed $\Delta\nu = 0.58$ volt should thus be essentially that of ClI^+ (predicted about 0.61 volt). Since a similar excellent check is repeated for the similar molecules IBr, BrCl, and is supported by other evidence, the foregoing interpretation seems well established, and indirectly verifies the predictions concerning ClI^+.

For CH_3I, a pair of absorption band-systems near λ1900 is known which closely resemble those of ClI^+, except for structural complications due to the additional nuclear degrees of freedom. The observed $\Delta\nu$ is 0.61 volt. The explanation is very probably like that in ClI^+, especially since a similar pair of band-systems is also found in

[1] R. S. Mulliken, Phys. Rev. **46**, 549 (1934).

CH_3Br. This strongly supports the prediction that the normal state of CH_3I^+ is a ^2E with two components, analogous to $^2\Pi_{1\frac{1}{2}}$ and $^2\Pi_{\frac{1}{2}}$ of CH_3I^+. Incidentally, the strength of the C−I bond should not be much affected by excitation of $5p\pi_I$ (non-bonding) to give the bands near λ1900 (this agrees with their structure), nor by its complete removal to give CH_3I^+. (By "strength" of bond is here meant vibrational force constant and C−I distance, rather than dissociation energy; the latter may be greatly changed.)

By methods given previously,[1] one can roughly predict I for removal of any non-bonding electron from a molecule. For removal of $5p\pi_I$ from ClI or CH_3I or HI, the predicted I (I_{pred}) is about 11.16 volts. This applies to a mean I for the two components of the $^2\Pi$ or ^2E; actually there should be two I's close together with predicted values $11.16\pm\Delta\nu/2$, i.e., 10.85 and 11.47 volts. The observed minimum $I(I_{obs})$ for CH_3I is 9.1 ± 0.25 volts.[2] The agreement with $I_{pred}=10.85$ is as good as experience[1] allows us to expect (cf., e.g., HI, where $I_{pred}=10.85$, $I_{obs}=12.75$ volts).

Configuration (1) applies also to CH_3Br and CH_3Cl, except that $4s_{Br}$ and $4p\pi_{Br}$ or $3s_{Cl}$ and $3p\pi_{Cl}$ appear. Ionization potentials, and ultraviolet bands, show relations analogous to those in CH_3I, although the bands are less sharp. CH_3F should differ from the others in the energy order of the orbitals in (1), I being larger for $2p\pi_F$ than for $[\sigma]$ or $[\pi]$, one of which, probably $[\pi]$, should give the minimum I. Also, ns_X should precede $[sa_1]$ in (1) in all cases except perhaps for X = iodine.

The structure of the molecules CH_3X can be understood better if they are compared with CH_4 as well as with the mixed halogen type XY exemplified by ICl. Except for non-bonding I atom orbitals present in (1), the analogy to CH_4 is probably closer than to XY. The structure of CH_4 (symmetry T_d) is[3]

$$(1s_Ca_1)^2[sa_1]^2[pt_2]^6, \quad {}^1A_1. \qquad (4)$$

If we suppose one H atom slightly displaced the symmetry can be reduced to C_{3v}. The degenerate orbital $[p]$ then splits up and we have an expression closely similar to that for CH_3I in (1):

$$(1s_Ca_1)^2[sa_1]^2[\pi e]^4[\sigma a_1]^2, \quad {}^1A_1. \qquad (5)$$

The twofoldly degenerate $[\pi e]$ here should be very nearly the same as $[\pi e]$ in CH_3I. Each is confined essentially to the CH_3 radical, and the only differences are due to secondary effects on shape and field of force within CH_3 which result when a C−I is substituted for a C−H bond. In particular, I should be nearly the same (14.4 volts) for $[\pi e]$ in CH_3I as for $[p]$, i.e., $[\pi]$ and $[\sigma]$, in CH_4. For $[\sigma]$ of CH_4, of course, I is the same as for $[\pi]$, but for $[\sigma]$ in CH_3I, in the writer's opinion, I must be somewhat smaller than for $[\pi]$, but certainly not small enough to be identified with the observed minimum I of CH_3I. The chemical conception of CH_3I as a "derivative" of CH_4, supported by quantum-mechanical calculations of Van Vleck, emphasizes the similarity of CH_3I to CH_4, insofar as the bonding electrons (here described by $[s]^2[\pi]^4[\sigma]^2$) are concerned.

We might now proceed to other CH_4 derivatives such as CH_2I_2, $CHBr_3$, CBr_4. We shall here only mention, however, that the minimum I of all these molecules, as well as of many others more complex (e.g., C_2H_5I, C_3H_7Br) must in ordinary cases be that of a non-bonding $5p\pi_I$ or $4p\pi_{Br}$ electron if I or Br atoms are present. If no Br or I but only Cl is present as a substituent, probably $3p\pi_{Cl}$, or perhaps sometimes one of the bonding orbitals, should give I_{min}. If only F is present, a bonding orbital surely gives I_{min}.

[*Added in proof:* Throughout this paper "I" means "vertical I." Except for non-bonding orbitals (e.g., $5p\pi_I$), ordinary ("adiabatic") I's should be appreciably smaller than vertical I's.[1] For the former, a different orbital may more often give I_{min} than for the latter; e.g., in Cl derivatives, the *adiabatic* I_{min} may perhaps usually belong to $[\pi]$ or $[\sigma]$ rather than to $3p\pi_{Cl}$.]

For any molecule, I_{min} determines to a great extent the region at which its ultraviolet absorption begins, as well as the character of the spectrum in this region. If I_{min} is small, absorption tends to begin at relatively long wavelengths. In other words, low ionization potential, other things being fairly equal, implies low excitation potential. This is the principal reason

[1] T. N. Jewitt, Phys. Rev. **46**, 616 (1934).
[2] R. S. Mulliken, J. Chem. Phys. **1**, 492 (1933).

why, for example, introduction of iodine tends to shift the beginning of absorption in an organic compound toward long wavelengths.

In conclusion, we return to the ultraviolet absorption spectrum of CH_3I, investigated by Herzberg, Scheibe, Henrici, and others.[4] This begins with a continuous region having an intensity maximum near λ2600. This we may attribute to transitions from the normal level, call it N (cf. (1)), to an excited electron level A, of unstable character such that dissociation into CH_3+I occurs. At shorter wavelengths are discrete bands. The first two groups of these, near λ1900 (upper electron levels "B" and "C") have already been discussed.

Careful consideration indicates that $N\rightarrow A$ involves transfer of one electron from $5p\pi_I$ to an excited orbital (αa_1), giving excited states

$$(\pi_I)^{-1}[\alpha a_1], \quad {}^{1,3}E, \tag{6}$$

where α is probably either s^* (cf. $[s^*]$ of CH_4[3]) or σ^* (cf. $A\sigma^*$ of ClI and $[\sigma^*]$ of CH_4). The transition is thus more or less analogous to the well-known transitions[1] in ClI to the states

$$(\pi_I)^{-1}(A\sigma^*), \quad {}^{1,3}\Pi, \tag{7}$$

where $A\sigma^*$ is a Cl−I anti-bonding orbital. By analogy with the transition from (2) to (7) in ClI, the CH_3I transition from (1) to (6), i.e., $N\rightarrow A$, may include two or three components; but because the absorption is continuous, these cannot be separately distinguished. Theory indicates that the dissociation products comprise unexcited CH_3 ($^2A_1$ state[5]), plus unexcited I (p^5, ^2P) in either its $^2P_{1\frac{1}{2}}$ or its $^2P_{\frac{1}{2}}$ state, or perhaps both of these, depending on the particular component of the group $^{1,3}E$ to which a particular absorption act leads. The B, C, upper levels may be described as $(\pi_I)^{-1}[\beta]$, where $[\beta]$, not in analogy to the corresponding ICl case given by (3), is most likely $[\pi^*e]$ or some other e type.

CH_3Br and CH_3Cl show analogous absorptions, shifted to shorter wavelengths because I is greater for π_{Br} and π_{Cl} than for π_I.

The foregoing interpretation receives strong support from recent work of Dr. W. C. Price, who has very kindly informed the writer of his results (cf. his Letter in this issue for details). Price finds Rydberg series in CH_3I absorption, leading to two I values 9.49 and 10.11 volts. These may evidently be identified with the two predicted components of ^2E of CH_3I^+ discussed above. The $\Delta\nu=0.62$ volt checks the prediction while the minimum I of 9.49 is nearer the approximately predicted 10.85 than is Jewitt's value 9.1 volts.[2]

[4] Cf. A. Henrici, Zeits. f. Physik **77**, 35 (1932); G. Scheibe et al., Zeits. f. physik. Chemie [B]**20**, 283 (1933); etc.

LETTERS TO THE EDITOR

Prompt publication of brief reports of important discoveries in physics may be secured by addressing them to this department. Closing dates for this department are, for the first issue of the month, the twentieth of the preceding month; for the second issue, the fifth of the month. The Board of Editors does not hold itself responsible for the opinions expressed by the correspondents.

The Near Infrared Spectrum of MgO

Quite recently it has become possible to obtain single crystals of MgO as large as 3×4×0.5 cm. These crystals are highly transparent to visible light, are quite hard and have much the appearance of glass. They are cubic crystals of the NaCl type, and may be cleaved quite easily, the cleavage surfaces being very plane and possessing a high degree of polish. Surfaces prepared in this manner require no further grinding or polishing before being used, and are very resistant to the effects of water, acids, heat, etc.

Since they are cubic in their structure, these crystals should, according to the classical theory of crystal structure possess only one absorption frequency in the infrared. Due to the high degree of symmetry of a cubic lattice, the overtones of this frequency should not appear, leaving the infrared spectrum extremely simple. Czerny and Barnes.[1] however upon examining other cubic crystals and in particular the alkali halide crystals, observed in every case several secondary absorption maxima upon the short wavelength side of the fundamental. The unexpected occurrence of these maxima was later explained by Born and Blackman[2] in a paper entitled *Über die Feinstruktur der Reststrahlen*, as being due to a slight, hitherto neglected anharmonicity of the forces existing between the atoms of the crystal. In view of the possible existence of such secondary maxima in MgO, the short wavelength side of the fundamental of these new crystals is of particular interest.

Using a rocksalt spectrometer the transmission curves for 5 thicknesses of MgO ranging from 3.05 mm to 0.075 mm were measured from 1μ to 16μ. In agreement with the result found by Tolksdorf[3] on a thin layer of MgO powder, the fundamental was located at 14.2μ. In addition weak transmission minima (absorption maxima) were found around 10.8μ, 8.3μ and 7.0μ. These do not form harmonic ratios with the fundamental and are therefore assumed to be analogous to the bands discussed above. It is hoped that in the near future a complete discussion of a comparison of these observed values with those calculated according to the equations given by Born and Blackman may be presented. Each of the plates measured was approximately 85 percent transparent from 1μ as far out as 6μ, the entire losses being reflection losses.

R. Bowling Barnes
R. Robert Brattain

Palmer Physical Laboratory,
Princeton University,
February 15, 1935.

[1] M. Czerny, Zeits. f. Physik **65**, 600 (1930); R. Bowling Barnes and M. Czerny, Zeits. f. Physik **72**, 447 (1931); R. Bowling Barnes, Zeits. f. Physik **75**, 723 (1932).
[2] M. Born and M. Blackman, Zeits. f. Physik **82**, 551 (1933); M. Blackman, Zeits. f. Physik **86**, 421 (1933).
[3] S. Tolksdorf, Berlin Dissertation, 1928.

Interaction of Low Energy Neutrons with Atomic Nuclei

A number of elements have been shown by Fermi and his collaborators to have remarkably high stopping power for the slow neutrons which are so effective in producing many types of artificial radioactivity. This letter is to report measurements of a different type on the stopping power, for slow and fast neutrons of a large number of elements, the stopping power being expressed in terms of the neutron-nucleus collision cross section, and especially to direct attention to the result that the cross section for the hydrogen nucleus is about 3.5 times that of the deuterium nucleus, although the two nuclei have about the same cross section when measured with high energy Rn-Be neutrons.

The Rn-Be source, contained in a platinum capsule and surrounded by 1 cm of additional lead to reduce the gamma-radiation, was placed in the center of a paraffin sphere of 6 cm radius, it having been found that this thickness of paraffin gave a sufficiently large number of slow neutrons,[1] and yet permitted fairly good geometrical conditions, as shown in Fig. 1. The slow neutrons were

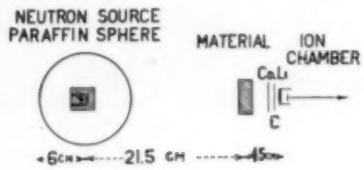

FIG. 1.

detected through the ionizing particles ejected by the neutrons from a layer of lithium placed in front of a shallow ionization chamber connected to an amplifier-recorder system.

The absorption and scattering of the neutrons was studied by interposing similar cylindrical samples of various materials in the path between the source and chamber. In order to separate out the effects of the slow neutrons from the fast neutrons, readings were taken with, and without a 1 mm thick Cd disk interposed. The Cd served as an effective slow neutron filter, absorbing practically all of the slow neutrons lying within its anomalous absorption region, but apparently had little effect on neutrons of higher (and possibly lower) energies. The number of recorded counts was reduced to about 35 percent when 1 mm of Cd was interposed, indicating that about 65 percent of the recorded neutrons were within the region strongly absorbed by Cd.

The results in Table I show the apparent neutron-nucleus cross sections, corrected approximately so as to

TABLE I. *Neutron-nucleus cross section for slow and fast neutrons.*

Material	Atomic weight	Neutron-nucleus cross section $\times 10^{24}$ cm^{-2}	
		Slow neutrons	Fast neutrons
H	1	13.3	1.68
D	2	3.4	1.71
Li	6.94	49	1.84
Be	9.02	3.8	1.65
B	10.82	600	1.60
C	12.0	2.8	1.65
O	16.0	3 est.	
F	19	<4	
Na	23	4.5	
Mg	24.3	2.5	
Al	26.97	1.9	2.4
Si	28.06	2.0	
P	31.03	7.2	
Cl	35.46	38	
K	36.1	34 est.	
Ca	40.07	<10	
Ti	48.1	<8	
Cr	52.01	7.4	
Mn	54.93	8.0	
Fe	55.84	7.8	3.0
Co	58.94	26	
Cu	63.57	5.9	3.2
Zn	65.38	3.6	3.3
Se	79.2	12	
Zr	91	17	
Sn	118.7	3.6	4.3
Sb	121.8	8	
I	126.93	10.1	4.6
Ba	137.37	100	
W	184.0	19	5.3
Hg	200.6	430	5.8
Pb	207.2	6.1	5.7
U	238.17	100	

express the cross-section value for those slow neutrons which disintegrate Li and are strongly absorbed by Cd. The results for high energy Rn-Be neutrons not slowed down by paraffin, from previous measurements,[2] are included in the last column. The corrections for the somewhat different geometrical conditions in the two sets of data have not yet been completely made, but measurements of the cross sections for high energy Rn-Be neutrons, using spheres of lead and copper instead of paraffin in the arrangement of Fig. 1, indicate that the high energy cross sections should be multipled by about 0.85 to make them correct relative to the slow neutron measurements. The nature of the measurements at this stage is such that the results, especially for the large absorptions, do not have much precision. We estimate that most of the smaller cross-section values are accurate to well within 10 percent, but the larger values within ±25 percent.

While the variation of the cross section of nuclei in general with slow neutrons compared to fast neutrons will certainly be of theoretical significance, some elements having practically the same value (considering the geometric factors), others increased only slightly, and some increased enormously, probably one of the most interesting points in the table is the large increase in cross section of the proton compared to the deuteron.

The relative effects of H_2O and D_2O in enhancing the efficiency of neutrons in the production of artificial radioactivity in silver was tested by activating a strip of silver suspended above a Rn-Be source at the bottom of a test-tube, first in air, then immersed in 200 cc of H_2O, then in the same volume of D_2O (99.8 percent). The 2-min. period radioactivities obtained in air, H_2O and D_2O were respectively as 1, 2.0 and 6.5. Subtracting the direct effect in air, the enhancing effect of H_2O was 5.5 times that of D_2O.

J. R. DUNNING
G. B. PEGRAM
G. A. FINK
D. P. MITCHELL

Columbia University,
Department of Physics,
February 19, 1935.

[1] Am. Phys. Soc. Bull., Feb. (1935).
[2] John R. Dunning, Phys. Rev. **45**, 586 (1934).

The East-West and Longitude Effects

In measuring the difference between the numbers of charged particles effecting a line of Geiger-Müller counters when it is tilted toward the west and then toward the east, the common practice is to rotate the line of counters about an axis normal to the equipotential gravitational surface at the location in which the experiment is being conducted. Now it has been shown in sea-level surveys by Clay[1] and by Millikan and Neher[2] that the variations in the surface magnetic field for the same geomagnetic latitude extend to sufficient heights to influence the charged particles coming in at the equator, giving rise to the "longitude effect." Our present surveys show this effect to be from 4 to 5 percent of the total intensity of the cosmic radiation at sea level. A glance at a map showing lines of equal horizontal intensity of the earth's magnetic field will show that these variations are quite large and extend over wide areas. As an example, on the coast of Peru where Johnson[3] and Korff[4] have studied the east-west effect; the horizontal intensity is 0.30 gauss while 8000 kilometers to the west it has increased to 0.35 gauss and has diminished to something like 0.28 gauss in the first 5000 kilometers to the east. These distances are of the same order as the radius of curvature of a charged particle which is just able to reach the earth's surface at this latitude and consequently will be influenced by these variations. A rough calculation shows that the surfaces of equal magnetic intensity in this region are tilted upward toward the west at an angle of several degrees. In order for the results of the east-west measurements to be interpretable, the axis of rotation of the counters must be more nearly normal to these surfaces of equal magnetic intensity. This means that the axis of rotation of the counters must be inclined *east* of the vertical.

Now it can easily be shown that the full east-west effect found by Johnson can be eliminated if the axis of rotation of the counters is tilted about two degrees west of the normal to the equipotential gravitational surfaces, and if the axis of the counters is set more nearly normal to the surfaces of equal magnetic intensity, this angle becomes two to four degrees in South America. The east-west effect then increases from six to eight percent to something like six to sixteen percent at sea level, the exact amount depending on the ratio of electrons to photons and the effect of the earth's atmosphere in absorbing each.

In the African region the effect should be in just the opposite direction, i.e., to perform an east-west effect experiment in this region one should tilt the axis of rotation of the counters toward the *west*. One should then expect to find an east-west effect near the equator in both South America and Africa even though there were equal numbers of positrons and negatrons with the same energy distribution coming into our atmosphere. Under these conditions in South America there would be a preponderance toward the east and in Africa a greater number toward the west.

The influence of the atmosphere, which lies between two equigravitational surfaces, would be to make the effective angle of inclination to the vertical of the axis of a line of counters less than it would be otherwise.

In support of this suggestion the experiments of Johnson in South America and Rossi[5] in Africa may be cited. At 8000 feet Rossi gets a maximum west excess of 16 percent at a point 11° *north* of the magnetic equator, while Johnson, *on* the magnetic equator would get about 12 percent.

The point to be noted is the fact that setting the axis of rotation of a line of counters parallel to the line of a plumb-bob loses its meaning as far as the east-west effect is concerned in certain locations and interpretations must be made by taking proper account of the dissymmetry of the earth's magnetic field.

I wish to make acknowledgment of the fact that studies leading to these suggestions have been supported by a grant from the Carnegie Corporation of New York.

H. V. NEHER

California Institute of Technology,
Pasadena, California,
February 18, 1935.

[1] J. Clay, P. M. Van Alphen and C. G. T. Hooft, Physica 1, 829 (1934).
[2] R. A. Millikan and H. V. Neher, Phys. Rev. **47**, 205 (1935).
[3] Thomas H. Johnson, Phys. Rev. **45**, 569 (1934).
[4] S. A. Korff, Phys. Rev. **46**, 74 (1934).
[5] B. Rossi, Phys. Rev. **45**, 212 (1934)

On the Low Temperature Diffusion of Solid Aluminum into Iron

The writer has recently noted the comparatively rapid diffusion of solid aluminum into steel at low temperature.

A built-up gasket of aluminum foil was used in a bolted tongue-and-groove type joint between the body and cover of a steel autoclave, being held under very considerable mechanical pressure by the bolts. After carrying out a digestion for six hours at 290°C, it was found that the gasket had welded to the groove at points near the bolts, where the pressure was greatest; and in machining out the aluminum, it was found to have penetrated into the steel to a depth of nearly a millimeter below the original surface of the groove at the points of welding.

The groove had been freshly cut and probably retained traces of machine oil. The foil had been moistened with turpentine, which strongly wets aluminum, before use. Although no direct measure of the pressure between the aluminum and steel could be made, the apparatus had been tight in previous work against water above its critical temperature, which would require a gasket pressure in the neighborhood of one thousand kg per sq cm.

As no notice was found on such low temperature diffusion of aluminum into steel or iron, the writer improvised a small nichrome furnace for heating under controlled atmosphere and has been studying the diffusion of aluminum into iron over the temperature range 300° to 900°. This study is still far from complete, but has progressed far enough to warrant the publication of a few general results, which are outlined below:

(1) Aluminum will diffuse into steel and into cast iron at 300° provided both surfaces are clean and sufficient pressure exists at the interface to assure full surface-to-surface contact.

(2) The rate of diffusion is a direct function of the pressure, as yet undetermined.

(3) The pressure necessary to produce a given rate of penetration varies as an inverse function of the temperature. Penetration without substantial pressure has not been observed below the melting point of aluminum.

(4) If the surface of either metal is old or oxidized, diffusion does not occur at any pressure within reach.

(5) The rate of penetration under similar conditions varies as much as fifty percent between different kinds of iron or steel.

(6) At the temperature of melting aluminum, this metal diffuses upward through a bar of iron or steel whose lower end is immersed in aluminum at the rate of one to two cm per day, depending on the character of the ferrous metal; and the penetration continues until the whole bar is impregnated.

(7) The specific gravity of the steel or iron so treated is increased; the largest observed increase being about 2½ percent. (Note that Al–Fe alloys prepared by fusion are of lower specific gravity than that of iron, though in general higher than the weighted mean of the specific gravities of the two metals.)

(8) The electrical conductivity of iron or steel wire is noticeably increased by low temperature impregnation with aluminum.

(9) Machining and grinding characteristics of iron and steel are not materially changed by low temperature impregnation with aluminum.

(10) Above the temperature of melted aluminum, the slow diffusion of iron into the aluminum becomes noticeable in addition to the reverse process; becoming more rapid as the temperature is raised. The original outline of a bar of steel immersed in aluminum was completely lost in 20 hours at 750°, and the original structure of a steel bar 2½ cm dia. by 10 cm long was lost throughout after 20 hours in aluminum at 900°. It had become hard, brittle and of lower specific gravity than the original steel.

The above notes make it appear that the low temperature penetration of iron by aluminum is mainly a capillary flow in the intercrystalline pores of the iron, with at the most only a superficial disturbance to the structure of the latter. This also seems probable on the basis of microscopic examination of etched specimens. If so, one would expect the treated iron to be both stronger and more impervious

to penetration by gases than the untreated material. This has not yet been tested.

Impregnated iron and steel are slightly more resistant to atmospheric rusting and much more resistant to high temperature oxidation than iron or steel alone. This may be due to the more adhesive nature of the oxide film first formed, to its lesser permeability or to lessened porosity of the metal.

The writer has also observed the moderately rapid diffusion of chromium powder into iron at 950°, and that of copper sheet into iron at 850°, as well as that of liquid aluminum, tin and zinc into copper, of liquid tin into iron and into chromium and of liquid aluminum into chromium. These, with the possible exception of the last, have been reported by others. The diffusion of liquid aluminum into iron has been noted by Grube, Chimie et Industrie **18**, 68 (1927), and by others, reference to whom is not at hand at the present moment.

The above work was started during the writer's engagement as a metallurgical technician at Ryerson Laboratory, University of Chicago, and has been continued since with his own facilities. He wishes to acknowledge with thanks and appreciation his indebtedness to Professor Gale for the latter's encouragement and for putting the facilities of the laboratory at his disposal, as well as to the laboratory staff for their helpfulness in this and other work during his stay at the university.

It is hoped that an opportunity will be forthcoming for the continuance of this study with better equipment for the maintenance and accurate measurement of high mechanical pressures and for the study of magnetic properties involved.

LEO G. HALL

Spalding Machinery Co.,
205 W. Wacker Drive, Chicago,
December 9, 1934.

The Far Ultraviolet Absorption Spectrum of Methyl Iodide

The author has shown in a number of cases[1] that the far ultraviolet absorption spectra of polyatomic molecules can be followed to their limits if a grating vacuum spectrograph and a Lyman continuum are used. From these limits very accurate values of the ionization potentials of the molecules can be deduced. Methyl iodide is an excellent example of this. Its ionization potential as determined by ordinary methods is given as $9.1 \pm .25$ volts.[2] An analysis of its absorption spectrum taken at very low pressures in the region 2000–1200A reveals two ionization potentials whose values can be given as 9.489 and 10.113 volts with a probable error of only 0.003 volt.

The bands down to 1650A have been reported by Herzberg, Scheibe[3] and others. Below this the bands are predissociated. They become somewhat sharper at shorter wavelengths and approach two very prominent heads at about 1300A and 1220A, respectively. Two strong electronic series going to each limit are observed, a comparatively large number of the higher members being visible in all cases. The upper members from about $n=5$ to $n=15$ conform very well to Rydberg formulas, and their limits are computed to be $76{,}920 \pm 15$ cm^{-1} and $81{,}980 \pm 15$ cm^{-1}. These correspond to the ionization potentials previously mentioned.

From $n=2$ to $n=5$ the bands are difficult to follow on account of their diffuseness and deviations from the Rydberg formulas. However, it can be established fairly definitely that the *B* and *D* bands of Herzberg and Scheibe are the first members of the two electronic series which go to the lower limit, and the *C* band and a band at about 1542A are the first members of the series which go to the upper one.

W. C. PRICE

The Rowland Physical Laboratory,
The Johns Hopkins University,
February 1, 1935.

[1] *The Absorption Spectra of Acetylene, Ethylene and Ethane in the Far Ultraviolet*, W. C. Price (to appear soon in Phys. Rev.); W. C. Price, Phys. Rev. **46**, 529 (1934).
[2] T. N. Jewett, Phys. Rev. **46**, 616 (1934).
[3] Herzberg and Scheibe, Zeits. f. physik. Chemie **B7**, 390 (1930).

Line Strengths in Intermediate Coupling—An Addition

In the paper of the above title (p. 295 of this volume), the following statement of the *J*-file sum rule is given: *For any coupling, in a transition array in which the jumping electron is not equivalent to any electron in the ion in either configuration, the strengths of the J files referring to the levels of the initial (final) configuration are proportional to the values of* $2J+1$ *for those levels.*

Mr. Goldberg of the Harvard Observatory has called my attention to the fact that in all the transition arrays which he has calculated in *LS* coupling, this sum rule holds for the files in *one* direction even if the jumping electron is equivalent to other electrons in *one* of the configurations. He finds that *the strengths of the J files referring to the levels of the initial (final) configuration are proportional to* $2J+1$ *provided that the jumping electron is not equivalent to any other in the final (initial) configuration*—it may be equivalent to others in the initial (final) configuration. By a simple extension of the method of § 2 of the paper cited, a general proof of this statement may be given, not only for *LS* coupling, but for any intermediate coupling. The values of the sums come out k times the value (4) of the above paper, if the jumping electron is one of k equivalent electrons in one of the configurations.

This means, for example, that for the array $d^4p \rightleftharpoons d^5$, the *J*-file sum rule holds with respect to the files referring to the levels of d^5, but not with respect to files referring to d^4p, and that the absolute strengths of these files, in terms of the one-electron matrix component, are five times those of the corresponding files of $d^4\,p \rightleftharpoons d^4\,d$.

This extension of the sum rule was recognized for the case $k=2$ in the above paper, but it is thought advisable to state the more general result here in order to collect, in as nearly one place as possible, all the sum rules which are applicable in intermediate coupling.

GEORGE H. SHORTLEY

Mendenhall Laboratory of Physics,
Ohio State University,
February 18, 1935.

The Masses of Be^8, Be^9 and B^{11}, as Determined from Transmutation Data

We[1] have investigated the gamma-ray spectrum resulting from the bombardment of Li by H^1. The spectrum is complicated but has a definite maximum at 16 mev $=0.0172$ mass units. The intensity of the gamma-radiation increases rather suddenly when the bombarding voltage reaches 600 kv, and decreases again at higher voltage.

This suggests that a large part of the radiation is due to

$$Li^7+H^1\rightarrow Be^8+E_1 \qquad (1)$$

and that the proton is captured on a level, presumably the ground level, in Be^8. It is not likely that any reaction involving Li^6 could yield sufficient energy.

We may equate the right-hand side of this reaction to the right-hand side of the well-known reaction

$$Li^7+H^1\rightarrow 2He^4+E_2 \qquad (2)$$

and solve for the mass of Be^8. From the data given by Oliphant[2] we find $E_2=17.5$ mev $=0.0188$ mass unit at 600 kv. This gives

$$Be^8=2He^4+E_2-E_1=8.0043+0.0188-0.0172=8.0059,$$

which is 0.0016 greater than the mass of two alpha-particles. It is, therefore, to be expected that Be^8 will have an extremely short lifetime, splitting up into two alpha-particles, each with an energy of 0.75 mev corresponding to a range of about 0.35 cm.

The first evidence for the existence of Be^8 was obtained by Kirchner[3] who gives 8.0074 for the mass. This determination depends, however, on the value 11.0110 ± 0.0015 for the mass of B^{11} as given by Aston. If, on the other hand, we use our value for the mass of Be^8 we find from Kirchner's data $B^{11}=11.0095$.

Almost the same value for B^{11} is obtained from the reaction

$$B^{10}+H^2\rightarrow B^{11}+H^1+E. \qquad (3)$$

Cockroft[4] has measured four groups of protons and we[5] have determined the gamma-ray spectrum. The agreement is satisfactory and the total energy in the reaction is 9.7 mev $=0.0104$ mass unit. Using Bainbridge's value for B^{10}, H^2 and H^1, we get $B^{11}=11.0093$, in good agreement with the above value.

Using the above mass values we may calculate the mass of Be^9 from several well-known reactions. Bonner and Brubaker[6] have recently investigated the energy spectrum of neutrons produced when Be is bombarded by H^3, and have shown that the maximum energy of these neutrons is 4.5 mev $\pm$0.1 mev. Presumably the reaction is

$$Be^9+H^3\rightarrow B^{10}+n^1. \qquad (4)$$

Using the above values and $n^1=1.0080$ (Chadwick), 0.0007 for the kinetic energy of the H^2 and 0.0005 for the kinetic energy of B^{10}, we find

$$Be^9=10.0135+1.0080+0.0048+0.0005-2.0136-0.0007=9.0125.$$

Dee[7] has observed a singly charged particle of short range from Be bombarded by protons. If we assume that this particle is H^2, the most probable reaction is

$$Be^9+H^1\rightarrow Be^8+H^2. \qquad (5)$$

Using Oliphant's[2] data for the kinetic energy of the H^2 particle and taking the mass of Be^8 to be 8.0059, we obtain

$$Be^9=8.0059+2.0136+0.0008-1.0078-0.0001=9.0124.$$

It should be noted that here the mass of B^{10} is not involved and the agreement therefore constitutes a check on the value 10.0135 for the mass of B^{10} as given by Bainbridge.

Oliphant[2] has observed 26 cm protons when Be is bombarded by H^2. We may assume that the reaction is

$$Be^9+H^2\rightarrow Be^{10}+H^1. \qquad (6)$$

We obtain the mass of Be^{10} from Meitner's[8] observation that Be^{10} is radioactive, changing into B^{10} and a negative electron with 0.3 mev energy. From this we obtain for the mass of Be^9

$$Be^9=10.0135+1.0078+0.0047+0.0003-2.0136-0.0002=9.0125$$

The excellent agreement among these three determinations of the mass of Be^9 is no doubt to some extent fortuitous, for the probable error is in each case about 0.0005. Nevertheless, we may conclude that the mass of Be^9 is very nearly equal to the sum of the masses of two alpha-particles and a neutron, namely, $8.0043+1.0080=9.0123$.

It is, therefore, not surprising that Be^9 may be disrupted by gamma-rays from radium, as found by Szilard and Chalmers.[9] Our masses of Be^8 and Be^9 lead us to predict that the lowest energy gamma-ray capable of disrupting Be^9 is 1.4 mev, which is the minimum required to produce the reaction

$$Be^9\rightarrow Be^8+n^1.$$

Disintegration into two alpha-particles and a neutron would probably require more energy, because of the mutual potential barrier of two alpha-particles, which is about 2 mev. This is in agreement with the results of Ridenour, Shinohara and Yost,[10] but not in agreement with those of Gentner.[11]

H. R. Crane
C. C. Lauritsen

Kellogg Radiation Laboratory,
California Institute of Technology,
February 14, 1935.

[1] Crane, Delsasso, Fowler and Lauritsen, to be published soon.
[2] Oliphant, Inter. Conf. of Physics, London, Oct. 1934.
[3] Kirchner and Neuert, Physik. Zeits. **35**, 292 (1934).
[4] Cockroft, Inter. Conf. on Physics, London, Oct. 1934.
[5] Crane, Delsasso, Fowler and Lauritsen, Phys. Rev. **46**, 1109 (1934).
[6] Bonner and Brubaker, L. A. Meeting, Am. Phys. Soc., Dec. 1934; Phys. Rev. **47**, 254A (1935).
[7] See reference 2.
[8] Meitner, Naturwiss. **22**, 420 (1934).
[9] Szilard and Chalmers, Nature **134**, 494 (1934).
[10] Ridenour, Shinohara and Yost, Phys. Rev. **47**, 318 (1935).
[11] Gentner, Comptes rendus **199**, 1211 (1934).

On the Electrostatic Deflection of Cosmic Radiation

Early in 1933, we arranged an experiment to study the deflection of cosmic-ray particles by strong electrostatic fields between parallel plates. Previous magnetic deflection experiments had left, of course, no reason to doubt that an electrostatic deflection should exist. Our object was rather to determine the relative numbers of rays in the lower energy range. In April, 1933, a small effect had been observed and was mentioned by the senior author in a lecture before the National Academy of Sciences. An abstract of this lecture has appeared in *Science*.[1] Further observations, however, resulted in a diminution of the electrostatic deflection relative to the probable error so that a complete report was postponed pending more exhaustive investigations.

Recently Lenz[2] has reported electrostatic deflection results of large magnitude and it becomes of interest to compare them with our own observations. We find it difficult to reconcile his large effects with the other existing data regarding the distribution of cosmic-ray electrons in energy. The considerations to be outlined here have led us to the conclusion that Lenz's low field-strength result is irreconcilable with our observations and that electrons of sufficiently small energy to have been deflected could not have penetrated the absorbing material present. Neither can we reconcile his large high field strength effect with the magnetic deflection result of Curtiss[3] nor with the cloud-chamber observations of Anderson.[4]

Lenz, Curtiss, and ourselves all used three or more Geiger-Müller counters in a vertical line with a region of deflecting field between two of them, and all found a diminution of counting rate when the electric or magnetic field was applied. Lenz's data with the bottom counter displaced will not be included in this discussion.

One of us[5] has computed, for each of the experiments, the fractional diminution (ϵ in the diagram) that would be observed if all the rays were of a given energy (V in the diagram). The actual diminution will be, of course, the integral of the product of ϵ by the energy distribution function. Table I shows the percent diminutions obtained in the four experiments and the amount of absorbing material, expressed in mm of lead, associated with each.

Considering any two deflection experiments, the one whose ϵ curve lies the farther to the right should give the larger effect. Comparing Lenz's 700 volt/cm result with the authors', and his 70,000 volt/cm result with Curtiss's, it appears from the curves that, as regards *a* and *b*, Lenz's 700 volt/cm effect should be less than ours; and as regards *c* and *d*, his 70,000 volt/cm effect should be less than that of Curtiss, whereas the reverse of these two conclusions is recorded. The diagram shows, further, that the electrons eliminated in Lenz's 700 volt/cm experiment lie below 10^7 volts, but Anderson's data indicate that such electrons cannot penetrate 10 mm of lead. Also, Lenz's 70,000 volt/cm result requires that at least 94 percent of the particles lie below 10^9 volts while Anderson reports 25 percent lying above 4×10^8 volts.

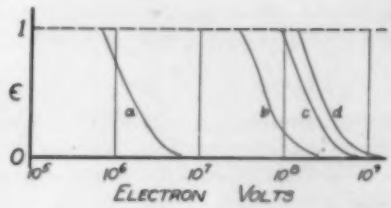

FIG. 1. Fractional number (ϵ) of electrons eliminated by deflecting field as function of their energy.

Curtiss worked under a thin roof while both Lenz and the authors had two concrete floors above them, but this could hardly produce sufficient differences in energy distribution to explain the discrepancies. And the difference in amounts of absorbing material inherent in the three counter systems are in the wrong sense to resolve the difficulties.

W. E. DANFORTH
W. F. G. SWANN

The Bartol Research Foundation
of the Franklin Institute,
Swarthmore, Pennsylvania,
February 11, 1935.

TABLE I.

Curve	Experiment	% Diminution Obs.	Equiv. Abs. in mm of lead
a	Lenz 700 v/cm	33% ±7%	10
b	Swann & Danforth	3% ±3%	7
c	Lenz 70,000 v/cm	94% ±2%	10
d	Curtiss	33% ±2%	6

[1] W. F. G. Swann, Science, May 19, 1933.
[2] E. Lenz, Nature **134**, 809 (1934).
[3] L. C. Curtiss, Bur. Standards J. Research **9**, 815 (1930).
[4] C. D. Anderson, Phys. Rev. **43**, 381 (1933) and a paper now in process of publication in the Proc. Roy. Soc.
[5] W. E. Danforth, J. Frank. Inst. **217**, 331 (1934) and a paper now in preparation.

The Virial Theorem and Quantum Statistics

Fock[1] has given a variational treatment of the virial theorem for the Thomas-Fermi method. But Jensen[2] has pointed out that because of the improper integrals occurring, the variations employed by Fock are invalid. Jensen then proceeds to amend the procedure, but at the expense of making an artificial assumption concerning a "perturbed" and an "unperturbed" solution. However, the difficulties of the variational method may be avoided by a simple treatment based on the following lemma.

The function of the scalar parameter λ,

$$M_\lambda = \frac{1}{2}\int\int \frac{\rho(r_1)\rho(r_2)}{|\lambda r_1 - r_2|}\,dr_1 dr_2 = \frac{1}{2\lambda}\int\int \frac{\rho(r_1)\rho(r_2)}{|r_1 - r_2/\lambda|}\,dr_1 dr_2$$

obviously reduces for $\lambda = 1$ to the mutual potential energy of a charge distribution of density ρ. In terms of the potential ϕ, M_λ becomes

$$M_\lambda = \tfrac{1}{2}\int \rho\phi(\lambda r)\,dr = 1/2\lambda \int \rho\phi(r/\lambda)\,dr.$$

If ρ is piecewise continuous then it is known from potential theory that ϕ together with its first derivatives is continu-

ous, so M_λ may be differentiated with respect to λ. There results when $\lambda=1$ since $d\phi(r\lambda)/d\lambda = r\cdot\text{grad}\ \phi(r\lambda)$,

$$\tfrac{1}{2}\int\rho\phi d\tau = -\int\rho r\cdot\text{grad}\ \phi d\tau.^3 \qquad (1)$$

Consider the Fermi statistics applied to a molecule with nuclear charges $e_1, e_2 \cdots, e_n$. Then in terms of the total potential, $V=\phi+\Sigma e_k/|r-r_k|$, the kinetic energy of the electron cloud is defined as

$$T=\tfrac{3}{5}\int\mu(V-\beta)^{5/2}d\tau \quad (V-\beta)>0, \qquad (2)$$

where $\mu=8\pi e(2me)^{3/2}/3h^3$ and $-e\beta$ is the maximum energy of an electron. Performing a partial integration,

$$T=-\tfrac{1}{2}\int\mu(V-\beta)^{3/2}r\cdot\text{grad}\ V d\tau.$$

The surface integral vanishes since $(V-\beta)=0$ on the boundary. But, by definition the charge density $\rho=-\mu(V-\beta)^{3/2}$, so

$$\begin{aligned}2T &= \int\rho r\cdot\text{grad}\ V d\tau \\ &= \int\rho r\cdot\text{grad}\ \phi d\tau+\Sigma\int\rho r\cdot\text{grad}\ e_k/|r-r_k|d\tau.\end{aligned}$$

The first integral on the right is an instance of lemma (1) and the second may be transformed by the identity

$$r\cdot\text{grad}\ |r-r_k|^{-1} = -|r-r_k|^{-1}-r_k\cdot\text{grad}_k\ |r-r_k|^{-1},$$

$$\begin{aligned}2T = -\tfrac{1}{2}\int\rho\phi d\tau &-\Sigma\int e_k\rho/|r-r_k| \\ &-\Sigma\int e_k r_k\cdot\text{grad}_k\ \rho/|r-r_k|.\end{aligned}$$

Here the first two terms represent the potential energy, U, of the electron cloud, so the virial theorem may be written

$$2T = -U-\Sigma\int e_k r_k\cdot\text{grad}_k\ \rho/|r-r_k|d\tau. \qquad (3)$$

Under the sole assumption that ϕ *is everywhere finite* it is possible to give a justification of the partial integration and differentiation under the integral sign here employed. Lack of space prevents its inclusion but it is, of course, necessary as near the nuclei the charge density is unbounded and all the integrands are quite improper. It is then found *essential to take the integral of Eq. (3), not in the general sense, but as a limit of an integral over the region resulting from the exclusion of the nuclei by means of small spheres.* Thus, the virial equation may be also expressed as

$$2T+U=\lim_{a\to 0}\Sigma e_k r_k\cdot\mathfrak{e}_a(r_k).$$

Here $\mathfrak{e}_a(r)$ is the electric field produced by all charges exterior to spherical regions of radius a surrounding the nuclei.

The case of a neutral atom is of interest. By symmetry Eq. (3) reduces to $2T=-U$. Also, $\beta=0$ so (2) may be written

$$T=-\tfrac{3}{5}\int\rho V d\tau = -\tfrac{3}{5}\int\rho(\phi+e_1/r)d\tau.$$

The potential energy is simply $U=\tfrac{1}{2}\int\rho\phi d\tau+e_1\int\rho/r d\tau$. By elimination from these three relations it is found that

$$T+U=\tfrac{3}{7}e_1\int\rho/r d\tau=\tfrac{3}{7}e_1\phi(0)$$

and

$$\tfrac{1}{2}\int\rho\phi d\tau=-\tfrac{1}{7}e_1\int\rho/r d\tau.$$

The first expression gives the total energy of the atom, and the second states that the mutual potential energy of the electron cloud is one-seventh that arising from nuclear attraction.

RICHARD J. DUFFIN*

Department of Physics,
University of Illinois,
Urbana, Illinois,
February 15, 1935.

[1] V. Fock, Physik. Zeits. Sowjetunion **1**, 747 (1932).
[2] H. Jensen, Zeits. f. Physik **81**, 611 (1933).
[3] This suggests the correspondent of Euler's theorem for functionals. Thus, $\int\cdots\int\rho\psi(x_1\cdots x_n)dx_1\cdots dx_p$ may be termed "homogeneous" of degree r in ψ provided

$$\int\cdots\int\rho\psi(\lambda^c x_1\cdots\lambda^c x_n)=\lambda^r\int\cdots\int\rho\psi(\lambda^{c-1}x_1\cdots\lambda^{c-1}x_n),$$

where c is a fixed constant. Then

$$r\int\cdots\int\rho\psi dx_1\cdots dx_p=\int\cdots\int\rho\Sigma_n x_i\partial\psi/\partial x_i \quad dx_1\cdots dx_p.$$

* University Fellow in Physics.

Concerning the Ionosphere

In his addendum[1] to my letter[2] in this journal I was pleased to note that Professor E. V. Appleton is in agreement with my theory of the diurnal and latitude variations in the F_2 region of the ionosphere based on the hypothesis of heating of the region by the sunlight with consequent vertical expansion of the region and horizontal spread due to winds. The theory, qualitatively at least, yields accord with the main F_2 features. Calculation indicates that the absorption of solar ultraviolet light by molecular oxygen and its decomposition to atomic oxygen is adequate to cause the heating and expansion of these outlying reaches of the atmosphere. In respect to the ionization above 180 km first observed by Breit and Tuve[3] and its daytime bifurcation into F_1 and F_2 first recognized and investigated in detail for a number of years by Kirby, Berkner and Stuart[4] and independently announced by Schafer and Goodall,[5] there is a slight discrepancy with the observations in England. Kirby, Berkner and Stuart[4] at Washington found from 1930 to 1933 that the maximum noon ionization of F_2 was roughly 1.5 to 2 times as great in winter as in summer. The continuance of the Washington observations by Kirby, Judson and Gilliland during 1933 and 1934 gave the same answer. On the other hand, Appleton[6] stated that in England the summer noon F ionization (he called it "F" ionization, whereas he was dealing with a region stratified into F_1 and F_2) was about 1.5 to 1.8 times the winter noon values during 1933. The discrepancy may possibly be due to a difference in latitude and in any case may be cleared up by further observations.

E. O. HULBURT

Naval Research Laboratory,
February 8, 1935.

[1] Appleton, Phys. Rev. **47**, 89 (1935).
[2] Hulburt, Phys. Rev. **46**, 822 (1934).
[3] Breit and Tuve, Phys. Rev. **28**, 554 (1926).
[4] Kirby, Berkner and Stuart, International Scientific Radio Union, Washington, April 27, 1933; Bur. Standards J. Research **12**, 15 (1934). The terminology, F, F_1 and F_2 which I have used is that originally proposed by Kirby, Berkner and Stuart and adopted at the International Scientific Radio Union meetings in London, September 1934.
[5] Schafer and Goodall, Nature **131**, 804 (1933).
[6] Appleton, Proc. Roy. Soc **A141**, 700 (1933).

A Note on the Production of Cosmic-Ray Showers

The cosmic-ray showers, which are shown so beautifully in the counter controlled cloud chamber,[1] have been investigated by numerous observers. The method in general has consisted in putting three Geiger counters below a thin plate of heavy material. The counters are usually arranged so that three particles emerging simultaneously from the plate are required to register a coincidence. Hence a shower will consist of at least three particles associated in time.

This note concerns an experiment dealing with the variation in the number of showers with depth below the top of the atmosphere. The experiment was performed in a tunnel of the Morris Dam of the City of Pasadena. Readings were taken at points where the solid angle down to 45° from the vertical was filled on all sides with a known depth of water. The coincidences were recorded with a vacuum tube circuit similar to those of Johnson and Rossi. The counters were 14 cm long and 2.5 cm in diameter. They were placed as shown in Fig. 1, beneath a lead plate 2.2 cm thick and 20×20 cm in area.

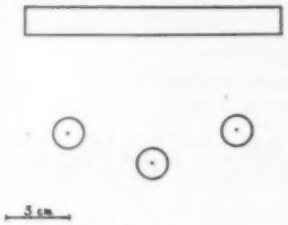

FIG. 1.

Measurements were made of the number of coincidences per hour at three locations as shown in the following table. This table gives the increase in the number of coincidences per hour due to the lead plate above the counters.

(i)	Apparatus on the top floor of Bridge Laboratory	8/hr.
(ii)	Under approx. 4 meters water equivalent below sea level	0.5/hr.
(iii)	Under approx. 10 meters water equivalent below sea level	0.1/hr.

The intensity of the vertical radiation at the three places was measured by putting the counters in a vertical line with about 6 cm between counters (i.e., 12 cm overall). Comparing this with the number of showers emerging from the 2.2 cm lead plate, one obtains,

		Vertical	Showers
(i)	At sea level	1.0	1.0
(ii)	4 meters below	0.38	0.06
(iii)	10 meters below	0.20	0.01

A few measurements have been made with varying thicknesses of lead, and these show that the thickness of lead for a maximum number of showers decreases greatly as one goes below sea level.

As a result of these experiments the following conclusions must be reached.

(i) The sea level radiation responsible for the type of coincidence here involved is softer than the average cosmic radiation.

(ii) The energy of the shower particles, as measured by the thickness of lead at which the coincidences are of maximum frequency, decreases when the shower producing radiation is filtered through water.

I wish to thank the Water Department of the City of Pasadena for permission to use the Morris Dam.

I also wish to thank C. D. Anderson and R. A. Millikan for many helpful suggestions.

W. H. PICKERING

California Institute of Technology,
February 6, 1935.

[1] Anderson, Millikan, Neddermeyer and Pickering, Phys. Rev. 45, 352 (1934).

The Thermal Equilibrium of Elementary Particles

We examine some new features of the equilibrium of matter and radiation at high temperatures $T \gtrsim 2mc^2/K$. At these temperatures the number of photons with energy $h\nu > 2mc^2$ capable of producing the creation of pairs of electrons cannot be neglected.[1] Also the collisions between the nuclei and other elementary particles, as neutrons, protons and electrons, produce the nuclear transformations in which the neutrons and protons can be captured or emitted.

We want to show that the application of the statistical laws permit the deduction from general assumptions of some properties of the elementary particles.[2]

Let us consider a region (for instance inside a star) in which nuclei, radiation and elementary particles are in thermal equilibrium. We want to assume the validity of the conservation laws of the charge, energy and momentum and of the exclusion principle for the electrons. We suppose also that it is possible to describe, at least in a first approximation, the states of the neutrons and protons by the antisymmetrical eigenfunctions and for some other particles (e.g., for photons) by symmetrical eigenfunctions.

The chief new feature of the equilibrium is that the total number of elementary particles of every kind will be variable with the temperature. The general statistical laws show, for each kind of elementary particles, the validity of the laws of Kirchhoff regarding the emission and the absorption of them by the nuclei, and the existence of a law of the spectral distribution of the number of particles among the various states which depend only on the temperature, and not on the kind of nuclei which take part in the equilibrium.

It is, for instance, noteworthy that by the usual statistical method[3] one can deduce the validity, for each kind of particles, of the asymptotical law of Wien for the density of particles with energy $W \to \infty$. Thus, from Kirchhoff's laws we conclude that the cross sections for the creation of pairs or the transformation of nuclei must tend to a constant limit when the energy of the incident particles tends to ∞.

A more detailed account of the application of the statistical method based on the assumption that, in a first approximation, the interaction among the particles can be described by some field of forces, will be given in another place.

GLEB WATAGHIN

University of São Paulo,
Department of Physics,
January 24, 1935.

[1] In a previous note we have considered the problem regarding the statistics of positive and negative electrons: Phil. Mag. [7] **17**, 910 (1934).
[2] The following remarks can also be applied to the hypothetic "neutrinos" and negative protons.
[3] Which we applied to the electrons in our preceding note, reference 1.

A New Method for Calculating Relative Multiplet Strengths in a Transition Array

The relative strengths of multiplets in a transition array such as $p^3 \cdot p - p^3 \cdot d$, where the jumping electron does not belong to a shell of equivalent electrons, may be calculated by the simple Kronig formulae.[1] When the jumping electron belongs to a shell of three or more equivalent electrons, as in the array $p^3 - p^3 d$, the relative multiplet strengths may be calculated by the method of Condon and Ufford,[2] which is based on the principle of spectroscopic stability. When more than one term of a kind occurs in a given configuration, however, their method gives only the sum of the strengths of the multiplets arising from all transitions between these terms and a term (or set of like terms) in the second configuration, and not the strengths of the individual multiplets. This apparent indeterminacy arises from the assumption that it is impossible to fix the ionic parentage for each term of the given configuration of equivalent electrons. Bacher and Goudsmit[3] have shown that the difficulty is purely formal, and that the parentage of any term in such a configuration may be expressed as a linear combination of all the terms of the ion. The coefficients may be found by quantum-mechanical methods. Thus, the parentages of the terms ^4S, ^2D and ^2P of p^3 are divided as follows among the terms ^3P, ^1D and ^1S of p^2: (^3P), $(1/2\,^3P + 1/2\,^1D)$ and $(1/2\,^3P + 5/18\,^1D + 2/9\,^1S)$. Accordingly, the relative multiplet strengths for the permitted transitions of $p^3 - p^2 \cdot d$ are the same as for the corresponding transitions of $p^3 \cdot p - p^2 \cdot d$, except for the factors 1/2, 5/18, etc., which must be introduced to take account of the fractional parentage of the term in question. It has already been noted that the strengths of $p^3 \cdot p - p^3 \cdot d$ may be calculated by the simple Kronig rules. Table I contains the multiplet strengths for the transition $p^3 - p^2 d$. The numbers in parentheses are the strengths given by Kronig's formulae for the corresponding multiplets of $p^2 \cdot p - p^2 \cdot d$. The parent terms are also given in parentheses. The missing multiplets are those forbidden by one or more of the ordinary selection rules. The resultant strengths may be compared with those computed by Condon and Ufford for the same transition array.

TABLE I.

p^3 \ $p^2 d$	(^3P) ^4P	^2F	^2D	^2P	(^1D) ^2F	^2D	^2P	^2S	(^1S) ^2D
(^3P) ^4S	(240) 240								
1/2 (^3P) ^2D		(504) 252	(90) 45	(6) 3					
1/2 (^3P) ^2P			(270) 135	(90) 45					
1/2 (^1D) ^2D					(336) 168	(210) 105	(54) 27		
5/18 (^1D) ^2P						(126) 35	(162) 45	(72) 20	
2/9 (^1S) ^2P									(360) 80

Tables for the cases of astrophysical importance will be given in the complete paper, which will be sent to the *Astrophysical Journal*.

DONALD H. MENZEL
LEO GOLDBERG

Harvard Observatory,
Cambridge, Massachusetts,
February 18, 1935.

[1] cf., review by Shortley, Proc. Nat. Acad. Sci. **20**, 591 (1934).
[2] Condon and Ufford, Phys. Rev. **44**, 740 (1933).
[3] Bacher and Goudsmit, Phys. Rev. **46**, 948 (1934).

The Action of Neutrons on Heavy Water

We have observed a large decrease in the radioactivity of a target activated by neutrons when heavy water is interposed between the target and neutron source. The water, weighing 46 g was contained in a Pyrex glass tube. It was prepared by Dr. H. L. Johnston and since it had been loaned for another purpose we were not at liberty to transfer it to a more suitable vessel. The neutron source consisted of 125 millicuries of radon in a 0.5 cc bulb containing powdered beryllium. This bulb was in turn surrounded by 20 g of powdered beryllium to utilize the production of neutrons by gamma-rays. The tube of water was placed close to the source and inclined at an angle to the target to increase the path of the neutrons through the water. This average path was about 5 cm. The target was a silver cylinder, 1 mm thick, placed around a screen-wall tube counter and inside the outer brass wall, 2 mm thick, of the counter.

In order to compare the effect with H^1 and H^2, measurements were made with a similar Pyrex glass tube containing the same quantity of ordinary water, and also with the empty container. The summary of the various activations under these conditions is given. Each value is the average count per minute above the normal background for the first 5 minutes, starting one-half minute after the source was removed.

Heavy water	*Light water*	*Empty tube*
2.8	22.6	13.4
6.8	16.8	19.2
3.0	18.4	22.8
7.8		
Ave. 5.1	19.3	18.5

One series was obtained with a copper target with a comparable result. When the source was placed in water to give a larger number of slow neutrons a smaller effect was observed. However the geometry on these experiments was such as to decrease the path of the neutrons through the heavy water and moreover the boron in the Pyrex glass was doubtless sufficient to absorb all of the very slow neutrons.

From the nature of the experimental set-up including the borosilicate glass and the outer brass wall of the counter, it seems probable that the decrease observed with heavy water is due to its action upon neutrons which have at least fairly high kinetic energies. It is not obvious, however, whether the effect is due to absorption or scattering.

We wish to thank Dr. L. R. Taussig and the University of California Hospital for the radon used in these experiments.

W. F. Libby
E. A. Long
W. M. Latimer

Department of Chemistry,
University of California,
Berkeley, California,
February 7, 1935.

Proceedings of The New England Section of the American Physical Society

MINUTES OF THE CAMBRIDGE MEETING, FEBRUARY 2, 1935

THE sixth regular meeting of the New England Section was held at Cambridge, Massachusetts, on Saturday, February 2, at Massachusetts Institute of Technology. The presiding officer at the sessions was Professor W. G. Cady, Chairman of the Section.

The morning session was devoted to contributed papers, whose Abstracts are printed below. After this session, the George Eastman Laboratory of Physics was open for inspection.

The afternoon session was devoted to invited papers. Professor G. Gamow gave a most interesting discussion of the theories of the beta-disintegration of nuclei. Professor Francis Bitter spoke on the relationship between the magnetic and mechanical properties of metals.

The program of the Section consisted of 9 papers, the Abstracts for which are given below.

PHILIP M. MORSE, *Secretary-Treasurer*

ABSTRACTS

1. Thomas-Fermi Method in Metals. H. M. KRUTTER, *Massachusetts Institute of Technology.*—Each atom in a metal is considered to be at the center of a cell formed in the manner suggested by Wigner and Seitz. To a first approximation this cell is assumed to be spherical. The Thomas-Fermi equation is solved numerically within this sphere subject to the two boundary conditions that the potential approach Ze/r at the nucleus, and the total electronic charge contained within the sphere is equal to $-Ze$. Expressions have been found for the kinetic, potential and total energies. The virial theorem has also been checked analytically. Calculations of the total energy as a function of internuclear distance show no minima. Potential field, momentum distribution, and other features obtained by this method promise to be of decided value as first approximations in more accurate treatment of metals. The Dirac modification of the Thomas-Fermi equation, which includes an exchange correction, has also been solved numerically for several atoms and should give more accurate potential fields.

2. On the Stokes Phenomenon for the Differential equations which Arise in the Problem of Inelastic Atomic Collisions. O. K. RICE, *Harvard.*—The problem of inelastic atomic collisions, involving exchange of energy between the atoms, depends upon the solution of a pair of coupled differential equations equivalent to a single differential equation of the fourth order, in which the independent variable is the distance r, between the two atoms. Asymptotic forms for the solutions of this pair of equations may be found. The probability of energy exchange may be shown to depend upon the connections between the solutions for values of r which correspond to regions of space where the relative kinetic energy of the two atoms is positive and the solutions for values of r corresponding to regions where the kinetic energy is negative. The finding of these connections involves a study of the asymptotic forms of the solutions when these forms are considered as functions of a complex variable. Such a study has been made in this paper, and the corresponding Stokes phenomenon investigated. It was not possible to attain the desired end, but results of interest have nevertheless been obtained. A brief discussion is given of the previous work of Stueckelberg.

3. A Contribution to the Theory of the W. B. K. Method. E. C. KEMBLE, *Harvard.*—Let $p(z,E)$ denote the classical local momentum $[2\mu(E-V)]^{1/2}$ in a one-dimensional problem in wave mechanics. Let $f_i = p^{-1/2}\exp\left\{\frac{2\pi}{h}i\int_{z_0}^{z} p\,dz\right\}$ and $f_r = p^{-1/2}\exp\left\{\frac{-2\pi}{h}i\int_{z_0}^{z} p\,dz\right\}$ denote the basic W. B. K. approximation functions. At every point of the complex z plane where p does not vanish it is possible to fit a linear combination $a_i f_i + a_r f_r$ to an arbitrary exact wave function $\psi(z)$ so that a_i and a_r become uniquely defined functions of z. A study of the differential equations of a_i and a_r makes it possible to put Zwaan's derivation of the Kramers connection formulas on a rigorous basis. The same method of attack yields a proof of the usual Bohr energy level formula applicable to the lower energy levels for which the connection formulas themselves are not valid. When applied to the problem of the transmission of matter waves through rounded potential hills, it gives an accurate transmission coefficient formula applicable through the entire range of positive and negative values of $V_{max}-E$.

4. Vacuum Tube Amplifier for Thermocouple e.m.f. R. P. JOHNSON, M. E. BELL AND W. B. NOTTINGHAM, *Massachusetts Institute of Technology.*—An amplifier has been developed for measuring small d.c. voltages arising in low resistance sources such as thermopiles. The source is placed in series with a "balancing out" e.m.f., a platinum to platinum cam driven contact, and the primary of a 1 : 100 ratio transformer. The contacts are closed about 90 percent of each revolution of the cam during which time the current builds up in the primary circuit, thus storing "magnetic"

energy in the iron of the transformer. The instant the contact opens an oscillation starts in the secondary. After one-quarter period of the oscillation practically the entire energy stored in the iron is delivered to charge the grid to filament capacity in parallel with the secondary distributed capacity. The voltage pulse delivered to the grid is practically equal to the thermal e.m.f. multiplied by the turns ratio and the ratio of the time constant (L_1/R_1) of the primary to the one-quarter period of the secondary circuit. Thus with an initial amplification of about 8000, it has been possible to detect thermal e.m.f.'s of 10^{-9} volt with reliability. In the present arrangement the pulsating current is rectified after passing through a three stage audio-amplifier giving a galvanometer output of 3 mm per 10^{-9} volt in an eight ohm primary circuit.

5. The Need of Physicists to Study the Problem of Hardiness and its Measurements. S. R. WILLIAMS, *Amherst.*—It is a conservative statement,—that among the tests for the suitability of materials in construction work the measurement of hardness holds an outstanding position as a test method. In spite of its wide use there is no satisfactory definition. We do not know what is meant by the term hardness. The methods thus far employed for measuring it are not based on any fundamental physical property. Modern atomic theories, colloid theories and theories of elasticity and plasticity should place the physicist in an advantageous position for studying the problem of hardness. Someone may wish to revive in connection with hardness the phenomenon of dilatancy as set forth by Osborne Reynolds. Hardness should not be left either to the metallurgists to study on metals alone or to the mineralogists on minerals. Desch has observed that "metallographic researches have resulted as yet in comparatively few far reaching generalizations." In the field of hardness measurements there is need for some generalization. It is this phase of the work which the physicist should consider. It may seem a far cry from hardness research to pedagogy. They are, however, intimately associated so far as the teacher of science is concerned. The investigation of hardness as a physical property of solids should percolate down through our science departments until the students in general physics are studying allied properties, such as density, elasticity, thermal and electrical conductivity and magnetic induction. This could be done with a series of alloys developed by a metallurgical department. The number of alloys would be legions. Such a program would give to the embryo physicist the "thrill of discovery" as well as to the older investigator. Students are interested in any project if it means being associated with something important and worth while. This would get away from the deadly practice students now have of trying to duplicate a number to be found in a table of physical constants and place the emphasis on the technique of experimentation.

6. Gamma-Ray Sensitivity of Tube-Counters and the Measurement of the Thorium Content of Rocks. ROBLEY D. EVANS, *National Research Fellow, University of California* (now at M. I. T.), AND R. A. MUGELE, *University of California.*—The useful sensitivity, S, of a tube-counter exposed to feeble gamma-radiation is proportional to $(N-B)/(N+B)^{1/2}$, where B is the background counting rate and N is the counting rate when the gamma-ray source is present. S depends upon the product of (a) the efficiency of production of secondary electrons in the counter by the incident radiation, and (b) the efficiency of the tube-counter in discharging once for each such secondary electron formed within its sensitive volume. Systematic comparison of many forms of tube-counters reveals that the sensitivity to gamma-radiation from a source of given strength and geometry, may be markedly increased (a) by increasing the effective area of the cathode by employing screen-wire cathodes or grooved tube cathodes in place of solid smooth cathodes, and by using cathodes of high atomic number. If the cathode is not radioactive, various cleaning treatments do not increase its sensitivity. Temperature changes between 0° and 45°C do not appreciably affect the copper cathode tube-counter. The sensitivity, S, may be increased further (b) by careful selection of the operating voltage and the pressure of the filling gas. For every counter an optimum pressure and voltage may be found at which the counter is many times more sensitive than it would be if no care were given to the selection of these operating conditions. For a tube-counter 12 cm long and 2 cm in diameter maximum sensitivity is obtained with a 100-mesh copper gauge cathode when the counter contains air at 6.5 cm Hg pressure and is operated 170 volts above threshold. The elevated sensitivity of these gamma-ray counters permits the direct measurement of the feeble gamma-radiation from the radioactive impurities in ordinary granitic rocks, and, when combined with independent measurements of the uranium content by the radon emanation method, leads to thorium measurements having a probable statistical error of about 2×10^{-7} g Th per g rock when only two hours of measurements are made on 1400 g of rock.

7. The High Pressure Transitions of Bismuth. P. W. BRIDGMAN, *Harvard.*—By an extension and improvement of the methods used in Phys. Rev. **45**, 844 (1934), the transition parameters of bismuth have been determined at high pressures. There are two new modifications of bismuth, each denser than the liquid. The transition line between I' (ordinary bismuth) and II (first high pressure modification) is linear and passes through the points 80°, 23,250 kg/cm² and 180°, 17,850 kg/cm². The transition line between II and III (second high pressure bismuth) is also linear and passes through 80°, 26,400 kg/cm² and 180°, 22,950 kg/cm². The triple point Liq.-I-II occurs at 184.0°. 17,600 kg/cm², with the parameters:

$\Delta V_{II\text{-}I}$	$=0.00474$ cm³/g	Lat.ht.$_{I\text{-}II}$	$=118$ kg cm/g
$\Delta V_{II\text{-}liq.}$	$=0.00025$	Lat.ht.$_{II\text{-}liq.}$	$=186$
$\Delta V_{liq.\text{-}I}$	$=0.00449$	Lat.ht.$_{I\text{-}liq.}$	$=304$

By calculation, rough values for the triple point Liq.-II-III are found to be: 187.0°, 22,700 kg/cm², and

$\Delta V_{III\text{-}II}$	$=0.00279$ cm³/g	Lat.ht.$_{II\text{-}III}$	$=44$ kg cm/g
$\Delta V_{II\text{-}liq.}$	$=0.00020$	Lat.ht.$_{II\text{-}liq.}$	$=186$
$\Delta V_{III\text{-}liq.}$	$=0.00299$	Lat.ht.$_{III\text{-}liq.}$	$=142$

Exploration has been made for still other modifications up to 50,000 kg/cm², but none have been found at room temperature or 125°. Antimony which crystallizes in the same system as Bi I shows no new modifications in the same range.

8. Problems of Beta-Disintegration. PROFESSOR G. GAMOW, *George Washington University.*

9. Relationship between the Elastic and Magnetic Properties of Metals. PROFESSOR FRANCIS BITTER, *Massachusetts Institute of Technology.*

THE AMERICAN INSTITUTE OF PHYSICS

INCORPORATED

GOVERNING BOARD

For The American Physical Society:

KARL T. COMPTON, *Chairman*
Massachusetts Institute of Technology

GEORGE B. PEGRAM, *Secretary*
Columbia University

JOHN T. TATE
University of Minnesota

For The Optical Society of America:

E. C. CRITTENDEN
Bureau of Standards

PAUL D. FOOTE
The Gulf Companies

F. K. RICHTMYER
Cornell University

For The Acoustical Society of America:

HARVEY FLETCHER
Bell Telephone Laboratories

VERN O. KNUDSEN
University of California at Los Angeles

WALLACE WATERFALL
The Celotex Company

For The Society of Rheology:

E. C. BINGHAM
Lafayette College

A. STUART HUNTER
du Pont Rayon Company

S. E. SHEPPARD
Eastman Kodak Company

For The American Association of Physics Teachers:

HOMER L. DODGE
University of Oklahoma

PAUL E. KLOPSTEG
Central Scientific Company

FREDERIC PALMER
Haverford College

ADMINISTRATIVE STAFF

HUBERT A. BARTON, *Director* JOHN T. TATE, *Adviser on Publications*

MADELINE M. MITCHELL, *Editorial Secretary*

Office: 11 East 38th Street, New York, New York

JOURNALS

THE PHYSICAL REVIEW
REVIEWS OF MODERN PHYSICS
PHYSICS

JOHN T. TATE, *Editor*
J. W. BUCHTA, *Assistant Editor*
E. C. BINGHAM, *Rheology Editor*

THE JOURNAL OF THE OPTICAL SOCIETY OF AMERICA
THE REVIEW OF SCIENTIFIC INSTRUMENTS WITH PHYSICS NEWS AND VIEWS

F. K. RICHTMYER, *Editor*

JOURNAL OF THE ACOUSTICAL SOCIETY OF AMERICA

F. R. WATSON, *Editor*

THE JOURNAL OF CHEMICAL PHYSICS

HAROLD C. UREY, *Editor*

THE AMERICAN PHYSICS TEACHER

DUANE ROLLER, *Editor*

The American Institute of Physics is a membership corporation of which five societies are the founding members. These five societies are the principal national societies devoted to pure and applied physics in America. Their names, and those of their representatives who form the Governing Board of the Institute, are given above. The principal work of the Institute is the publication of journals sponsored by the societies or by itself. The names and the editors of the journals are also listed above.

The broad purpose of the Institute is to represent, in all matters of wide or common interest, the five thousand or more members and subscribers associated with the Founder Societies and the journals. It aims to advance the science and profession of physics, and to promote cooperation between pure research, the applied sciences and the industries. To achieve these aims, it is greatly in need of an endowment and is empowered by law to administer grants and funds of any kind.

Dunham 343
. . . . . McMillan and Professor O. Lawrence 343
. . . . . Allan E. Parker 349
. . . . . F. H. Crawford and T. Jorgensen, Jr. 358
. . . . . Arthur H. Compton 367
. . . . . Walter Albertson 370
. . . . . E. N. Seaman and Frank Morgan 377
. . . . . Glenn M. Webb 379
. . . . . Glenn M. Webb 384
. . . . . Walter F. Colby 388
. . . . . J. E. Armstrong 391
. . . . . P. W. Bridgman 393
. . . . . K. P. T. Tyndall 398
. . . . . Frederick Seitz 400
. . . . . Rudolph S. Mulliken 413

. 416
. . . . . J. R. Dunning, G. B. Pegram, G. A. Fink and D. P. Mitchell 416
. . . . . H. V. Neher 417
. . . . . Leo G. Hall 418
. . . . . W. C. Peirce 419
. . . . . George H. Shenkley 419
. . . . . H. R. Crane and C. C. Lauritsen 420
. . . . . W. R. Dampier and W. F. G. Swann 421
. . . . . Richard J. Drivin 421
. . . . . R. O. Hulburt 422
. . . . . W. H. Pickering 423
. . . . . Glen Wasserman 423
. . . . . Duncan H. Bishop and Leo Gallagher 424
. . . . . W. P. Lucas, R. A. Lewis and W. M. Lucas 424

. 426

Lancaster Press, Inc., Lancaster, Pa.